SURFACE ELECTRICAL PROPERTIES EXPERIMENT

STUDY PHASE

FINAL REPORT

NASA CONTRACT NAS 9-10748

January 1973 Vol. 1 of 3

CENTER FOR SPACE RESEARCH
MASSACHUSETTS INSTITUTE OF TECHNOLOGY

CSR-TR-73-1

SURFACE ELECTRICAL PROPERTIES EXPERIMENT

STUDY PHASE

FINAL REPORT

NASA CONTRACT NAS 9-10748

January 1973 Vol. 1 of 3

SURFACE ELECTRICAL PROPERTIES EXPERIMENT

STUDY PHASE

FINAL REPORT

NASA CONTRACT NAS 9 10748

January 1973

Prepared for:

National Aeronautics and Space Administration
Manned Spacecraft Center

Prepared by:

James W. Meyer
Richard H. Baker
Leonard B. Johnson

Approved by:

Gene Simmons, Principal Investigator
John V. Harrington, Director

Center for Space Research
Massachusetts Institute of Technology

TABLE OF CONTENTS

APPENDICES

1.0 INTRODUCTION AND SUMMARY

This final report describes work leading to the evolution of a conceptual design of the flight hardware for the Surface Electrical Properties Experiment (SEP), the definition of requests for proposals, the analysis of proposals submitted by prospective flight hardware subcontractors, and recommendations for the flight configuration to be implemented.

Initial efforts were made to assess the electromagnetic environment of the SEP Experiment. An EMI receiver and tri-loop antenna were constructed and tests of opportunity were performed with a Lunar Roving Vehicle (LRV). Initial analyses were made of data from these tests with support from this contract, analyses which were continued in depth under the hardware contract.

Extensive theoretical work was performed in an effort to reduce to a conveniently tractable form, the difficult problem of finding an analytic solution for the near-, intermediate-, and far-field components of a radiating dipole deployed at the interface between two dielectric media. The problem was further complicated by the addition of layers with varying dielectric "contrast" in one of the media.

Field tests were performed on glaciers to evaluate several engineering design concepts, and to acquire empirical data to support design performance criteria identified in the conceptual design. Glacier data along with measurements made on samples of lunar rock and soil returned by Apollo astronauts were used to refine the scientific conceptual design

of the experiment, and as an aid in forecasting the kind of information that could be derived from the experiment as it applied to the first few thousand meters of the lunar surface.

Preliminary electronic, thermal, and mechanical designs were completed and tested in breadboard and model form. These yielded information which proved valuable in the evaluation of the sub-contractor proposals.

The salient features of the conceptual design evolved during this study are as follows:

The SEP flight hardware was to consist of a transmitter and a receiver of combined weight not to exceed 30 pounds. The transmitter was to be equipped with a pair of dipoles, designed to operate efficiently at each of six frequencies when deployed by the astronaut orthogonal to one another on the lunar surface. The overall length of each leg of each dipole was not to exceed 70 meters. The transmitter was to power each orthogonal dipole alternately for a period of 200 milliseconds at each of the six frequencies totalling 400 milliseconds on-time at each frequency. The transmitter would be off for two 400 millisecond periods before the pattern was repeated at 3.2 second intervals. The desired transmitted power output at each of the frequencies was given as follows:

Frequency (MHz)	Radiated Power (Watts)
0.5	6
1.0	3
2.0	1.5
8.0	1.5
16.0	1.5
32.0	1.5

The receiving antenna was to consist of three mutually orthogonal loops approximately one third meter in diameter, but not necessarily circular, with minimum cross coupling between the loops.

The Data Storage Electronics Assembly (DSEA) was prescribed as the magnetic tape recorder to be used for recording the experiment data. The receiver was to acquire and synchronize automatically with the transmitter signal pattern. Each of the three orthogonal loops was to be connected to the receiver input sequentially for equal times during each 200 millisecond interval. It was envisaged that the receiver would be mounted on the LRV as a source of locomotion during traverses needed for interferometic operation.

Detailed information on the various parts of this program is contained in reports and memoranda which are referenced in the main body text and appended in full text to principal copies of this report. There are a few instances in which the bulk of the work, but not all, reported in a given document was supported under this contract. In these instances, the document is included in full for completeness.

2.0 SURFACE ELECTRICAL PROPERTIES EXPERIMENT, CONCEPTUAL DESIGN

The objectives of the SEP experiment were to detect layering in the lunar subsurface as revealed by significant changes in the dielectric properties (e.g., dielectric constant, conductivity) on the scale of a wavelength. The dramatic difference between the dielectric constant of water (80) and ice (3) or lunar soil (3-15) makes it possible to detect the presence

of water at depth. The detection and measurement of the depth of a water-ice interface (0° C. isotherm) would make it possible to obtain an independent estimate of the lunar thermal flux.

The electrical properties of the lunar material were to be measured in situ over the seven octave frequency range to be employed by the experiment. Under favorable conditions, it might be possible to estimate the number and size of subsurface scattering bodies through an analysis of their impact on the interferograms taken at each of the six operating frequencies.

The status of the SEP experiment conceptual design as of October 28, 1970 was described in detail in a M.I.T. Center for Space Research Technical Report CSR TR 70-7, attached as Appendix 2.1 to principal copies of this report. The Technical Report contains sections on administrative/biographical information, plus discussion of technical, engineering, and operational aspects of the conceptual design. An appendix details a rotating beam direction finding concept which at the time of the report writing was being considered as a prime candidate solution to the problem of tracking and locating the LRV during a traverse.

The conceptual design at this stage envisaged a transmitter providing a rotating beam pattern from an orthogonally driven turnstyle antenna. Eight frequencies (0.5, 1, 2, 4, 8, 16, 24, 32 MHz) each radiated for 0.1 seconds were called for, plus two 0.1 second periods during which the transmitter would be off in the total cycle time of 1 second. Anticipated radiated powers were 2 watts at 0.5 MHz, 1/2 watt at 1.0 MHz,

and 1/8 watt at each of the other frequencies. The estimated weight of the transmitter was 11.1 lb. The receiver equipped with three mutually orthogonal loops was to be designed for a logarithmic response to accommodate the large dynamic range of signals expected in the experiment. The data were to be recorded on the DSEA which was to be returned to earth. The weight of the receiver in this conceptual design was estimated at 10.8 lbs. The estimated time required for deployment by one astronaut was 31 minutes, with an additional 3 1/2 minutes required for other experiment-related activities.

As a result of engineering tests on the glacier, and of further analytical work, the rotating beam antenna concept was abandoned. The multiple conductor flat ribbon wire transmitting antenna concept also had to be abandoned because glacier tests showed break-up of the dipole patterns resulting from interactions of the contiguous wire elements. To improve the signal to noise ratio, more transmitter power was deemed necessary. Also, two of the original eight frequencies (4 & 24 MHz) were dropped from the conceptual design.

This conceptual design, as modified, was used as a baseline guide in the writing of the several proposals and requests for proposal prepared to implement the acquisition of the flight hardware.

3.0 PROPAGATION AND ANTENNA ANALYSIS

One of the most intriguing aspects of the Study Phase was the investigation of electromagnetic propagation phenomena and antenna problems associated with the lunar environment. In the case of the transmitter, a radiating antenna lying on the lunar surface was to be operated at the boundary of different dielectric media. In the case of the receiver, the antenna was to be portable and capable of sensing the separate orthogonal magnetic field components of the transmitted electromagnetic wave.

One problem was the characterization of the basic propagation phenomena associated with the lunar environment, which involved the simultaneous interaction of electromagnetic waves propagating above the lunar surface, energy propagating below the surface, and propagated energy reflected by one or more contrasting layers within the dielectric material. In addition, the experiment posed many antenna unknowns of a practical nature such as input impedance, efficiency, radiation patterns, and power division into the dual media in the case of the transmitting antenna; and field strengths and cross-coupling levels in the case of the receiving antenna. The problems were attacked in somewhat different fashions by different investigators.

Within the Center for Space Research, Laboratory for Space Experiments, the principal analytic effort to develop propagation conditions in layered media was pursued by W. W. Cooper who approached the problem by a direct method which obtained the field components associated with orthogonal Hertzian dipoles without using electromagnetic potentials. His work,

begun in the Study Phase was continued in the Hardware Phase resulting in Report TR 71-3 in June 1971 entitled "Patterns of Dipole Antenna on Stratified Medium," and later in January 1972 a report entitled "TE/TM Patterns of Hertzian Dipole in Two- or Three-Layered Medium" which is included as Appendix 3.1.

Simultaneously, Professor J. A. Kong of the M.I.T. Electrical Engineering Department conducted propagation studies based on a dielectrically stratified model of the moon, the results of which are summarized in Appendix 3.2, in a memo of February 17, 1971 entitled "Model Study of Lunar Subsurface Electrical Properties; Formal Solutions of Radiation from Dipole Antennas over Stratified Media". Professor Kong's studies have also continued in the Hardware Phase.

Toward the end of the Study Phase, J. Lozow of the Charles Stark Draper Laboratory, M.I.T., formed a review and extension of the work of Annan as a prelude to the determination of the electrical and radiation properties of the SEP antenna. The results of his brief effort, terminated by depletion of Study Phase funds, are given in Memo 23S 70-81 of 23 December 1971, entitled "Resonant Dipole on the Surface of a Dielectric Half Space," which also appears as Appendix 3.3.

In addition, propagation and antenna studies were carried out by LSE personnel. Typical results of this effort are abstracted in Appendix 8.1.

4.0 FIELD TESTS

Two field tests were carried out. Early tests at the Gorner Glacier in Switzerland were designed to verify the validity of the experimental concept. During the Study Phase tests were performed at the Athabasca Glacier to evaluate the conceptual design. A preliminary report on the Athabasca expedition and a heuristic interpretation of the results appear in Appendix 4.1.

5.0 ENGINEERING DEVELOPMENT AND FEASIBILITY PROGRAM

In the first portion of the Study Phase starting May 5, 1970, and covering a period of approximately three months, the bulk of the CSDL engineering effort was directed toward the evolution of a design concept for implementation of the experiment. The result of this early effort is represented in the "Conceptual Design Report", forwarded to MSC on July 23, 1970. It contains a description of the mechanical aspects of the concept, thermal design considerations, tape recorder requirements, astronaut deployment description, weight estimates, power requirements, and equipment requirements. This document, reproduced in Appendix 5.1, described the original design concept to which many modifications were later made.

In addition, a portion of the early engineering effort was expended in the generation of a technical specification which subsequently became part of a proposed statement of work by CSDL for hardware development. The S.O.W. was forwarded to MSC on July 31, 1970. The original expiration date for this Study Phase effort was August 7, 1970.

The engineering feasibility program, which involved the design, construction and laboratory evaluation within CSDL of breadboard system elements implementing the conceptual design, was not initiated until after receipt of the Study Phase contract extension notification of August 17, 1970. Under this extension, preliminary circuit, mechanical and thermal breadboards were contructed, based on conceptual design information available in early September of 1970, for the purpose of facilitating the development of a Field Evaluation Model of both the SEP trans-

mitter and receiver as well as a special EMI receiver to survey LRV interference.

5.1 SEP TRANSMITTER ELECTRICAL DESIGN ACTIVITY

At the start of the breadboard design effort, the salient SEP transmitter requirements differed from those which ultimately evolved and are summarized as follows:

(1) RF frequencies of 0.5, 1, 2, 4, 8, 16, 24, 32 MHz.

(2) A rotating dipole field using a crossed dipole transmitting antenna.

(3) Power delivered to the transmitting antenna of 2 watts @0.5 MHz; 1 watt @ 1 MHz, 0.5 watts @2 MHz; 0.25 watts @ 4 MHz; and 0.125 watts @ 8, 16, 24, and 32 MHz.

The frequencies were derived from a 32 MHz TCXO. Low power TT logic was used in a count-down chain to derive the RF frequencies. This section was built and tested in-house.

The square-wave outputs of the logic were buffered and then filtered using high-Q filters of 2-, 4-, and 6- pole Tchebycheff design. This section was built and tested in-house.

Diode switches were used to select the RF frequencies to be transmitted. In-house design as well as commercially available switches from companies such as Lorch and Meriman Research were tested and evaluated.

Power dividers, balanced modulators, and baluns used in the transmitter design were obtained commercially from companies such as Meriman Research.

The rotating dipole field was implemented by amplitude modulating the N-S dipole RF excitation with a 15 Hz sine wave

and the E-W dipole RF excitation with a 15 Hz cosine wave. The sine-cosine generator used a linear approximation approach which digitally locked the phasing of the sine and cosine outputs.

Linear amplifiers were chosen to drive the N-S and E-W antennas as it was required to have a differential phase error of less than 5° and a gain error of less than 1 db over the required frequency and temperature range. LEL division of Varian and Advantek were two companies who were approached for the supply of these amplifiers.

Preliminary negotiations were concluded with both M.I.T. - Lincoln Laboratory and Raytheon for the design of the antennas, as the proper facilities were not available at Draper Laboratory.

This design effort was accomplished with approximately 3 man-months of engineering time and 3 man-months of technician time.

5.2 SEP RECEIVER ELECTRICAL DESIGN ACTIVITY

In early September 1970, based on tentative specification information received from CSR, CSDL began breadboarding an eight-channel single hetrodyne Field Evaluation receiver, using a log amplifier for data compression. To meet the tight schedule, outside RF specialists were consulted in the areas of their expertise.

Efforts to obtain log amplifiers from two competitive sources were initiated with Varian, (LEL Division) and RHG. These companies agreed to supply working samples of small hybrid log amplifiers deemed potentially applicable to the receiver.

"Off-the-shelf" local oscillators, mixers, combiners, etc. were ordered in parallel to the in-house design efforts initiated in this area.

Breadboards of diode switches, front-end RF preamplifiers, and a telemeter VCO, were built and tested in-house. Specialized RF instrumentation to support the in-house design and build effort was rented (Vector voltmeter, spectrum analyzer, etc.) Some of the in-house built electronics was used to construct a special EMI investigation receiver, a coincident effort described in Paragraph 5.5.2.

In the area of antenna design, consultations were initiated with the M.I.T. Lincoln Laboratory and the Raytheon Company. In addition, preliminary negotiations for resident RF design and system engineers to backup the effort were undertaken with the Raytheon Company, RCA, and Varian (LEL Division).

The preliminary effort described above began in early September 1970 and terminated in early December 1970, a period of approximately 3 months. During this period, approximately 2.5 man-months/ month staff effort and 2 man-months/month staff effort and 2 man-months/month technician effort was applied to the receiver design. In addition, gratuitous study efforts by engineers at Varian (LEL Division), RHG and Lorch were expended, the results of which were used by CSDL to supplement the in-house effort.

5.3 SEP MECHANICAL AND THERMAL DESIGN ACTIVITY

The mechanical and thermal design was started before the conceptual design of the experiment had been hardened, in order to meet the imposed schedule. The design described here was based on information available in September and October, 1970.

A minimum weight design requires that the mechanical design incorporate the required thermal isolation while providing the necessary mechanical structure. The structural design must also make provision for ease of handling by the astronauts and mounting on the LEM and LRV. The thermal design must provide the proper thermal environment for the electronics, recorder, batteries, and solar cells under anticipated stowage and use conditions.

Major assumptions made were that the 4 transmitting antenna arms would consist of 8 parallel elements of various lengths up to 70 meters in the form of a flexible ribbon and that the receiving antenna would consist of 3 orthogonal common-center loops about 1 foot in diameter as set forth in the Conceptual Design document dated 8 October 1970. A receiver mockup is shown in Figure 5.1. It was also assumed that the astronaut would have the physical ability to reach the lunar surface if necessary during deployment.

A transmitter mockup is shown in Figure 5.2. This model does not show a system for attaching the transmitter feet to the pallet, but effort was expended in designing a tighter hold-down system than the oft-used pip pin. The T carrying handle also doubled as a fastener for holding the crossbar reel securing device. The reels were made as big in diameter

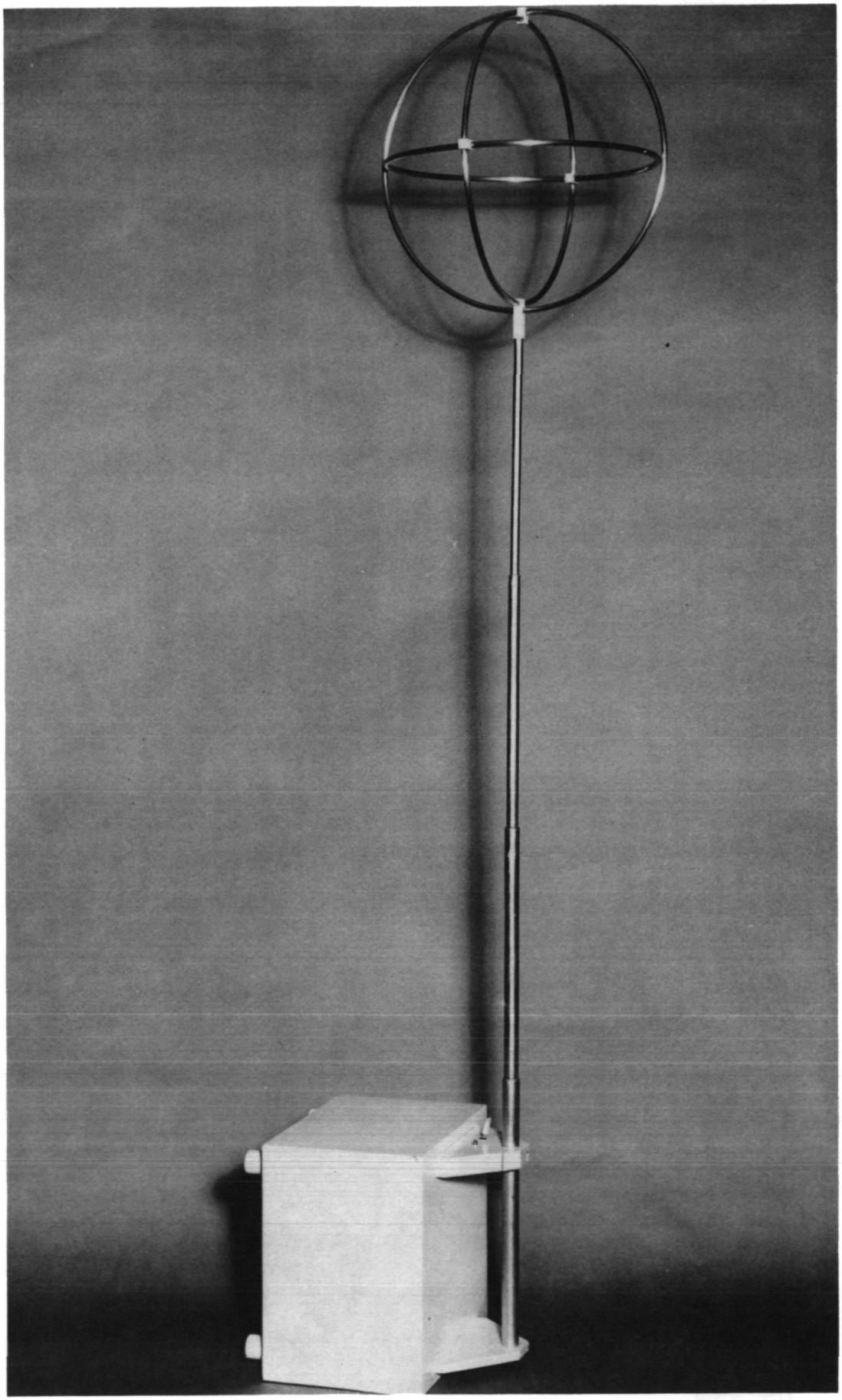

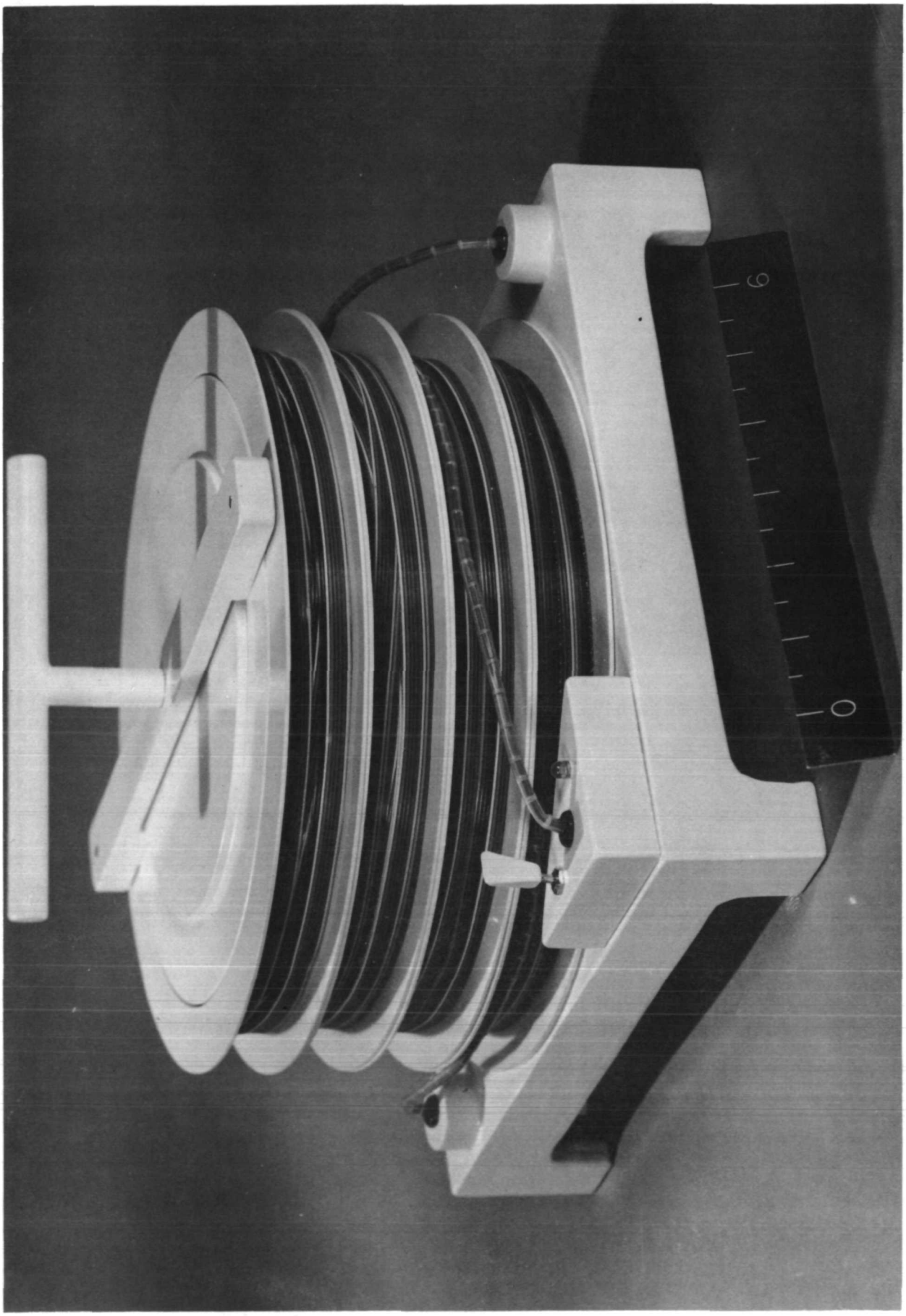
9
0

as possible to reduce set in the coiled antenna. The three-section solar panel was stored in the base of the transmitter. The electronics in the cylindrical section were suspended from the top plate which serves as a radiator. The electronics were packaged employing welded, heat-sinked, cordwood construction as used in the Apollo Guidance Computer.

5.4 REPORTING OF ENGINEERING DEVELOPMENT ACTIVITIES AND RESULTS

The evolution of the SEP conceptual design leading to the "Conceptual Design Report" of July 23, 1970 and to the later SEP Preliminary Technical Specification in August of 1970 may be traced in SEP memos SEP-4-T, dated 8 June 1970 and SEP-5-T, dated 12 June 1970, both of which appear in Appendix 5.2.

Interim reporting on the status of the CSDL breadboard effort was covered in Weekly Memos, the most pertinent of which appear in Appendix 5.3.

A summary report on the status of the engineering development effort at the termination of the Study Phase first contract extension was included in an M.I.T. presentation to MSC on December 11, 1970. A collection of presentation Vu-Graphs comprises Appendix 5.4.

5.5 EMI CONSIDERATIONS

One of the major design uncertainties associated with the SEP Experiment was the level of electromagnetic interference produced by the Lunar Rover Vehicle should the decision be made to transport the sensitive SEP receiver by this method. During the period of the first extension of the Study Phase, two efforts were mounted to reduce this uncertainty, one being an

EMI test of a breadborad LRV traction drive system, and the second being the design and fabrication of a special EMI receiver for use with the LRV.

5.5.1 INITIAL EMI TESTS

The first tests giving an indication of the possible level of LRV interference with SEP were conducted by CSDL personnel on October 26 and 27, 1970 on a breadboard Rover Traction Drive Motor System located at the Marshall Space Flight Center. A description of this test activity and its results is given in CSDL SEP memo SEP-10-T, dated November 2, 1970 which is included in this report as Appendix 5.5.

5.5.2 DEVELOPMENT OF THE EMI RECEIVER

During the three-month Study Phase extension, CSDL undertook the design and fabrication of a special EMI receiver, self-contained and similar in its important characteristics to the SEP receiver, and capable of being mounted on an LRV for high confidence determination of LRV interference effects on the SEP experiment. The completed receiver is pictured in Figs. 5.3, 5.4, 5.5 and 5.6. This unit was ultimately used to record the interference environment during Apollo System EMI and Compatibility Tests at MSC, performed on March 29, 1971. A brief description of the test conditions, the receiver characteristics and the test results is given in the CSDL memo entitled "EMI Test Results, Quick Look (Using MIT EMI Receiver), dated 19 February 1971, which is also included in this report as Appendix 5.6. Later, during the execution of NASA Contract NAS 9-11540, a detailed error analysis of all circumstances of

the EMI tests as well as extensive post-test calibration checks of the EMI receiver led to slight revisions of the "quick look" results and provided the highest-confidence data to date.

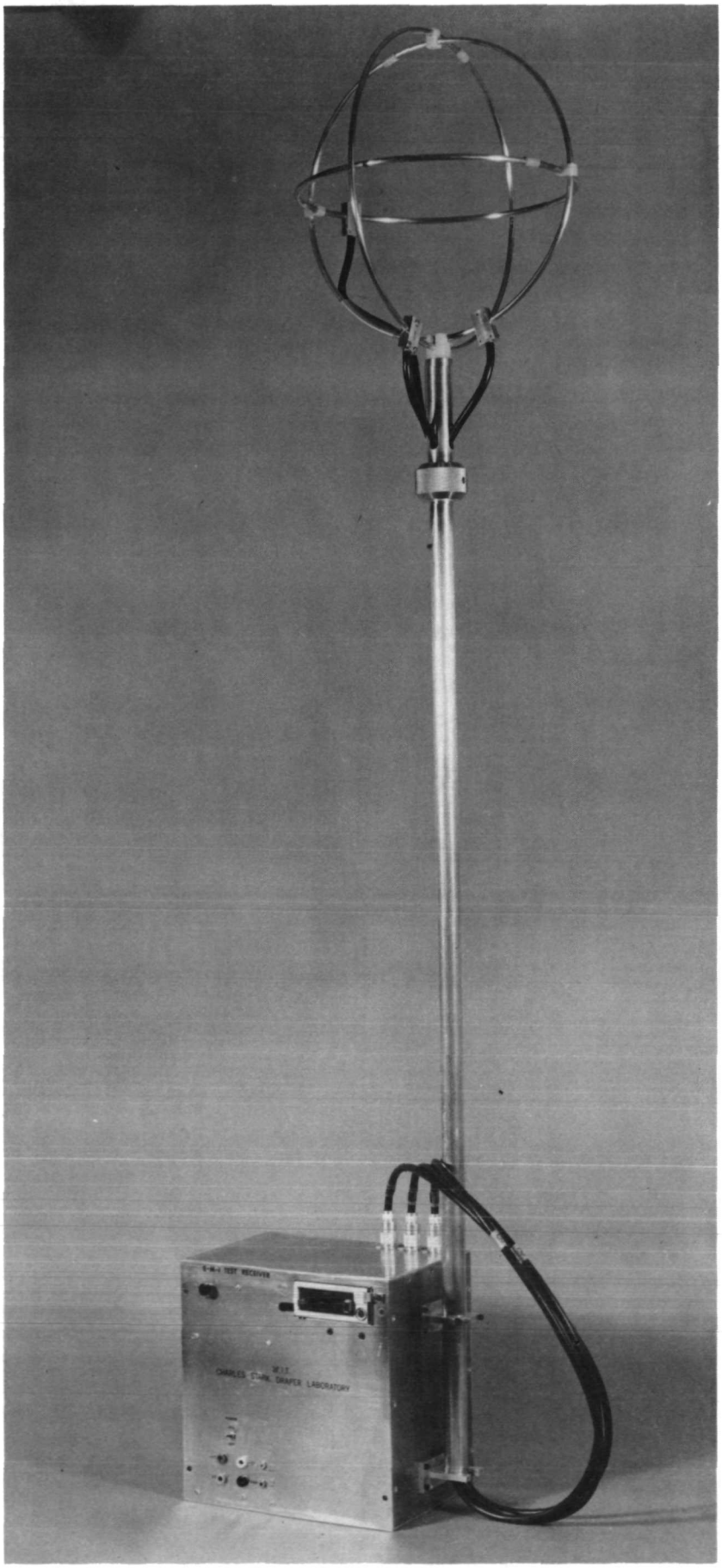
M.I.T.
CHARLES STARK DRAPER LABORATORY

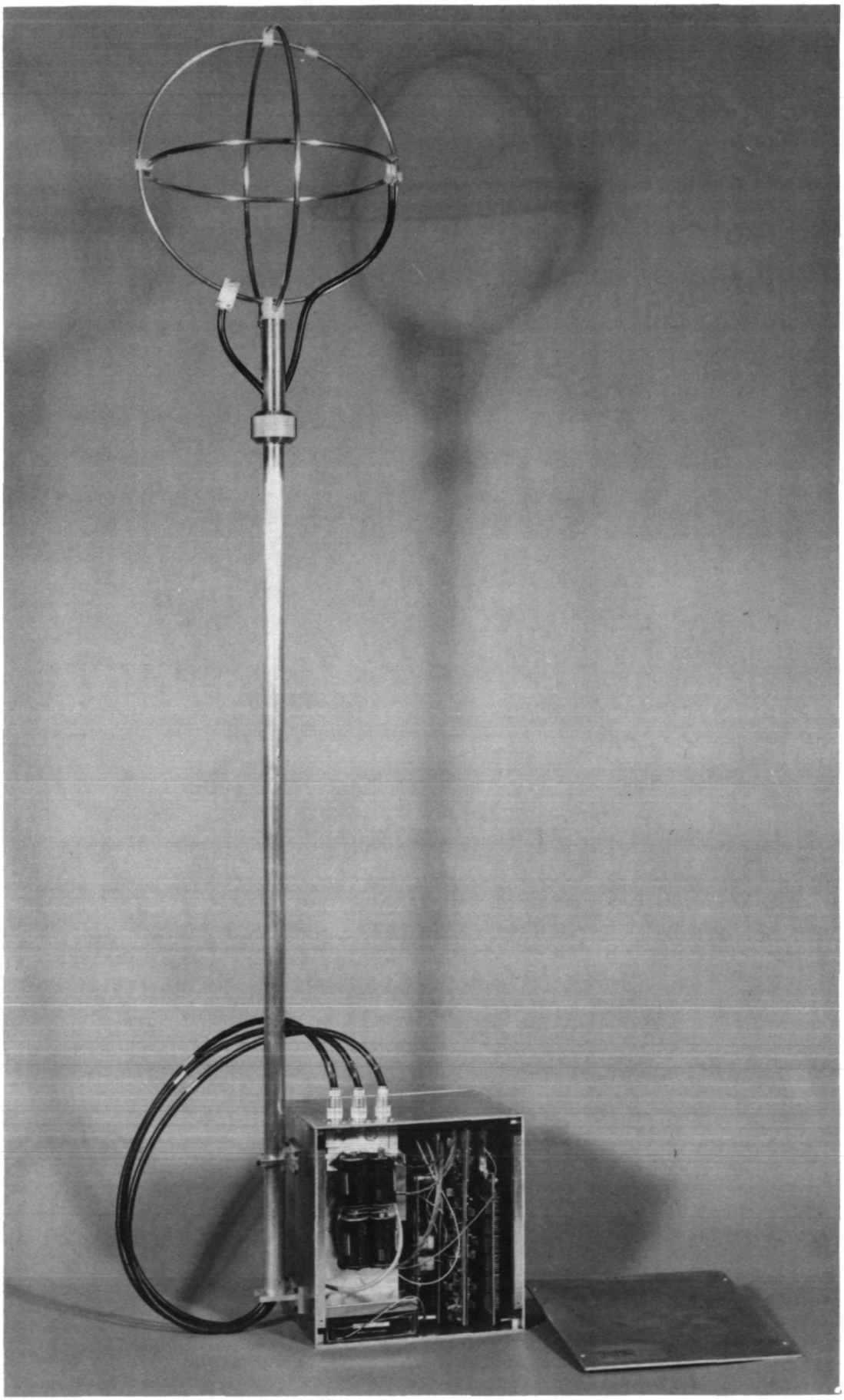

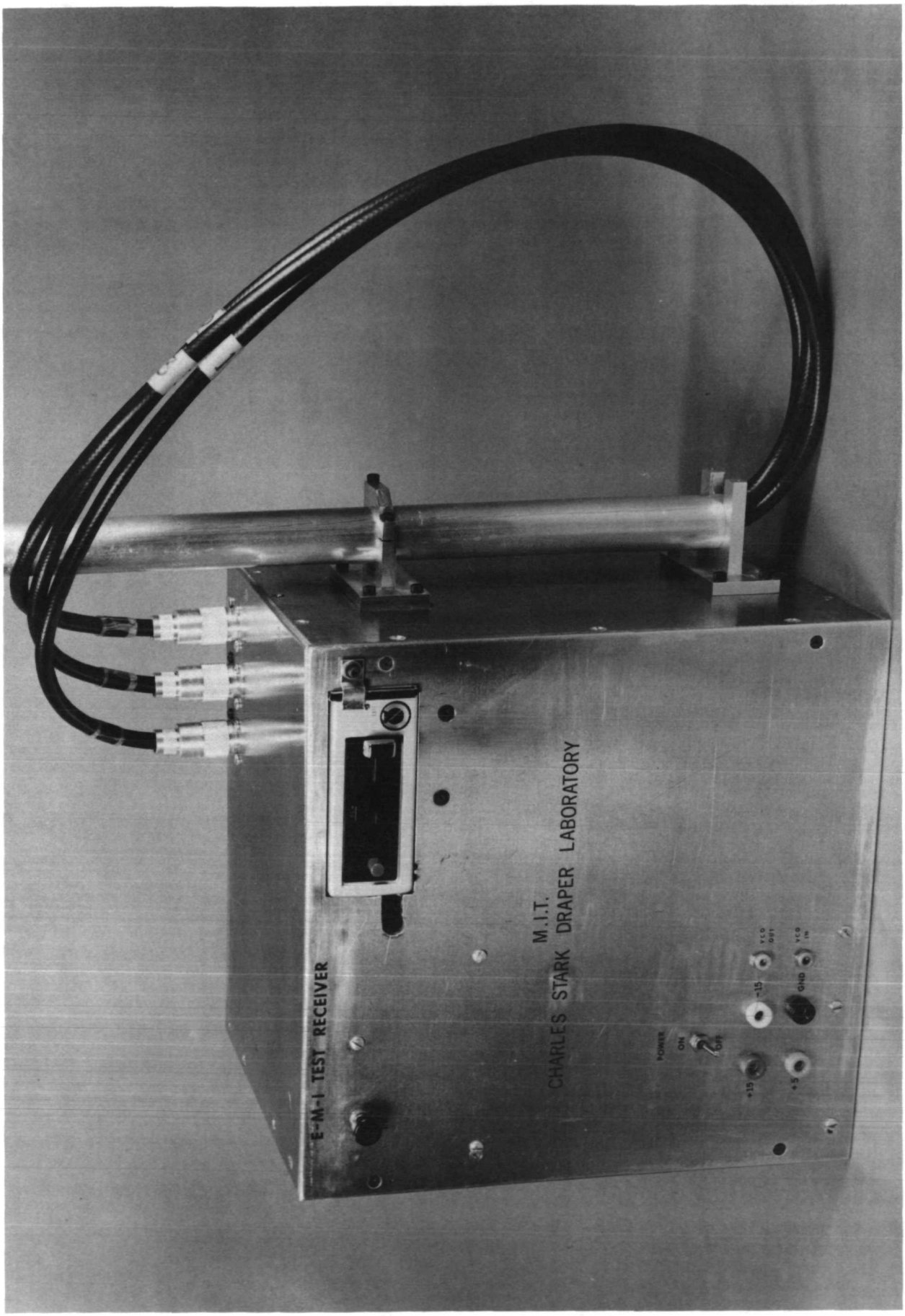
E-M-I TEST RECEIVER
M.I.T.
CHARLES STARK DRAPER LABORATORY
POWER
ON
OFF
+15
-15
VCO OUT
GND
VCO IN
+5

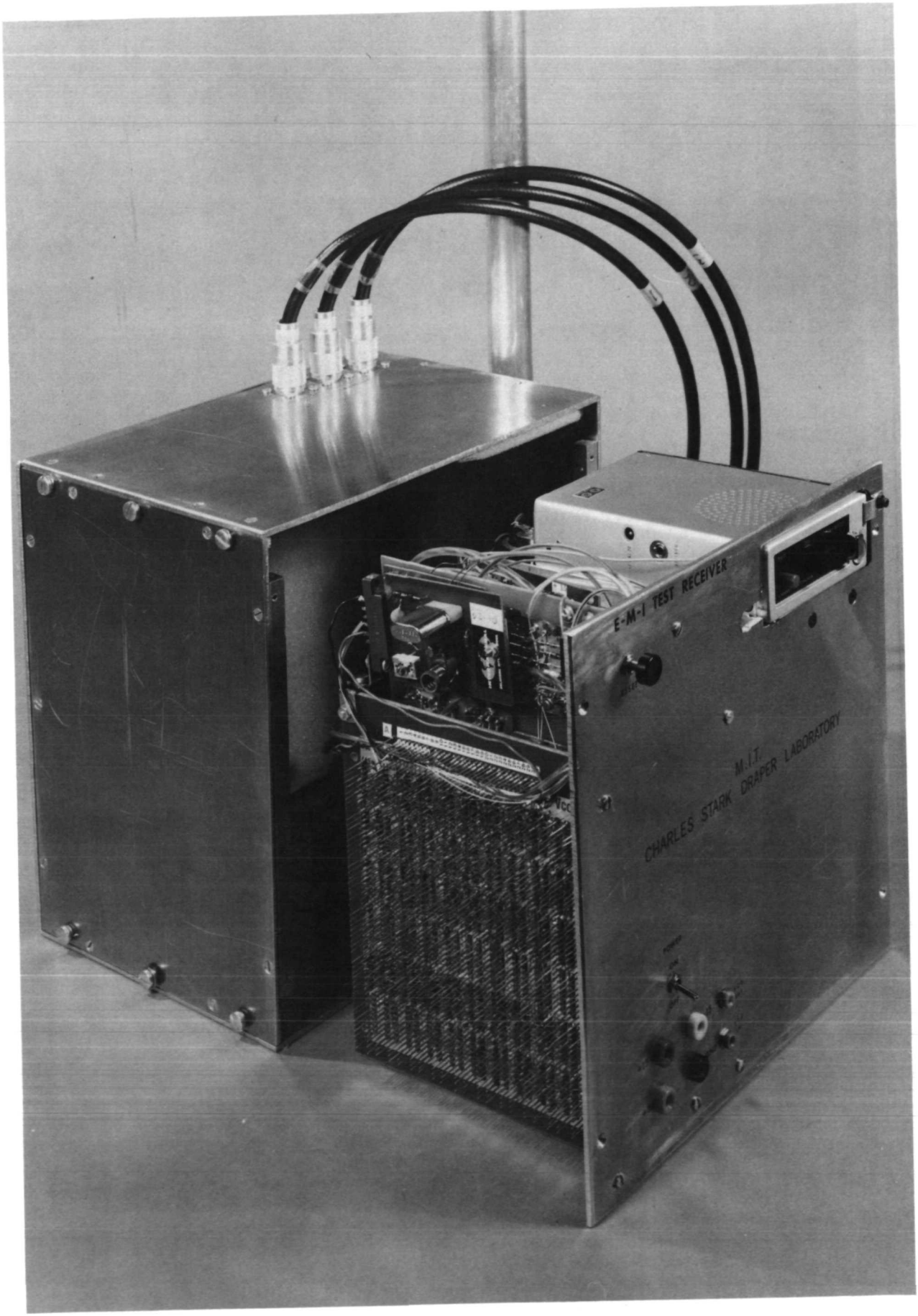
E-M-I TEST RECEIVER
M.I.T.
CHARLES STARK DRAPER LABORATORY

6.0 PHASE I DOCUMENTATION

In addition to design activity, a complementary documentation effort was pursued by CSDL during the Study Phase resulting in documentation important to further evolution of experiment hardware. Among the more significant documents produced were the following:

(1) A preliminary Hardware Technical Specification which served as the basis for Part 1 of a preliminary End Item Specification.

(2) Part 1 of a preliminary End Item Specification (See Appendix 6.1)

(3) A Configuration Management Plan suitable for follow-on hardware fabrication (See Appendix 6.2).

(4) A Reliability and Quality Assurance Plan suitable for follow-on production (See Appendix 6.3).

(5) A Procurement Specification for the Data Storage Electronic Assembly (See Appendix 6.4).

(6) A preliminary parts list for the proposed hardware design.

7.0 CONTRACT AND SUBCONTRACT DEFINITION, PROPOSAL, PREPARATION AND EVALUATION

For CSDL, an objective of the extended Study Phase effort was the preparation and submission to NASA MSC of a technical and cost proposal for development and manufacture of the SEP Experiment hardware, in response to request for Proposal No. JC931-88-1-165P. The work accomplished under the Study Phase was applied in the generation of CSDL Proposal No. 70-238 responding to the RFP. In this document, CSDL proposed the in-house development and manufacture of essentially all the SEP hardware, except for the ground support equipment and antennas which would be designed and built by a subcontractor. In addition, the subcontractor was to furnish resident engineering support, engineering field support and certain other local support to supplement the CSDL capability.

The Raytheon Company was invited by CSDL to bid on the subcontract activity, and requested to prepare supporting technical and cost proposals. For this purpose, the necessary contacts were established between M.I.T. and Raytheon personnel to define the subcontract requirements, identify the tasks and specify the level of effort.

Several aspects of the completed proposal were regarded as unsatisfactory by MSC, and the proposal was not accepted in its original form. Of particular concern to MSC were potential manpower problems attributable to in-house manufacture of all SEP hardware requiring a rapid but short-term peaking of production manpower to produce the flight hardware.

To meet these objections, CSDL subsequently substantially revised the original proposal by placing the manufacture of the Compatibility Unit, the Qualification Unit, and the two Flight Units with the subcontractor, in addition to the other fabricated items and support defined in the original proposal. Because of the magnitude of the subcontract effort under this revision, it became necessary for CSDL to solicit competitive bids from competent potential subcontractors, and a vigorous effort was mounted by CSDL to develop the request for proposal package. Because of the ever-dwindling time remaining before the Apollo 17 scheduled launch date of July, 1972, an accelerated bid effort was dictated and only two industrial contractors RCA-Camden and Raytheon were solicited. Technical and cost proposals subsequently received in November of 1970 from both organizations, were carefully reviewed by CSDL and Raytheon was selected as the successful bidder. Then followed intensive discussions with Raytheon to coordinate details of the subcontract effort with CSDL's revised proposal plan. This effort culminated late in November 1970 with CSDL "Technical Proposal for the Surface Electrical Properties Experiment", Proposal Number 70-238, Revision 1. A copy of the technical portion of this document appears in appendix 7.1.

MSC was concerned about coordination problems that might occur in a program in which the prototype design was the responsibility of CSDL and the productizing and manufacture of the end items was the responsibility of the subcontractor under CSDL supervision. In addition, the estimated cost of the program was considered high and MSC foresaw possible coordination problems

within M.I.T. arising from the organizational relationships outlined in the proposal. The revised proposal was not approved. This disposition terminated the role of CSDL as prime bidder for SEP hardware implementation.

A review of the situation by the M.I.T. Administration eventually resulted in a policy decision to proceed with a third proposal which placed responsibility for implementation of the SEP experiment in the hands of the M.I.T. Center for Space Research supported by a SEP Program Management Office to administer a major subcontract with an industrial subcontractor for the design, development, test and manufacture of the SEP hardware and supporting equipment. This effort required the generation of two major documents: (1) A detailed request for proposal defining for bid purposes the tasks and responsibilities of the industrial subcontractor for implementation of SEP, and (2) a proposal from M.I.T. to NASA responsive to RFP JC931-88-1-165P and delineating the role of the M.I.T. Center for Space Research as prime contractor, and as manager and administrator of a major subcontract. The task of preparing these documents on an accelerated basis was performed by CSDL and CSR personnel whose familiarity with the details and problems of the program, developed through the course of the Phase I effort, offered the best chance of accomplishing the task within permissible time limits.

During this period, plans for the operation, organization and staffing of the Program Management Office were formulated and activated. Several of the individuals who were expected to comprise the PMO were brought together to carry on the tasks of contract and subcontract definition, proposal preparation, and

subcontract bid response evaluation. Among these were Dr. James W. Meyer of the M.I.T. Lincoln Laboratory, who would assume the role of Program Manager under the Hardware Phase implementation contract, and L. B. Johnson of CSDL, prospective Assistant Program Manager, who would coordinate back-up support from CSDL. In addition, special assistance was to be available from Dr. L. J. Ricardi of Lincoln Laboratory on antenna problems and from Dr. J. A. Kong on questions relating to electromagnetic propagation. Generation of cost information was accomplished under the supervision of L. E. Beckley, Administrative Officer of CSR.

The request for Proposal for the SEP subcontract effort was completed early in January 1971, and mailed to prospective bidders on 4 January with a closing date for response of 18 January. Because of the extremely short time available for preparation of responses by the bidders and for evaluation of the responses by CSR, only two industrial organizations were solicited, RCA-Camden and Raytheon. A bidders conference, supported by CSDL, CSR, and Lincoln Laboratory personnel, was held 6 January, 1971 at M.I.T. Subsequently in response to CSR's invitation, each bidder made an individual interim presentation prior to the proposal deadline.

The CSR technical proposal in response to MSC RFP JC931-88-165P was completed in early January and copies were forwarded to MSC prior to an M.I.T. technical proposal and preliminary budget presentation made at MSC on January 20, 1971. A copy of the technical proposal is contained in Appendix 7.2.

In the latter part of January, a Proposal Review Committee comprised of personnel from CSR, LSE, the projected PMO, CSDL and Lincoln Laboratory, was formed to review the subcontract

proposals from RCA and Raytheon. The team worked intensively in the period from January 18 to January 28 to review the designs as proposed by the two bidders and summarized in Tables 1 and 2, as well as to assess the cost and other factors on which to base an award decision. On the latter date, the Committee presented the results of their review to members of M.I.T. Administration who concurred in the decision to award the SEP subcontract to Raytheon.

The final efforts under the extended Phase I SEP study entailed support of MIT-MSC negotiations for Contract NAS 9-11540 and preparation for immediate additional EMI tests.

TABLE I

PROPOSED TRANSMITTER DESIGNS

ITEM	RCA	RAYTHEON
Structure	Pressurized metal case housing machined metal modules	Unpressurized cylindrical epoxy fiberglass case housing cylindrical metal modules.
Electronics	(a) Six individual xtal. oscillators for transmitted frequency generation. (b) Class C RF power amplifiers of 6 watts max. capability for each dipole.	(a) One master xtal. oscillator and divider chain to generate transmitted frequencies. (b) Class B RF power amplifiers of 12 watts max. capability for each dipole.
Antenna	Two, multi-frequency, strip-line dipoles with built-in transmission line isolating traps.	Two, thin-wire, multi-frequency dipoles with lumped-parameter isolating traps
Thermal Control	Multilayer thermal blanket surrounding case	Insulation inside case; passive radiator.
Power	Regulated solar panel	Regulated solar panel plus small battery for peak power

TABLE 2

PROPOSED RECEIVER DESIGNS

ITEM	RCA	RAYTHEON
Structure	Metal container housing machined metal modules	Epoxy fiberglass container housing electronic modules
Electronics	(a) Superhetrodyne (b) Synchoronization scheme with spike noise protection (c) Sensitivity calibrated in mfg. and temperature compensated for stability	(a) Tuned radio frequency (b) Dual synchronization channels; coded sync word (c) Built-in noise diode sensitivity calibration
Antenna	Triple, co-centered, orthogonal loops	Triple, co-centered, orthogonal loops
Thermal Control	Exterior thermal blanket; Optical solar reflectors plus phase change (wax) heat sink	Thermal paint on housing; internal insulation; phase change (wax) heat sink
Power	Battery	Battery

8.0 SCIENCE - PRINCIPAL INVESTIGATOR

The efforts of the science team were focused on keeping the evolution of the experiment hardware consistent with the objective of deriving the most scientific information from the experiment when performed on the moon. Inevitably the necessity of compromise arises as the factors of manned space flight come to bear on the hardware in addition to the requirements imposed by science. The science team consisted of a mix of scientists and engineers who worked to keep requirements current and consistent and to develop the rationale necessary to the choice from among the alternatives of compromise.

8.1 THEORY

The theoretical treatment of a dipole antenna lying on the interface between two dielectric media, one of which may or may not be further stratified as applied to our experiment is very complex. Ordinary radiation and propagation theory is neither accustomed to treatment of the boundary conditions arising out of the experiment configuration or to the detailed treatment of electromagnetic wave components in the near and intermediate zones. Yet, experimental data is to be taken beginning and hopefully ending within the space occupied by the transmitting dipole itself. Therefore in a given traverse the receiver would pass from the near through the intermediate into the far zones of the dipole with the

receiving pickup loops a finite distance (probably not an insignificant fraction of the shortest wavelength) above the interface.

Because of the difficult nature of the problem several different approaches to its solution were believed desirable and hence were undertaken.

8.2 RELATED EXPERIMENTAL DATA

It was also necessary to assay related experimental data such as that obtained on glaciers and the dielectric properties of samples returned from the moon to make sure that transmitter power, for example, would be adequate for the experiment but not excessive which would increase experiment weight. A significant amount of the science team effort was in the planning, execution, and analysis of experimental tests carried out on glacier field trips. Experience with these tests indicated the need of a field evaluation model of the experiment hardware in the electrical configuration of the flight model but specially adapted to meet the requirements of field testing on glaciers.

8.3 TECHNICAL MEMORANDA

Selected technical memoranda written during this phase of the program are included in full text in Appendix 8.1 attached to principal copies of this report.

9.0 A Brief Summary of Task Evolution of the SEP Study Contract NAS 9-10748

May 7, 1970 $49,989

Phase I

Tasks:

P.I. - Provide SEP performance specs.

- Provide SEP preliminary operational criteria & procedures
- Determine SEP additional studies & spec. Equip.
- Determine SEP format and processing of the returned data and expected analysis effort.

Tasks:

Instr. Contractor:

- Provide conceptual design for SEP equipment including weight, volume and power requirements.
- Provide integration requirements for spacecraft and handling
- Provide Schedules and Cost Estimates for SEP equipment
- Provide SEP technical specs.
- Provide SEP design feasibility plan

Amend 1 S extended to February 6, 1971 and added $300,000

Tasks: - Preliminary design analysis

- Preliminary design layout

- Functional verification of design analysis and layout in elec., thermal, structural, human factors, and conceptual feasibility.
- Preparation of preliminary R & QC Plan and Procedures for Qual. Tests.
- Determine requirements for GSE and Generate Preliminary Design
- Preliminary analysis and define SEP interface to spacecraft and Rover
- Conduct FMEA of SEP Equipment
- " design analysis of final engr. layout for SEP equipment

Amend 4 S added $98,000

Tasks: Design & analysis of data format and tape recorder interface

- Design and analysis of transmitter antenna config. and interface with range determination technique
- Design and analysis of the receiver antenna and interface with Rover
- A third field evaluation (New Zealand cancelled)

Amend 6 C added $87,000

Overrun costs with no change in tasks

Total $534,989

Amend 8 C extended period to April 30, 1971

GLACIER TRIPS

No. 1 Athabasca - August & September 1970

No. 2 Athabasca - November- December 1970

New Zealand - Jan-Feb. 1971
(Authorized, but cancelled by M.I.T.)

10.0 CONCLUSION

In summary, the work accomplished under the Study Contract put M.I.T. in a position to proceed with confidence with the fabrication of flight hardware. A conceptual design was evolved, mechanical and thermal configuration studies were carried out, field tests were conducted, radio noise environment was studied, theoretical studies were initiated, and key problem areas were identified. With this experience M.I.T. was able to more accurately define for prospective bidders, performance criteria for the experiment equipment, and to evaluate critically the responses to the request for proposals.

Key problems that emerged from this study include:

(1) Efficient transmitter antenna design for multiple frequency operation/with constraints on length and weight while deployed directly on the lunar surface.

(2) Tri-loop receiver antenna design with emphasis on symmetry of pattern and loop-to-loop isolation.

(3) The increase of transmitter radiated power within weight and prime power constraints.

(4) The achievement of wide dynamic range in the receiver.

(5) The design of an effective interface with the Data Storage Electronics Assembly (DSEA) for purposes of recording and returning to Earth all experiment data.

(6) The development of a thermal control system for both the transmitter and the receiver that keeps the equipment within the design limits under a variety of lunar

environmental conditions.

(7) The derivation from theoretical studies of a mathematical formalism simple enough to permit solution yet representing the physical situation adequately for correlation with field results.

(8) The design of field tests on Earth to provide critical evaluation of engineering approaches, data for comparison with theory, and data to aid in the interpretation of that returned from the moon.

The resolution of these problems make up a major share of the effort necessary to conduct the experiment on the moon along with the resolution of the problems that inevitably arise in connection with the design, development, and manufacture of man-rated space hardware.

APPENDIX 2.1

SURFACE ELECTRICAL PROPERTIES EXPERIMENT

CONCEPTUAL DESIGN

Massachusetts Institute of Technology

Center for Space Research

SURFACE
ELECTRICAL PROPERTIES
EXPERIMENT

CONCEPTUAL DESIGN

CSR TR 70-7

Principal Investigator: Gene Simmons

Principal Administrator: John V. Harrington

October 28, 1970

TABLE OF CONTENTS

Table of Contents continued

SECTION I - ADMINISTRATIVE/BIOGRAPHICAL

I-1. APPLICANT INSTITUTION

Massachusetts Institute of Technology
77 Massachusetts Avenue
Cambridge, Massachusetts 02139

Telephone: (617) 864-6900

Principal Administrator Responsible for Experiment:

John V. Harrington

Title: Director, Center for Space Research

Telephone: (617) 864-6900 ext. 7501

I-2. PRINCIPAL INVESTIGATOR

Name:

Gene Simmons

Title:

Professor of Geophysics

Mailing Address:

Massachusetts Institute of Technology
54-314
Cambridge, Massachusetts 02139

Telephone:

(617) 864-6900 ext. 6393

Biographical Sketch:

The principal investigator has received a B.S. in electrical engineering, an M.S. in geology, and a Ph.D. in geophysics. He is a co-investigator on the Lunar Heat Flow Experiment, a part of ALSEP, and has served on various committees for NASA. He has experience in collecting and interpreting geophysical field data as well as laboratory data. Dr. Simmons is currently on leave of absence from MIT and is serving as Chief Scientist, NASA Manned Spacecraft Center, Houston.

"Page missing from available version"

I-2 — I-3

I-5. Principal Investigator's Role in Relation to this Experiment

This experiment is expected to be truly a team effort. Accordingly, the principal investigator will participate in all of the phases--equipment design and manufacture, preparation of analog models for data reduction, collection of data on the lunar surface, reduction of data, and finally, the interpretation of data. It is anticipated that each of the other team members will carry their share of the work on this experiment; their responsibilities are detailed below in Section I-6. Although the principal investigator will be responsible for both the engineering and the scientific aspects of this experiment, most of the actual engineering work will be done by the engineers, or contractors working for them, at the MIT Center for Space Research. The scientific aspects of the work will be done by the principal investigator and by David Strangway, Tony England, and their associates.

The principal investigator expects to spend an average of 10 percent of his working time on this experiment in the early phases. During the execution of the experiment on the moon and the early data reduction, full time will be devoted. Finally, in the interpretation phases, about half-time will be spent on this experiment. It should be possible to phase the periods of heavy load with those of other work that are currently expected to be in progress during the next few years,

namely the continuation of the lunar samples program and the lunar surface heat flow experiment.

I-6. Responsibilities of other key personnel

Dr. David W. Strangway, a co-investigator, is an associate professor of Physics at the University of Toronto, and will become Chief of the Geophysics Branch of the MSC in the fall of 1970. He will assist in the general design of the experiment, and will supervise analog scale-model studies, field experiments to test prototype apparatus, and data interpretation. He will devote an average of 20 percent of his time to this project.

Anthony W. England, an astronaut at MSC, also is a co-investigator. He will assist with the field tests of the engineering models and will help with the design of the experiment. He will be particularly valuable in coordinating the interfaces of the experiment with MSC and with the astronaut office. He will participate in the interpretation of the data from the moon. It is expected that he will devote from 5 to 10 percent of his time to this experiment.

Dr. John V. Harrington, Director, MIT Center for Space Research, will be responsible for administration of those portions of the program concerned with implementation of this lunar surface experiment, and will devote 5 percent of his time to this project.

Richard H. Baker, Head, Laboratory for Space Experiments within the Center for Space Research, will spend 25 percent of his time on administrative functions and technical considerations involved in the design and fabrication of the lunar surface properties experiment.

Lawrence H. Bannister, Staff Member, Center for Space Research, will be Project Leader for the Experiment Design, and will devote 50 percent of his time to this project. He and Mr. Baker will lead the engineering group that designs, constructs, and tests various models through the engineering hardware stage.

Dr. Ajit K. Sinha, a postdoctoral fellow at the University of Toronto, is computing theoretical mastercharts to demonstrate the effects of various physical parameters expected on the moon. These will be used with scale-model and field results to develop methods of interpreting lunar data. He will devote 100 percent of his time to this project.

Raymond D. Watts is completing his Ph.D. requirements at the University of Toronto and will be a research associate at the Lunar Science Institute in the fall of 1970. He will develop computerized techniques to interpret the data returned from the moon. He will devote 50 percent of his time to this project.

Gerald A. LaTorraca is a graduate student at MIT. He will work closely with the CSR in developing engineering models

and will assist in testing these models in the field. He will devote 75 percent of his time to the project.

James R. Rossiter is a graduate student at the University of Toronto and will be a graduate fellow of the Lunar Science Institute in the fall of 1970. He is conducting analog scale-model studies and will assist in field tests of apparatus and in data interpretation. He will devote 75 percent of his time to this project.

The Charles Stark Draper Laboratory of MIT will be Principal Contractor responsible for detailed design and fabrication of qualified flight hardware. John V. McKenna, of the Draper Laboratory, will be Program Manager and will devote 100% of his time to this project.

SECTION II - TECHNICAL INFORMATION

II-1. OBJECTIVES

The chief objectives of this experiment are to determine layering in the lunar subsurface, and to search for the presence of water at depth. In addition, the electrical properties of the lunar material will be measured in situ. Under favorable conditions, it may be possible to obtain an independent estimate of the lunar thermal flux and an indication of the number and size of subsurface scattering bodies.

II-2. SIGNIFICANCE

It is difficult to overstate the significance of a clear demonstration of the presence or absence of water in the lunar interior. Many of the surface features have been attributed to past erosion by water or ice. Igneous processes, as we know them on earth, depend on the presence of water to reduce the melting points of silicates. But the absence of water in the moon would demonstrate that igneous processes do not operate on the moon in an analogous fashion to those on the earth. This would imply greatly different thermal models for the two bodies. Thus the search for water in the lunar interior is scientifically very important.

Examination of the samples returned on Apollo 11 and Apollo 12 indicated an unusual absence of water. Few hydrous minerals were found. The assemblage of iron-troilite-ilmenite suggests a very low partial pressure of H_2O during formation of the rocks which are now residing on the surface. This finding is in agreement with radar measurements made from Earth and from Lunar Orbiters, which indicate a very low electrical conductivity of the material at the surface of the moon. Therefore, the amount of water, either free or bound in crystal lattices, at the surface of the moon is known to be extremely low. However,

the available data leave completely unanswered the critical question of whether or not water exists at depth in the moon.

It is the purpose of this experiment to measure the electrical properties of the lunar subsurface as a function of depth. Since the presence of even minute amounts of water in rocks changes the electrical conductivity by several orders of magnitude, any moisture present would be easily detected by this experiment. Thus upper bounds can be set on the amount of water in the lunar subsurface to depths of a few Kilometers.

The frequency range of the experiment has been selected to allow determination of layering over a range of depths from a few meters to a few Kilometers. Accordingly it may be possible to determine the thickness of the outer layer, commonly referred to as the regolith or the 'gardened layer', in the vicinity of the landing site. Such layering could be detected by the expected change in dielectric properties and conductivity. This subsurface topographic information holds considerable implications for the history of the outer few Kilometers of the moon.

Moreover, the presence of water in the moon would allow a determination of the amount of heat flowing from the interior of the moon to the surface. The electrical properties experiment, under favorable conditions, could provide a determination of the depth at which any moisture

present changed from the solid to liquid form. Thus the approximate depth to the zero-degree isotherm could be found. This depth, together with the knowledge of thermal conductivity estimated from lunar samples, could give an estimate of the lunar thermal flux. This, in turn, would provide important clues to the nature of the moon's core.

Recent seismic experiments have indicated that a large amount of scattering material may be present in the lunar subsurface. Since electromagnetic propagation in this experiment will be sensitive to these scattering bodies, and since a number of different wavelengths are being used, a measure of the size and number of scattering bodies also might be possible. This would give additional valuable information on the nature of the outer few Kilometers of the moon.

Therefore, the experiment will provide a wealth of information on the properties of the lunar subsurface. It is a valuable experiment which will help to determine the lunar history better than previously possible, and which relates to, and complements, other scientific studies of the moon already in progress.

II-3. DISCIPLINARY RELATIONSHIP

a. Brief history of related work.

Most geological environments on earth are too conductive due to the presence of moisture, to allow penetration of high frequency electromagnetic radiation. Therefore, radio frequency interferometry has had little development as a geophysical tool. However, the idea is not new. It was suggested by Stern (reported by Evans, 1963) as early as 1927, but was not developed as a field technique. Although the interpretation of his field results is open to some question, El-Said (1956) attempted to use the method to determine the depth to the water table in the Sahara Desert.

For this technique of sounding to be effective, the medium being probed must have low electromagnetic losses. Ice provides one of the few earth environments which meets this condition. It is highly resistive (Evans, 1965) and the bottom offers a good contrast. For this reason, radar pulses have recently been used to sound large ice sheets and glaciers (Evans, 1963; Rinker et al, 1964; Bailey et al, 1964; Walford, 1964; Jiracek, 1967), and glaciers have provided suitable sites to test the interferometry technique. (Annan, 1970).

There are many indications that the lunar surface is also very resistive. Radar measurements have indicated that lunar surface material has electrical properties similar to

those of dry, powdered, terrestrial rocks and is, therefore, transparent to radio waves (England et al, 1968; Campbell and Ulrichs, 1969; Strangway, 1969; St. Amant and Strangway, 1970). Initial experiments on lunar samples indicate that the dielectric constant and loss tangent of lunar rocks are, in fact, similar to those of dried terrestrial rocks (Chung et al, 1970; Gold et al, 1970).

b. State of present development in the field.

The present state of development of the experiment is based largely on the research conducted by the group of investigators who are submitting the proposal, and their co-workers. This research falls into four main areas:

(i) electrical properties of both terrestrial and lunar rocks;

(ii) theoretical solutions of the various field components associated with magnetic and electric dipoles above a dielectric layer, including computed results;

(iii) scale model studies of a dipole over a dielectric layer; and

(iv) field results using prototype apparatus on glaciers.

The state of development of each of these areas will be summarized here.

(i) Electrical properties of rocks

Several workers have now completed initial studies of the electrical properties of the returned lunar samples.

The results of these studies, summarized in Table II-1, indicate that the electric properties of lunar rocks are not much different from those of dried terrestrial rocks. The losses for a variety of dried terrestrial rocks in a vacuum are very low; the loss tangent, tan δ, typically is less than 0.01 at 1 Megahertz. The dielectric constant K, depends largely on the density and ranges from about 3 for the powders, up to about 10 for the solid rocks.

Gold et al (1970) measured the attenuation distance of some Apollo 11 fines to be about 10 wavelengths at 450 MHz., which is in agreement with many previous radar studies. This gives a loss tangent of about 0.02; the dielectric constant of these fines was about 2.4. Work on various solid samples from Apollo 11 has been completed by Chung et al (1970). Their lunar breccia has a dielectric constant between 15 and 20 for the frequency range around 1 MHz., and the igneous sample has a K between 11 and 14. At 25°C. these samples show a loss tangent of about 0.05 and 0.16 respectively. These losses are somewhat higher than those of the terrestrial rocks, possibly due to residual moisture in the sample. This is partly confirmed by work done on Apollo 12 sample 12002 (Chung, 1970) under very dry conditions, for which k = 10, and tan δ = 0.055, at 1 MHz. at 25°C.

Table II - 1 Summary of Dielectric Properties of Terrestrial and Lunar Rocks

Material	Bulk Density (gm/cc)	High Frequency Dielectric Constant K_∞	Loss Tangent tan δ	D.C. Conductivity (mhos/m.)
Powders (St. Amant and Strangway, 1970)			at 1 MHz., 27°C	27°C
Plagioclase	1.54	3.3	0.003	1×10^{-15}
Augite	1.66	4.4	0.03	-
Hypersthene	1.67	3.1	0.001	-
Basalt (1)	1.46	3.1	0.01	1×10^{-13}-6×10^{-12}
Basalt (2)	1.42	3.2	0.01	6×10^{-15}-7×10^{-17}
Granite	1.44	2.9	0.003	5×10^{-16}
Dunite	1.83	3.4	0.003	1×10^{-16}
Solids				
Basalt (2)	2.95	10.1	0.03	3×10^{-10}
Granite	2.71	6.4	0.01	6×10^{-13}
Dunite	3.32	8.2	0.003	1×10^{-15}
Lunar Powder (Gold et al, 1970)				
Apollo 11 fines	1.57	2.4 at 450 MHz.	0.02 at 450 MHz.	-
Lunar Samples (Chung et al, 1970)				
10020 (igneous)	3.18	10 - 15	0.09 - 0.2	10^{-7} - 10^{-9}
10057 (igneous)	2.88	9 - 13	0.09 - 0.2	10^{-7} - 10^{-9}
10046 (breccia)	2.21	6 - 9	0.05 - 0.09	10^{-8} - 10^{-9}
12002 Unpublished data		10	0.055	

The lunar samples of Chung et al have losses which show a fairly strong increase with temperature. This effect also is seen at lower frequencies in terrestrial rocks.

Some work has been done on the magnetic losses of the lunar samples using pulses (Olhoeft and Strangway, 1970). There appears to be some magnetic induction effects, but these are not likely to be pronounced at frequencies around 1 MHz.

A summary of the attenuation distance of electromagnetic waves, estimated from various lunar measurements, is shown in Figure II-1.

It is concluded from these studies that the electromagnetic losses to be expected on the moon may be greater than those for very dry terrestrial rocks, but are still very low. Typical penetration depths are in the range of Kilometers for frequencies around 1 MHz.

(ii) Theoretical solutions

Several theoretical results of interest have been derived by the group of investigators and their co-workers. The easiest solutions are for the configuration of a vertical magnetic dipole, over a dielectric layer, over a horizontal reflector, as shown in Figure II-2. The field component of interest is $E\phi$, the electric field measured tangential to an imaginary cylinder which encloses the dipole and has the same axis. These results are covered by Annan (1970). Suites

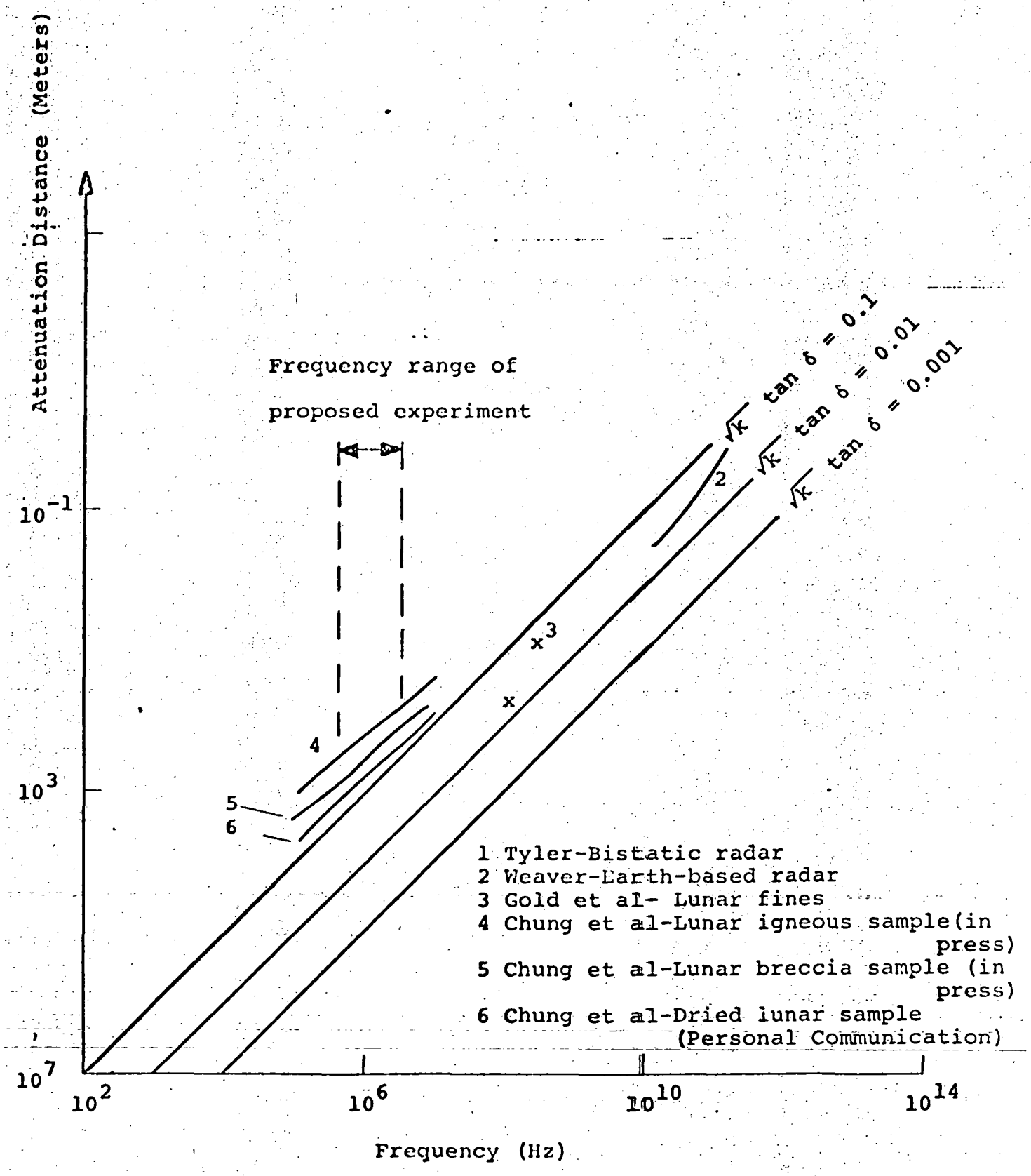

Figure II-1: ATTENUATION DISTANCE DEDUCED FROM VARIOUS LUNAR MEASUREMENTS.

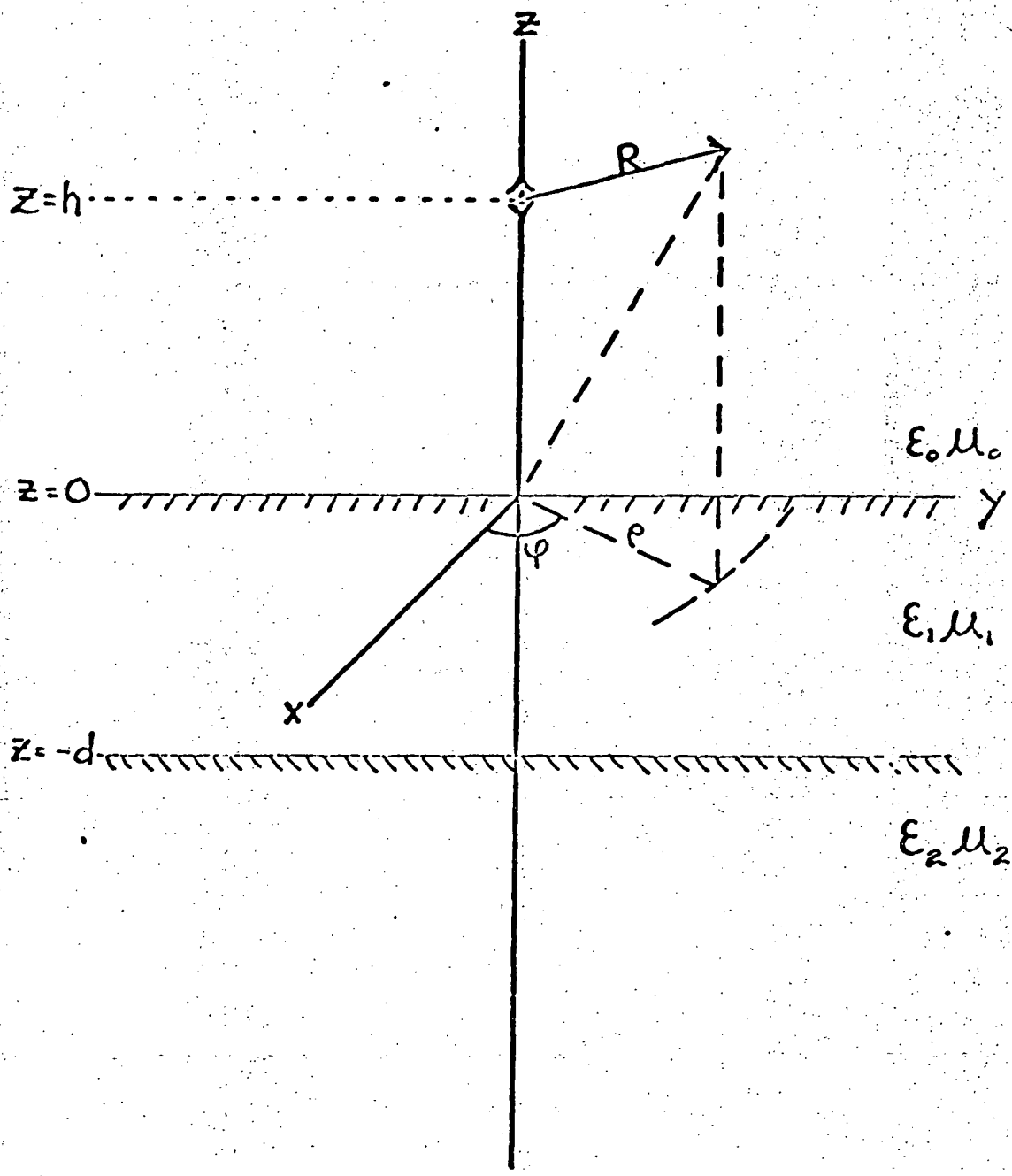

Figure II-2 VERTICAL MAGNETIC DIPOLE OVER A TWO LAYER EARTH

of curves have been computed, and samples of these are shown in Figures II-3 to II-5. These curves show how sensitive the technique is to the depth of the reflector, d, the dielectric constant, K, and the loss tangent, tan δ.

Solutions for a horizontal electric dipole over a dielectric layer, which is the system we propose to use, are more complex. To illustrate the components of interest, Figure II-6 shows the orientation. Results have been computed for the vertical magnetic field, Hz, and the radial magnetic component, $H\rho$. The Hz component should be simply related to the tangential electric field of the vertical magnetic dipole, $E\phi$, and this has been verified in the field. $H\phi$, the tangential magnetic field, theoretically should equal zero for a homogeneous layer over a horizontal reflector. Since in the field it has been found that this component does not always vanish, it can be used as a measure of inhomogeneity and scattering. A typical suite of curves for $H\rho$ is shown in Figure II-7.

(iii) Scale-model experiment

The theoretical results have been backed up by scale-model studies. Using a vertical magnetic dipole over a layer of sand covering an aluminum reflecting sheet, Annan got good agreement with the theory. Typical model results are shown in Figure II-8 along with their theoretical counterparts in Figure II-9. Although the agreement is not perfect, most of

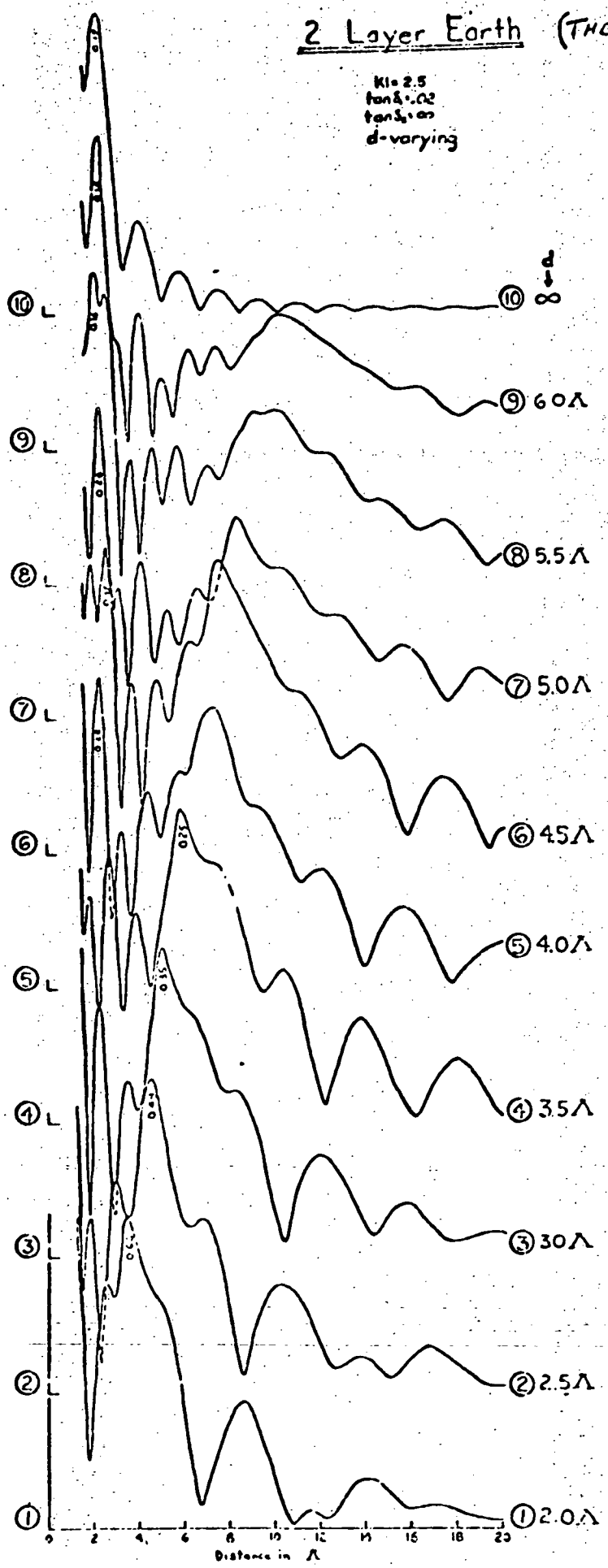
2 Layer Earth (THEORETICAL)
K1= 2.5
tan δ1 = .02
tan δ2 = ∞
d-varying
d
⑩ ∞
⑨ 6.0Λ
⑧ 5.5Λ
⑦ 5.0Λ
⑥ 4.5Λ
⑤ 4.0Λ
④ 3.5Λ
③ 3.0Λ
② 2.5Λ
① 2.0Λ
0 2 4 6 8 10 12 14 16 18 20
Distance in Λ

Figure II-3

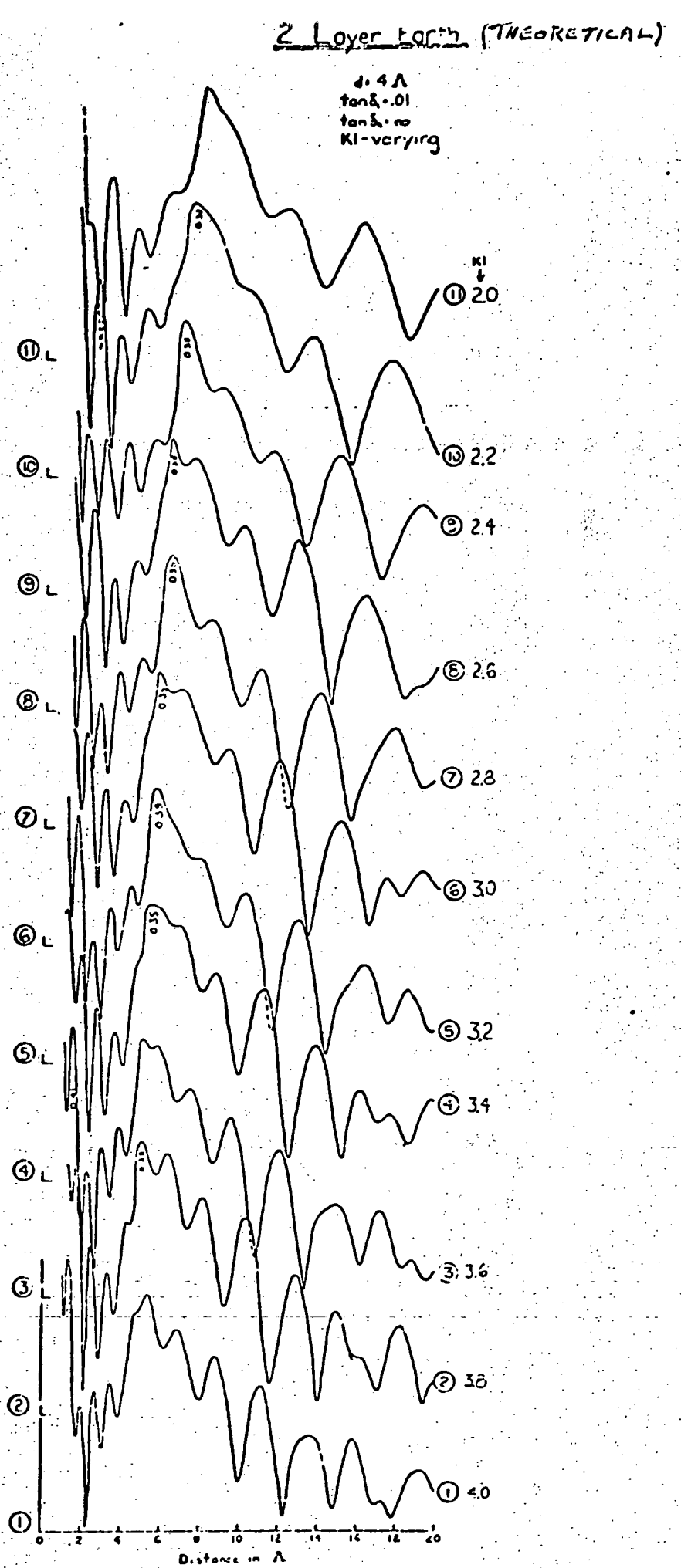
2 Layer Earth (THEORETICAL)
d = 4 λ
tanδ = .01
tanδ = ∞
K1 - varying
K1
⑪ 2.0
⑩ 2.2
⑨ 2.4
⑧ 2.6
⑦ 2.8
⑥ 3.0
⑤ 3.2
④ 3.4
③ 3.6
② 3.8
① 4.0
⑪L
⑩L
⑨L
⑧L
⑦L
⑥L
⑤L
④L
③L
②L
①
0 .2 4 6 8 10 12 14 16 18 20
Distance in λ

Figure II-4

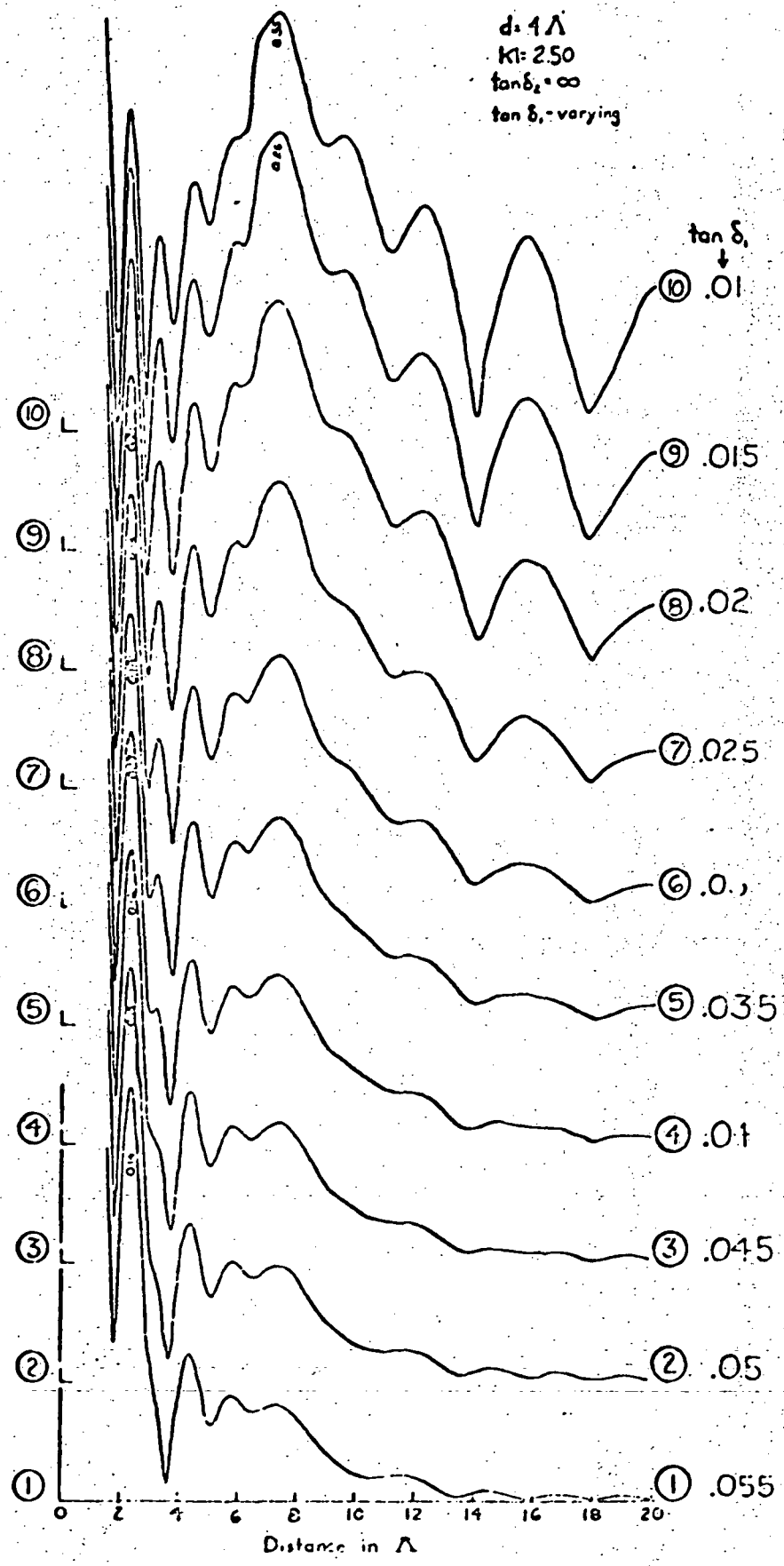
2 Layer Earth (THEORETICAL)
d = 1 Λ
K1 = 2.50
tan δ2 = ∞
tan δ1 = varying
tan δ1
⑩ .01
⑨ .015
⑧ .02
⑦ .025
⑥ .0.,
⑤ .035
④ .01
③ .045
② .05
① .055
0
2
4
6
8
10
12
14
16
18
20
Distance in Λ

Figure II-5

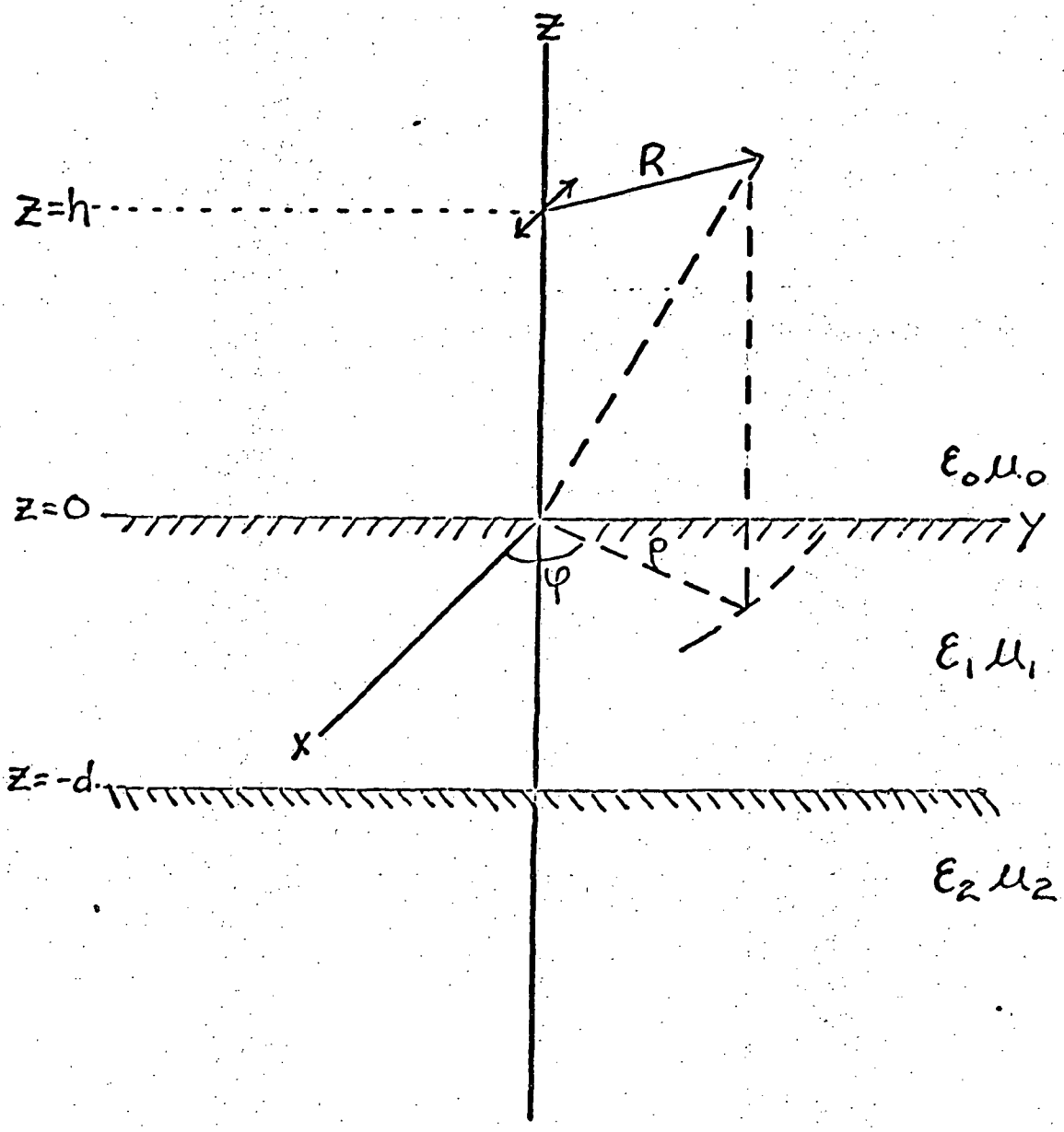

Figure II-6 HORIZONTAL ELECTRIC DIPOLE OVER A TWO LAYER EARTH

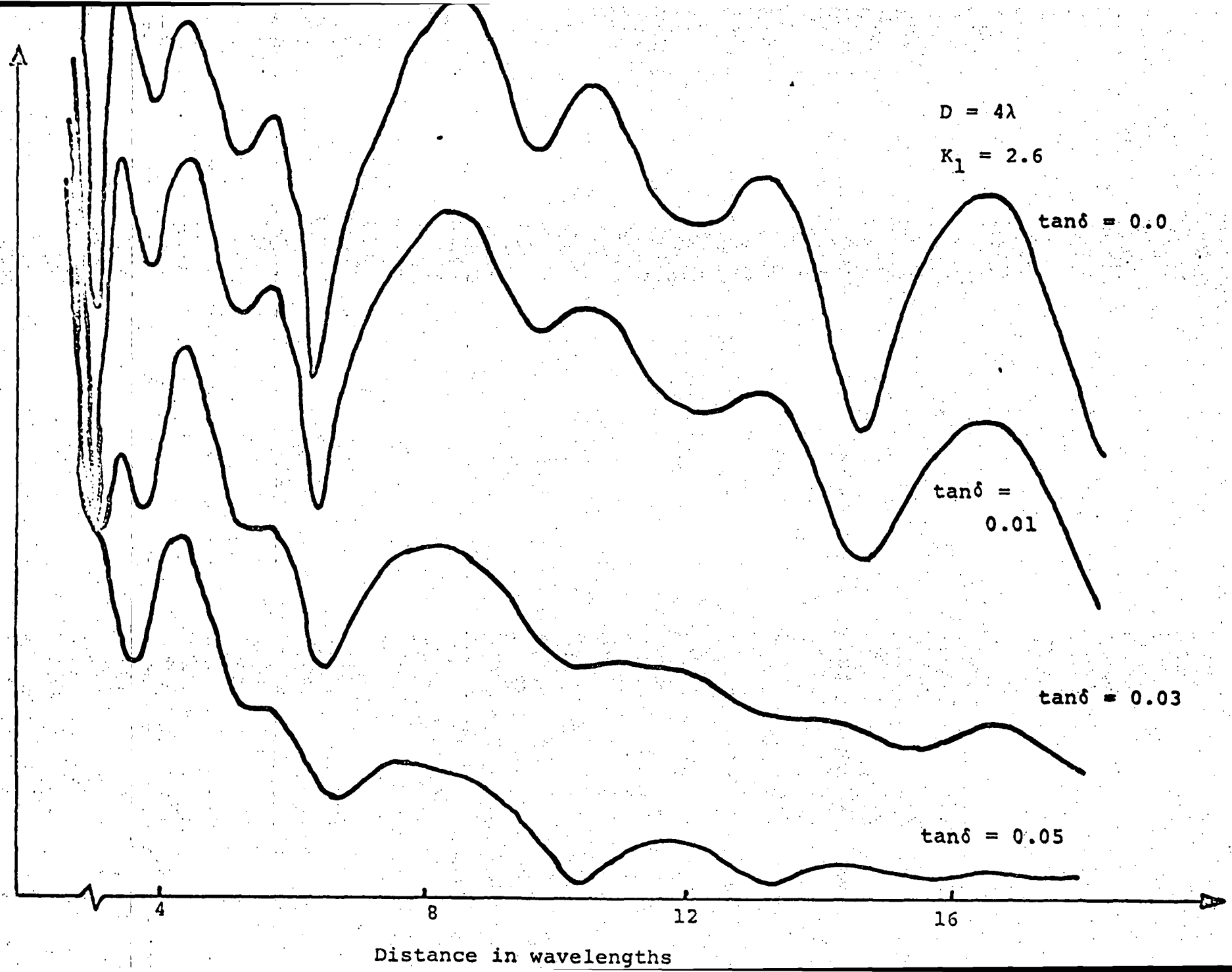

Figure II-7 THEORETICAL COMPUTATIONS, Hρ

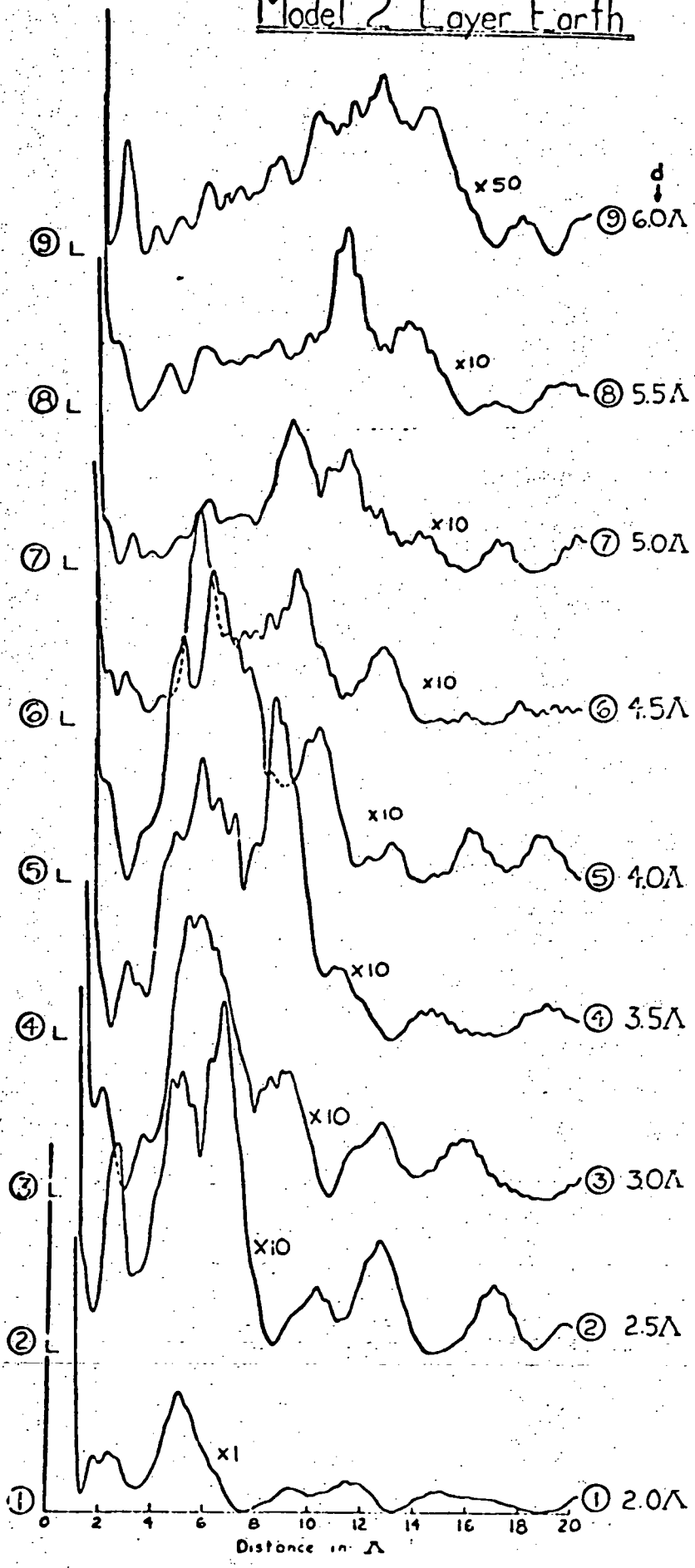
Model 2 Layer Earth
d
⑨ L
x50
⑨ 6.0Λ
⑧ L
x10
⑧ 5.5Λ
⑦ L
x10
⑦ 5.0Λ
⑥ L
x10
⑥ 4.5Λ
⑤ L
x10
⑤ 4.0Λ
④ L
x10
④ 3.5Λ
③ L
x10
③ 3.0Λ
② L
x10
② 2.5Λ
① L
x1
① 2.0Λ
0 2 4 6 8 10 12 14 16 18 20
Distance in Λ

Figure II-8

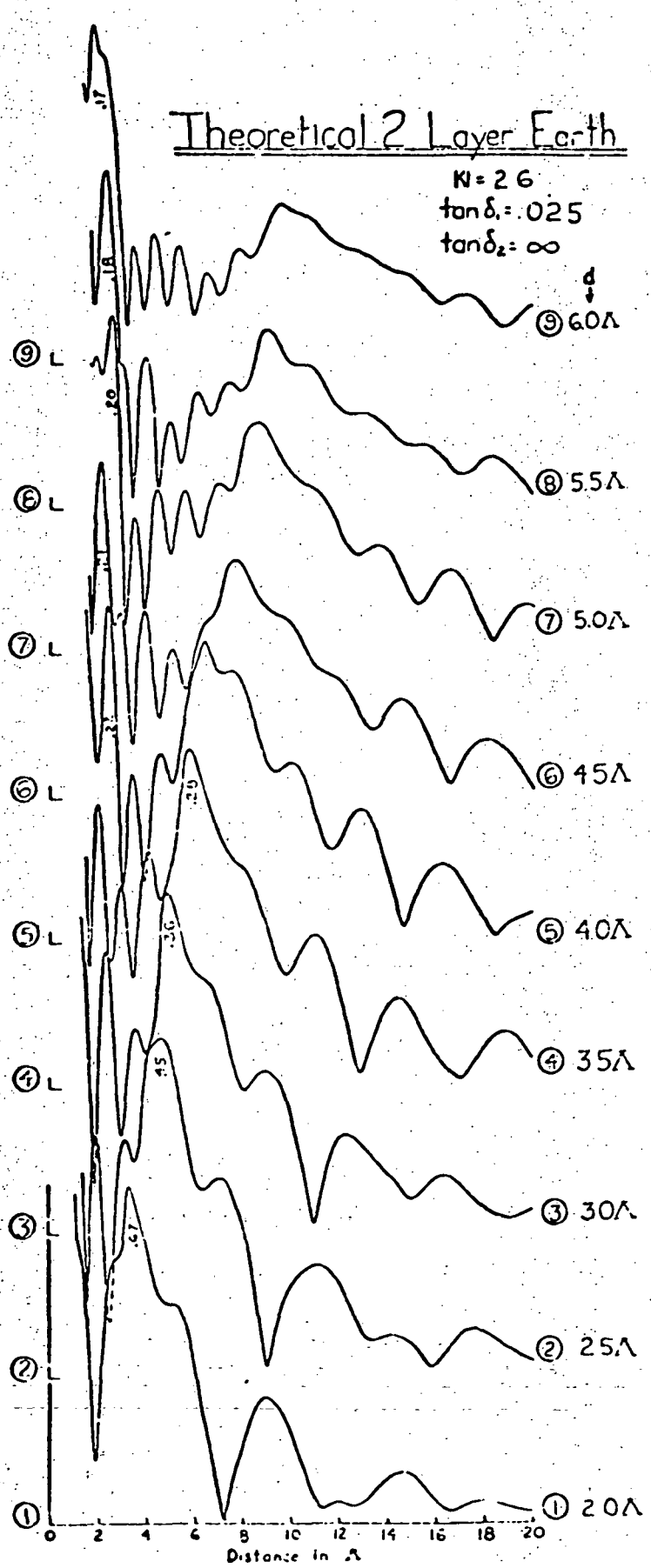
Theoretical 2 Layer Earth
K = 2 6
tan δ₁ = .025
tan δ₂ = ∞
d
⑨ 6.0Λ
⑧ 5.5Λ
⑦ 5.0Λ
⑥ 45Λ
⑤ 4.0Λ
④ 35Λ
③ 30Λ
② 25Λ
① 20Λ
⑨ L
⑧ L
⑦ L
⑥ L
⑤ L
④ L
③ L
② L
① L
.17
.18
.20
.31
.32
.29
.36
.45
.67
0 2 4 6 8 10 12 14 16 18 20
Distance in Λ

Figure II-9

the discrepancies can be explained by the limitations of the experimental model. Work is now in progress to construct a more sophisticated model, which will hopefully overcome most of the observed difficulties and will have the capability of modeling a larger variety of cases.

(iv) Glacier tests

The ultimate test of a new method is in the field. In order to evaluate the interferometry technique, two major field tests have been conducted. The first, over the 450 meter deep Gorner Glacier, gave conclusive proof that the method is able to determine the electrical properties of a dielectric medium in situ. This is shown by Figure II-10, where it can be seen that the dielectric constant of ice is about 3.2 as expected.

Using an engineering breadboard of the transmitter described in the hardware section of this proposal, a series of field trials were made on the shallower, 150 meter deep, Athabasca Glacier. Although a complete interpretation of the results is not yet available, the experiment indicated that the technique will give the depth to a reflector in a geological environment which has low electromagnetic losses. The transmitter performed flawlessly and the proposed multiple-frequency antenna was easily tunable for each frequency used. The data gave reasonable agreement with the theoretical results produced so far, in spite of their

Comparison of Theoretical and Experimental Profiles

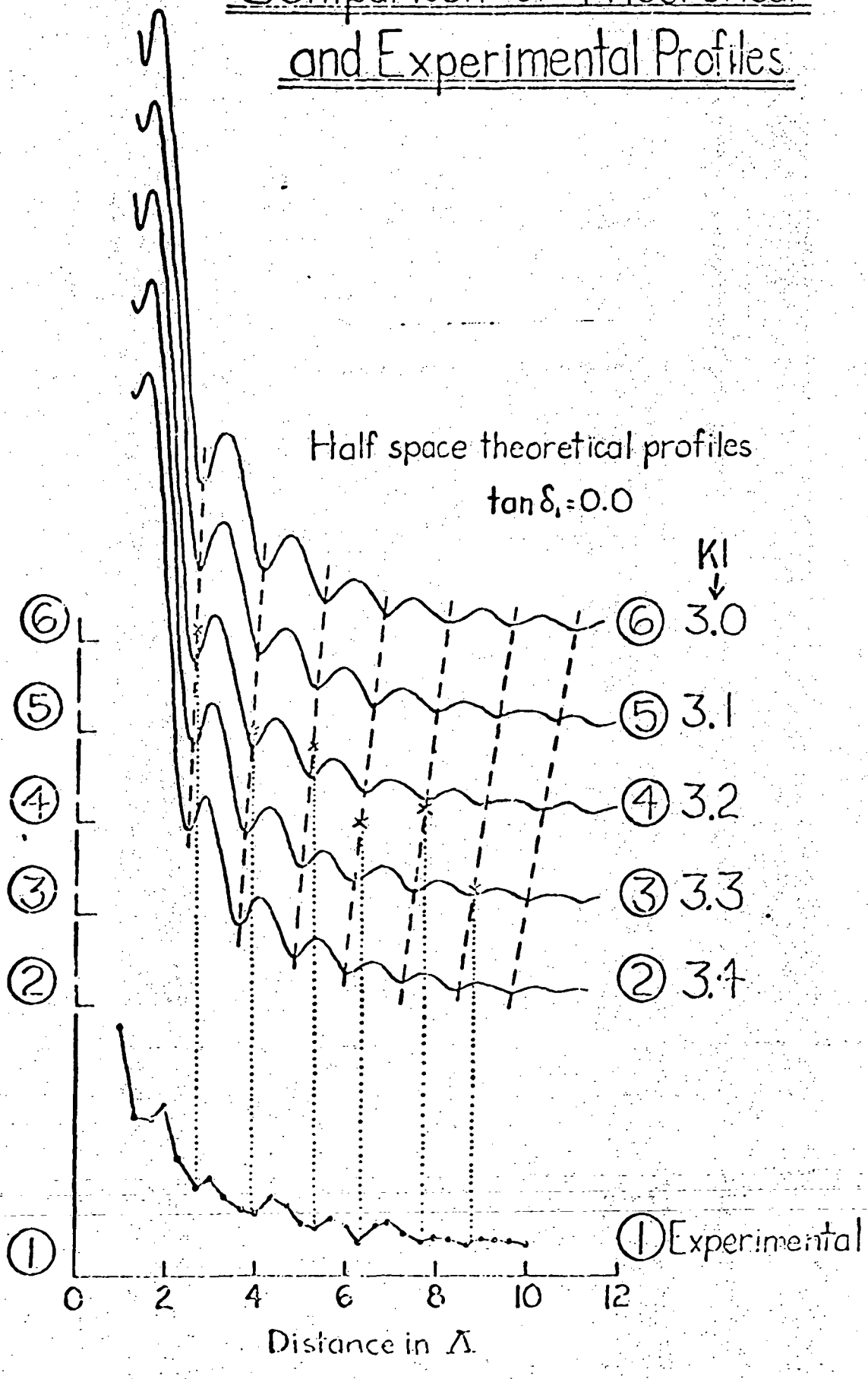

Figure II-10

inherent limitations. A few typical comparisons are shown in Figures II-11 to II-14.

(v) Summary of present developments

Studies of the electrical properties of lunar material indicate that the electromagnetic losses are adequately small in the chosen frequency range. The interferometry technique has been studied theoretically with scale models and in the field. Although work is continuing, the present results agree sufficiently well to show that the technique will give in situ electric properties and the depth to a subsurface reflector.

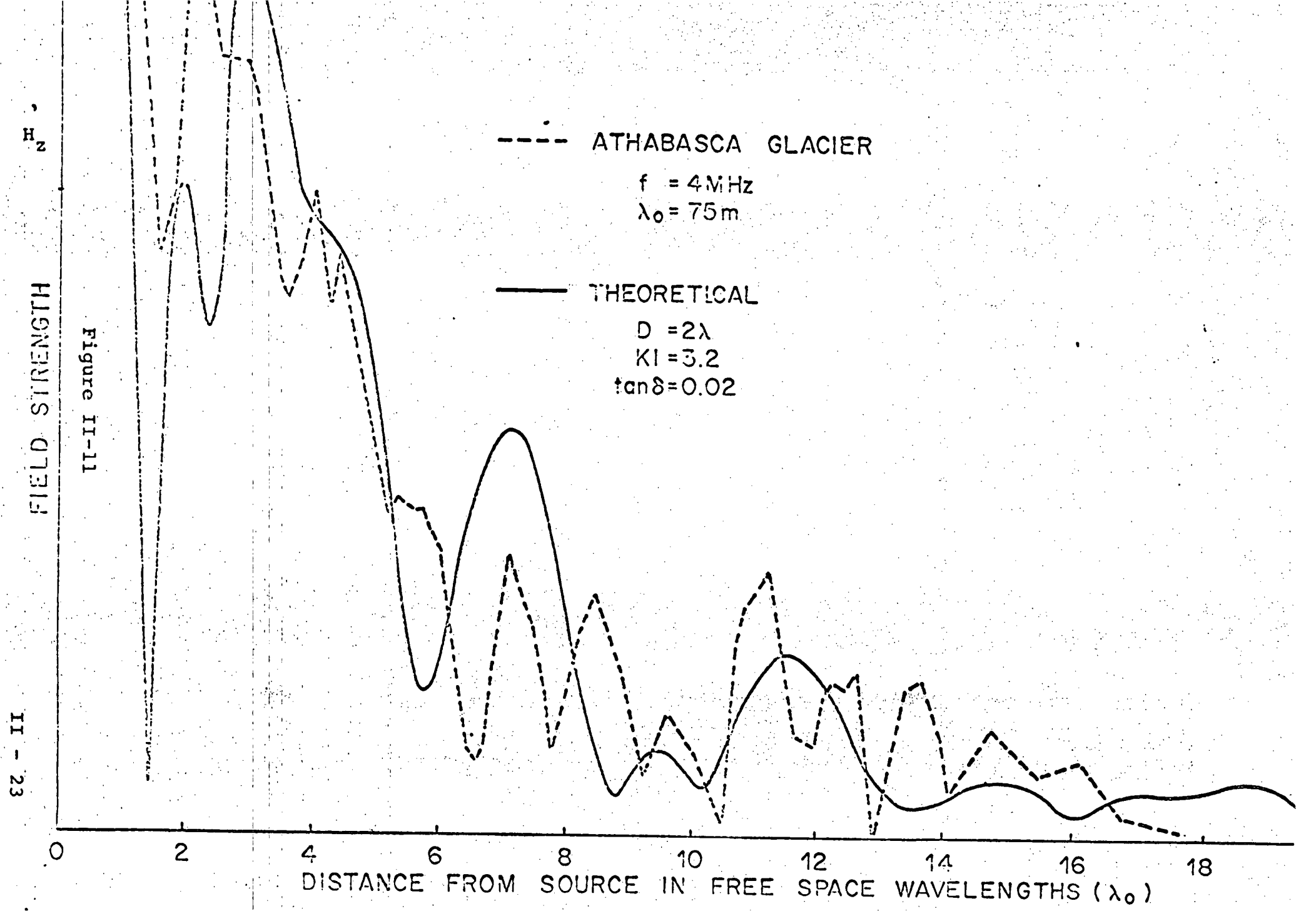
FIELD STRENGTH H_z
ATHABASCA GLACIER
f = 4 MHz
λ_o = 75 m
THEORETICAL
D = 2λ
KI = 3.2
tanδ = 0.02
0
2
4
6
8
10
12
14
16
18
DISTANCE FROM SOURCE IN FREE SPACE WAVELENGTHS (λ_o)

Figure II-11

ATHABASCA GLACIER
f = 4 MHz
λo = 75 m
THEORETICAL
D = 2λ
KI = 3.2
tanδ = 0.05
FIELD STRENGTH
Ho
DISTANCE FROM SOURCE IN FREE SPACE WAVELENGTHS (λo)
0
2
4
6
8
10
12
14
16
18

Figure II-12

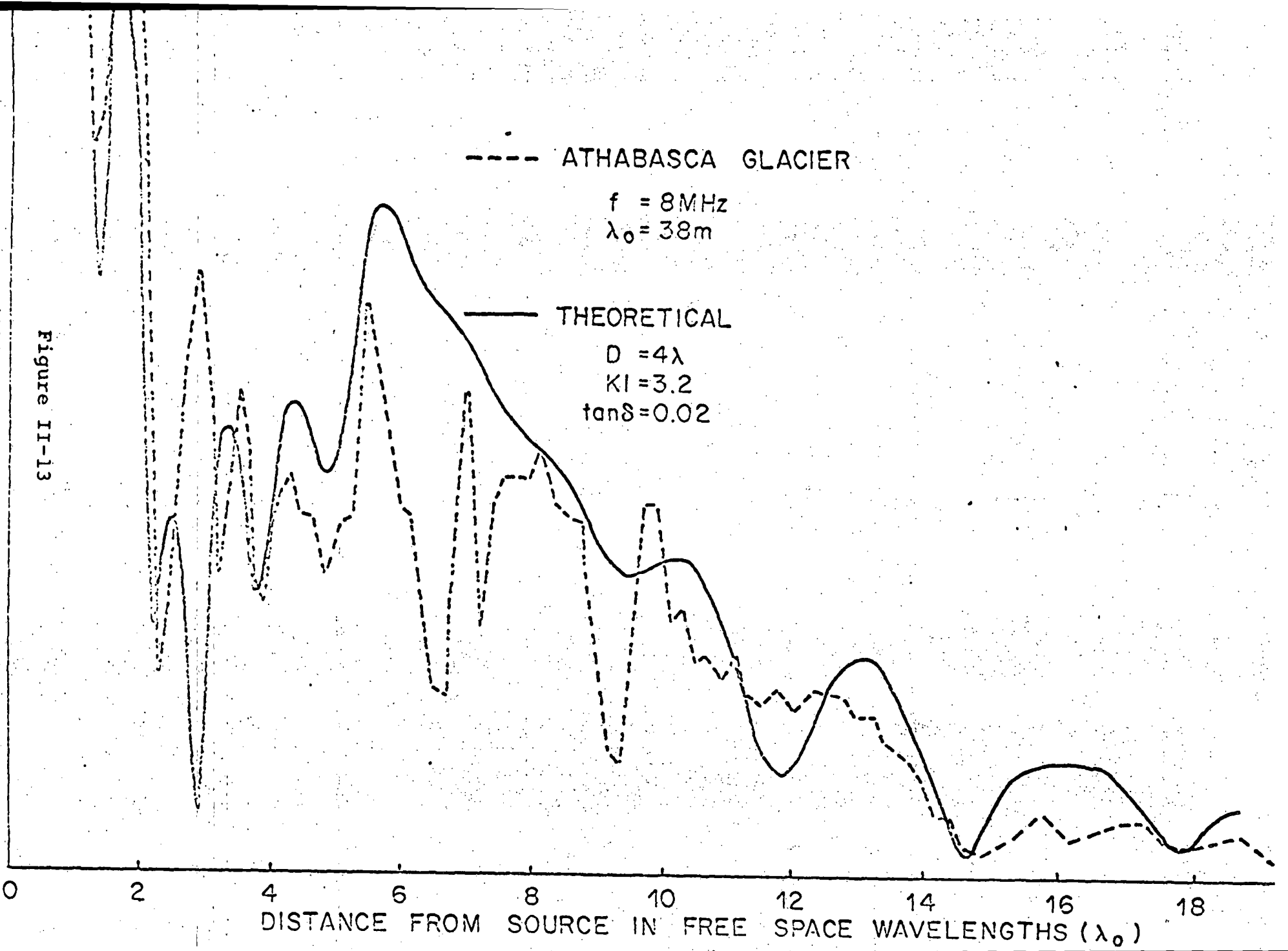
ATHABASCA GLACIER
f = 8MHz
λo = 38m
THEORETICAL
D = 4λ
KI = 3.2
tanδ = 0.02
FIELD STRENGTH
H_N
0
2
4
6
8
10
12
14
16
18
DISTANCE FROM SOURCE IN FREE SPACE WAVELENGTHS (λo)

Figure II-13

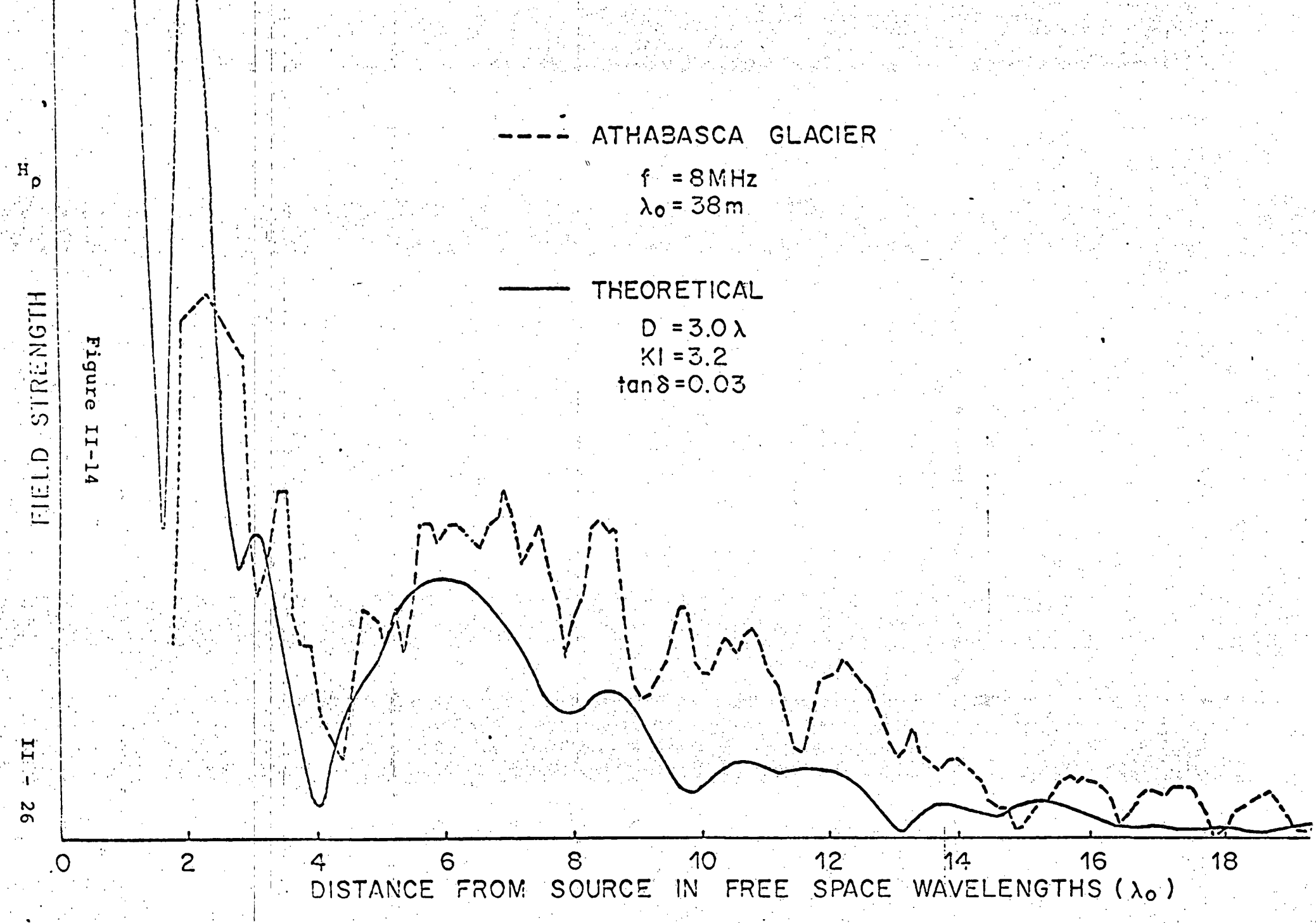

Figure II-14

II - 26

References for Section II-3.

Annan, A.P., "Radio Interferometry Depth Sounding," M.Sc. Thesis, Dept. of Physics, U. of Toronto, 1970.

Bailey, J.Y., Evans, S., and Robin, G. de Q., "Radio Echo Sounding of Polar Ice Sheets," Nature, v. 204, pp. 420-421, 1964.

Campbell, J.J., and Ulrichs, J., "Electrical Properties of Rocks and Their Significance for Lunar Radar Observations," J. Geophys. Res., v. 74, pp. 5876-5881, 1969.

Chung, D.H., Westphal, W.B., and Simmons, Gene, "Dielectric Properties of Apollo 11 Lunar Samples and Their Comparison with Earth Materials," J. Geophys. Res., in press, 1970.

El-Said, M.A.H., "Geophysical Prospection of Underground Water in the Desert by Means of Electromagnetic Interference Fringes," Proc. I.R.E., v. 44, pp. 24-30 & 940, 1956.

England, A.W., Simmons, Gene, and Strangway, D., "Electrical Conductivity of the Moon," J. Geophys. Res., v. 73, pp. 3219-3226. 1968.

Evans, S., "Radio Techniques for the Measurement of Ice Thickness," Polar Record, v. 11, pp. 406-410 & 795, 1963.

Evans, S., "Dielectric Properties of Ice and Snow - A Review," J. Glaciol., v. 5, pp. 773-792, 1965.

Gold, T., Campbell, M.J., and O'Leary, B.T., "Optical and High-Frequency Electrical Properties of the Lunar Sample," Science, v. 167, pp. 707-709, 1970.

Jiracek, G.R., "Radio Sounding of Antarctic Ice," Research Report Number 67-1, Geophysical and Polar Research Center, U. of Wisconsin, 1967.

Rinker, J.N., Evans, S., and Robin, G. de Q., "Radio Ice-Sounding Techniques," Proceedings of the Fourth Symposium on Remote Sensing of Environment, U. of Michigan, 1966.

St. Amant, M., and Strangway, David W., "Dielectric Properties of Dry, Geologic Materials," Geophysics, in press, 1970.

Strangway, D.W., "Moon: Electrical Properties of the Uppermost Layers," Science, v. 165, pp. 1012-1013, 1969.

Walford, M.E.R., "Radio Echo Sounding through an Ice Shelf," Nature, v. 204, pp. 317-319, 1964.

II-4. EXPERIMENT APPROACH

a. Experiment concept

The basic concept of the experiment is very simple. A transmitting antenna is set up on the surface that is to be probed, and a receiver is moved over the surface at some distance from the transmitter. As shown in Figure II-15, there are at least two waves which reach the receiver: a direct wave along the surface and a reflected wave from the subsurface.

In general, these two waves travel different distances at different velocities and therefore interfere with each other. In some cases, the interference is destructive, in others, constructive. The result is a series of peaks and nulls in the received field strength as the separation between the receiver and the transmitter is changed. It is this interference pattern of peaks and nulls which is indicative of the electrical properties of the medium and of the depth to the reflector.

In practice the situation is not quite so simple. There are, in fact, a number of different waves generated. As shown by Figure II-16, there are two spherical waves, A and C, travelling directly between the transmitter and the receiver. Wave C travels in the upper medium and wave A in the earth. Since these two waves have different velocities, they will interfere with each other. It is this interference which

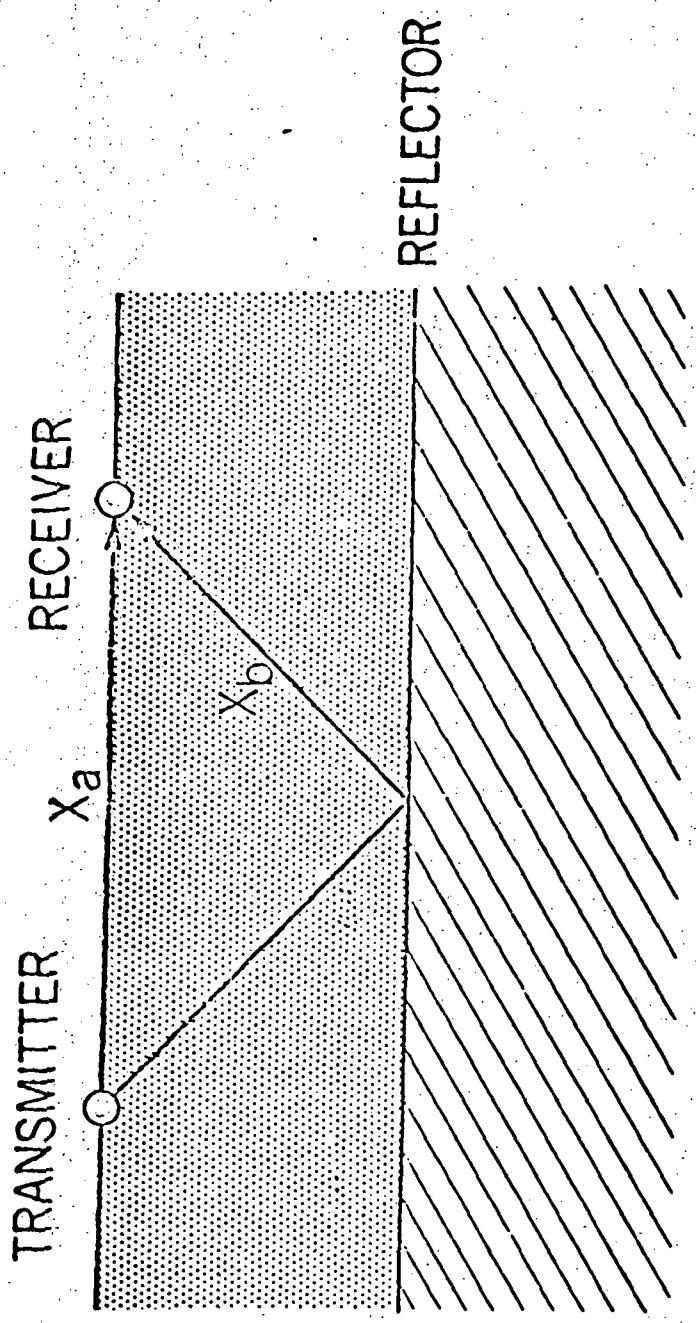

Figure II-15: Basic Experiment Concept.

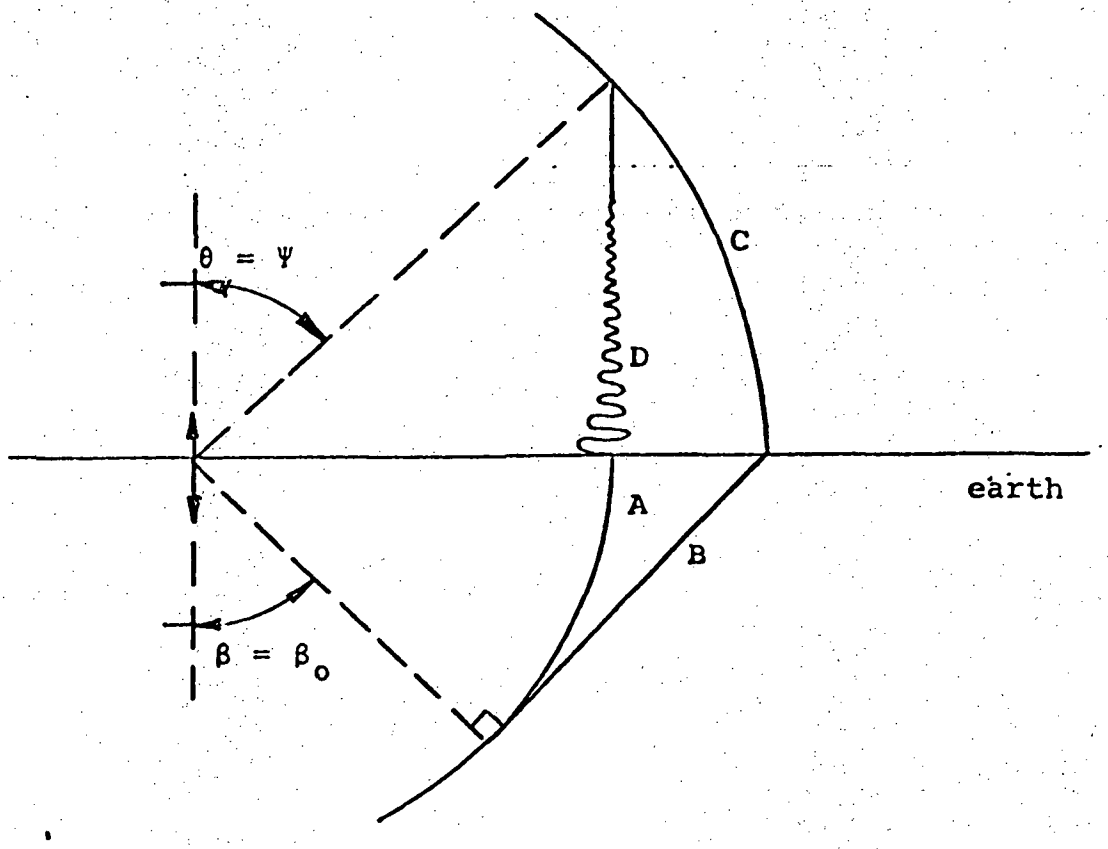

A - spherical wave in earth

B - flank or head wave in earth

C - spherical wave in air or vacuum

D - inhomogeneous wave in air or vacuum

Figure II-16: SKETCH OF WAVEFRONTS AT THE AIR-EARTH INTERFACE

gives a measure of the dielectric constant of the lower medium, since the greater the difference in the velocities of these two waves, the greater will be their rate of interference.

Another wave of some importance is the flank, or "head", wave, B. This wave is responsible for the directionality of the antenna pattern below the surface. It develops in order to satisfy the boundary conditions of wave C at the interface, since the phase velocity of some wave in the earth must be the same as the phase velocity of wave C, in the upper medium. This condition is satisfied if plane wave B propagates downward to some extent. The tilt is given as β, the angle of total internal reflection between the two media. Hence, $\sin \beta = \sqrt{\frac{E_o}{E_1}}$, where β is the angle between the z-axis and the direction of the wave, and $\frac{E_o}{E_1}$ is the ratio of refractive indices across the boundary. The importance of this wave is that it effectively gives the antenna radiation pattern a lobe at angle β.

The spherical wave A, travelling in the lower medium, also matches the boundary conditions, but in a different way. An inhomogeneous wave, D, is produced at the surface; this wave is directed upwards and decays exponentially with height above the surface. This wave is not as significant as the others discussed above.

Evidently, the practical usefulness of this method for depth sounding depends upon two major implicit assumptions. First, the medium being probed must not be too lossy, or the amplitude of the reflected wave will be too low to interfere well with the direct waves. And, second, there must exist some strong electric contrast below the subsurface, or there will be very little energy reflected.

It has been shown previously that the lunar surface should be very transparent to radio waves. The contrast necessary for reflecting energy from depth could come from a change in dielectric properties, electrical conductivity, or density. A range of frequencies, with wavelengths from 10 meters to 600 meters is planned, since these wavelengths correspond to the range of depths under consideration. Hence there is little fear that these conditions will not be met on the moon.

Interpretation of the data evidently requires a knowledge of the location of the receiver relative to the transmitting antenna. Position determination will be done in this experiment by determining an azimuth and a distance.

Two crossed transmitting antennas will be driven with differing modulations in such a way that first one antenna will be powered and then the other. This will have the effect of making the radiation pattern rotate. The azimuth will be determined by measuring the time of occurence of the maximum

received signal. The transmitter will radiate a sequence of eight discrete frequencies used in the experiment; switching between these frequencies will be synchronized to occur at a time coincident with the zero-azimuth aiming of the radiation pattern. This will provide the time base for the azimuth measurement and it is not necessary for the receiver to contain a clock. Since azimuth determination can be done at all eight frequencies, the problems of multipath and beam distortion can be sorted out. It is expected that accurate directions can be determined in this way.

The second part of the system will consist of analysis of the field strengths to give distance from the source. In general, the received field strength will be inversely proportional to the distance from the source and so can be used to determine the distance. Although any individual observation may be disturbed significantly by interference, the data can be averaged readily to give smooth curves. Moreover, this can be done using many frequencies so that there is inherent redundancy in the system.

It is planned that, as part of the traverse, the astronaut will walk along one arm of the transmitter antenna, locating himself precisely by means of markers along the antenna. This will give location data for the high frequencies where precision is required, and also will serve to calibrate the ranging system.

The use of these two approaches is expected to locate the receiver system at all times with the required accuracy. At greater distances along the traverse, the low frequencies are of most interest, so that the accuracy required in position decreases as the astronaut moves away from the transmitter. Internal checks using several frequencies will be available and the use of smoothing along the path will be most helpful.

b. Experiment procedure

A schematic diagram of the procedure is shown in Figure II-17. The source will be a center-fed half-wave dipole antenna laid on the surface near the LM. It will be powered by a small transmitter producing continuous waves at discrete frequencies of 0.5, 1, 2, 4, 8, 16, 24, and 32 Megahertz successively. This sequence will be repeated once per second. As described previously, another identical antenna will be laid out at right angles to the source antenna so that a rotating radiation pattern can be created for the purpose of azimuth determination.

The receiving antenna will consist of three orthogonal coils about one foot in diameter. These will detect the three orthogonal components of the received field at each successive frequency. The strength of the three field components will be recorded separately on a small tape recorder. The recorded information will be returned to earth

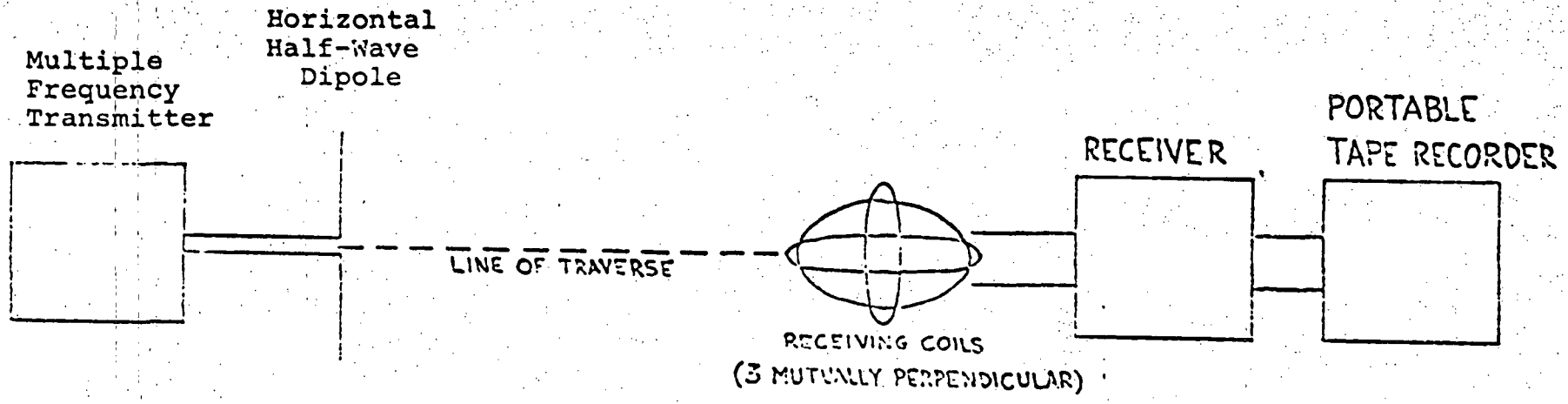

Figure II-17: Layout of Basic Experiment

for data analysis.

It is anticipated that the receiving coils will be fixed to the MET or to the Lunar Rover. Initially, the astronaut will have to deploy the transmitter and the two associated dipole antennas. The astronaut then will move away from the transmitter in a direction that is roughly perpendicular to one of the, identical, dipoles but will not be constrained to walk in a straight line. A traverse to a distance of three Kilometers or more is desirable, but shorter distances also can yield useful data at the higher frequencies.

During the first stages of the traverse, the most useful data will be that derived from the highest frequencies and since the position of the receiver must be known within about one-fifth of a wavelength, an initial accuracy in position of about two meters is necessary. This will be achieved by having the astronaut walk along any one arm of the antenna, which will be marked with fixed distance points, either pausing for about one second at each marked point or reading his position into the voice record. This procedure also will calibrate the ranging system.

During the remainder of the traverse, although it is desirable that the astronaut travels approximately perpendicular to one of the transmitting dipoles, this is not critical. He will be free to roam anywhere in a sector of about 20 degrees, and entirely free to conduct other

studies and activities. The range information also is not so critical at greater distances so, after the initial stages, the experiment will require only a minimal amount of astronaut attention.

Three receiving coils are necessary to record information on both the vertical and horizontal magnetic fields at each point. Since these two fields create independent interference patterns, interpretation ambiguities will be reduced by having both fields recorded separately. Since the horizontal field propagates in a radial direction from the transmitter it is not necessary to orient the three coils precisely with respect to the transmitter, it is only necessary that the plane of one coil be approximately horizontal. However, if the coils could be aimed roughly (say within $\pm$5 degrees) occasionally during the traverse, and so noted by the astronaut on the voice record, a useful estimate of the amount of lateral inhomogeneity could be made.

The above operating procedure has been determined largely on the basis of field trials made on glaciers. A one watt engineering breadboard of the proposed transmitter, constructed by the MIT Center for Space Research, was used to feed a tuned ribbon-wire half-wave dipole antenna. Receiver coils of one and three feet diameter were used with a commercial Galaxy R530 communications receiver.

Tests on the Athabasca Glacier, Alberta, gave results typified by Figures II-18 to II-20. Agreement between theory and data is not perfect for several reasons. First, the theoretical solutions are approximate, due to the mathematical complexities. Second, they are for an infinite, plane, horizontal, layer, which the glacier is not because it has sloping interfaces. And, third, some scattering is probably present in the field data. Nevertheless, the general shape of the curves is reasonably good, giving a depth to the bottom of the glacier of about 150 meters. This agrees completely with previously published seismic and gravity results of several workers.

Frequencies of 2, 4, 8, 16, and 24 MHz. were used. Although the results for the lower frequencies were tolerably noise free, those for the higher frequencies showed a large amount of scattered energy. This is probably because irregularities are approximately the same size as the wavelengths of the higher frequencies. The rapid changes of the field strength with position make it necessary to sample the field at least every one-fifth of a wavelength.

Studies were also made with the one-foot antenna strapped on a person's back. Although the interference of the human body was greatest at the higher frequencies, the results of this test are not dissimilar to the others (compare Figures II-19 and II-20).

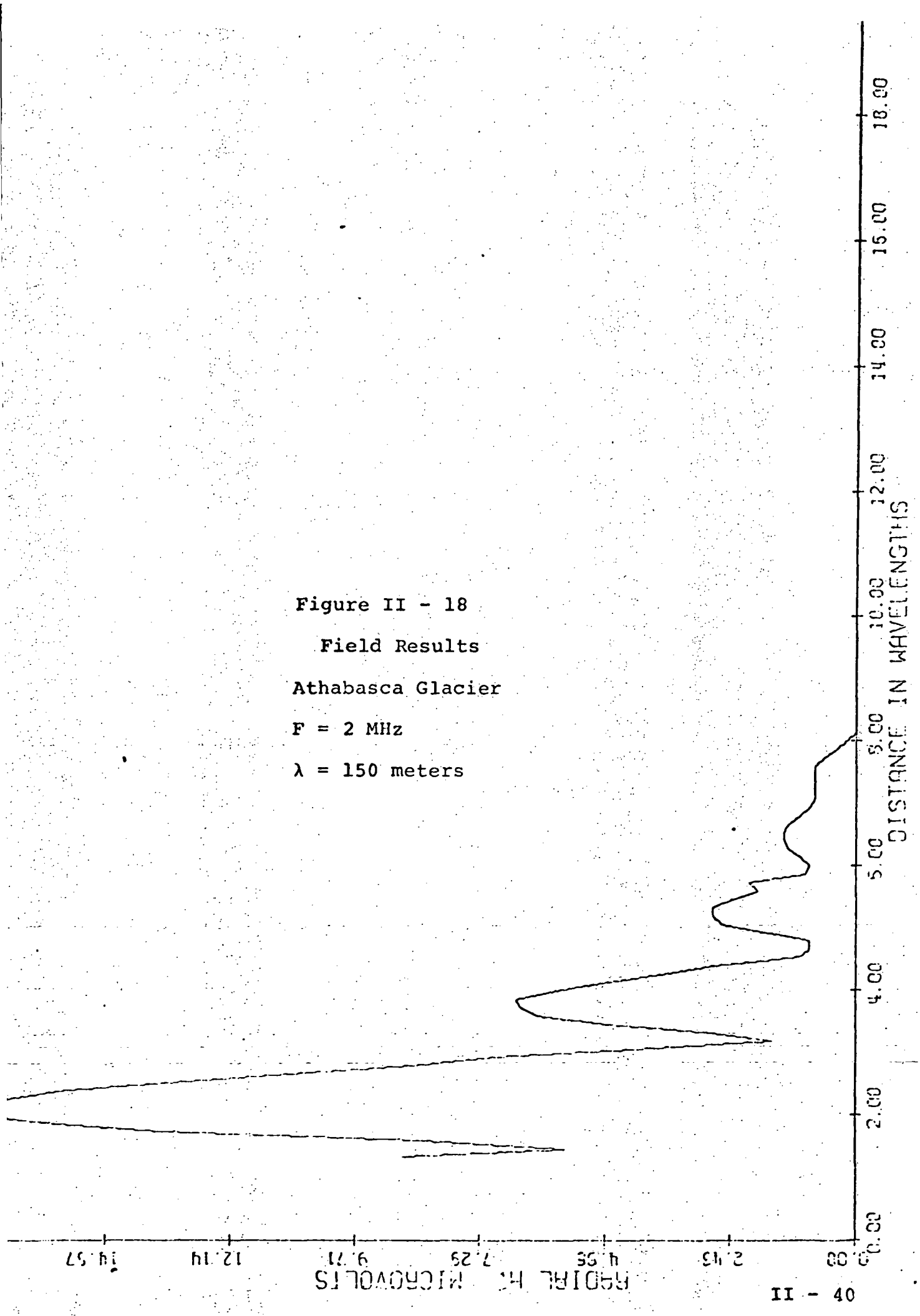

Figure II - 18

Field Results

Athabasca Glacier

F = 2 MHz

λ = 150 meters

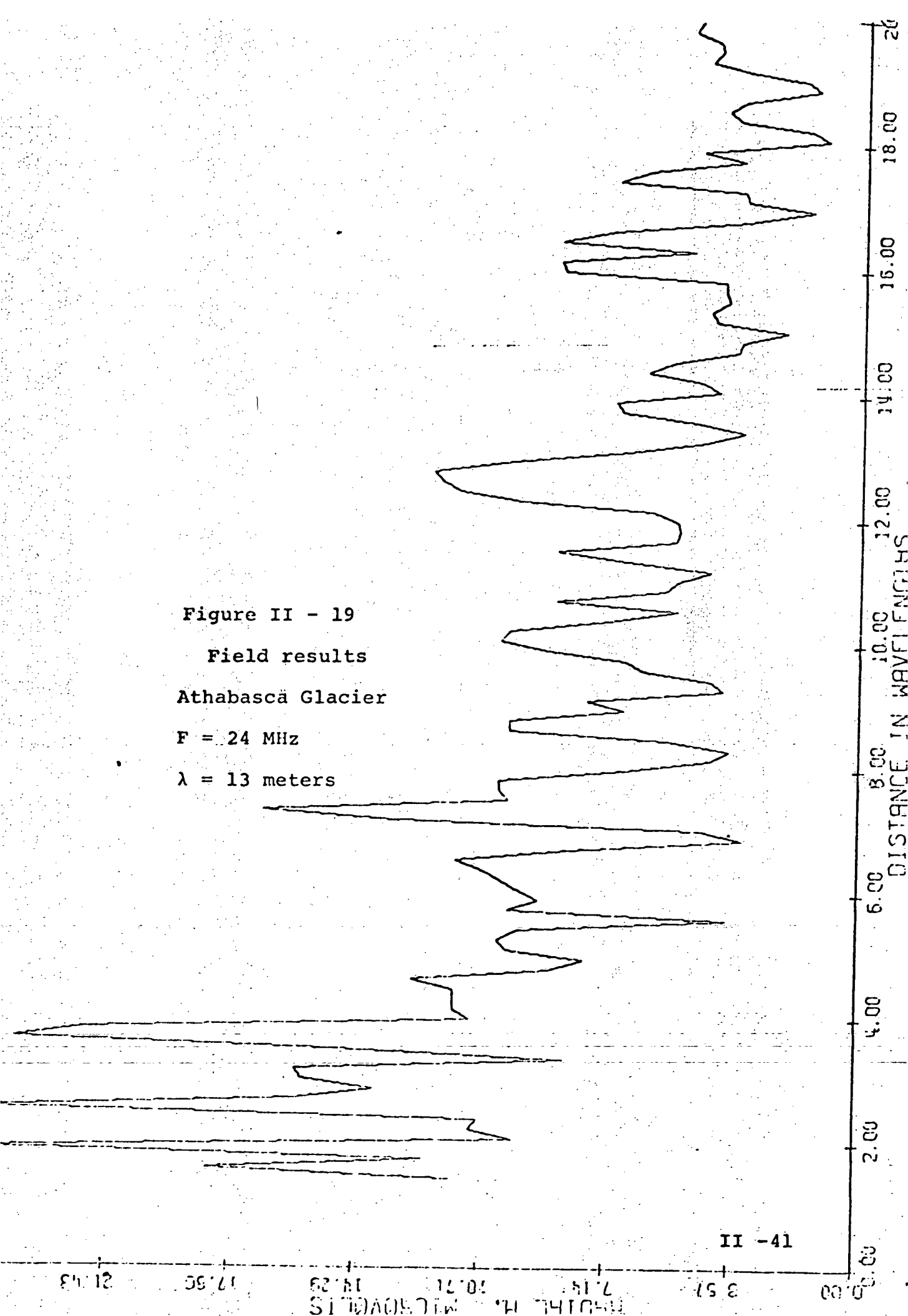

Figure II - 19

Field results

Athabasca Glacier

F = 24 MHz

λ = 13 meters

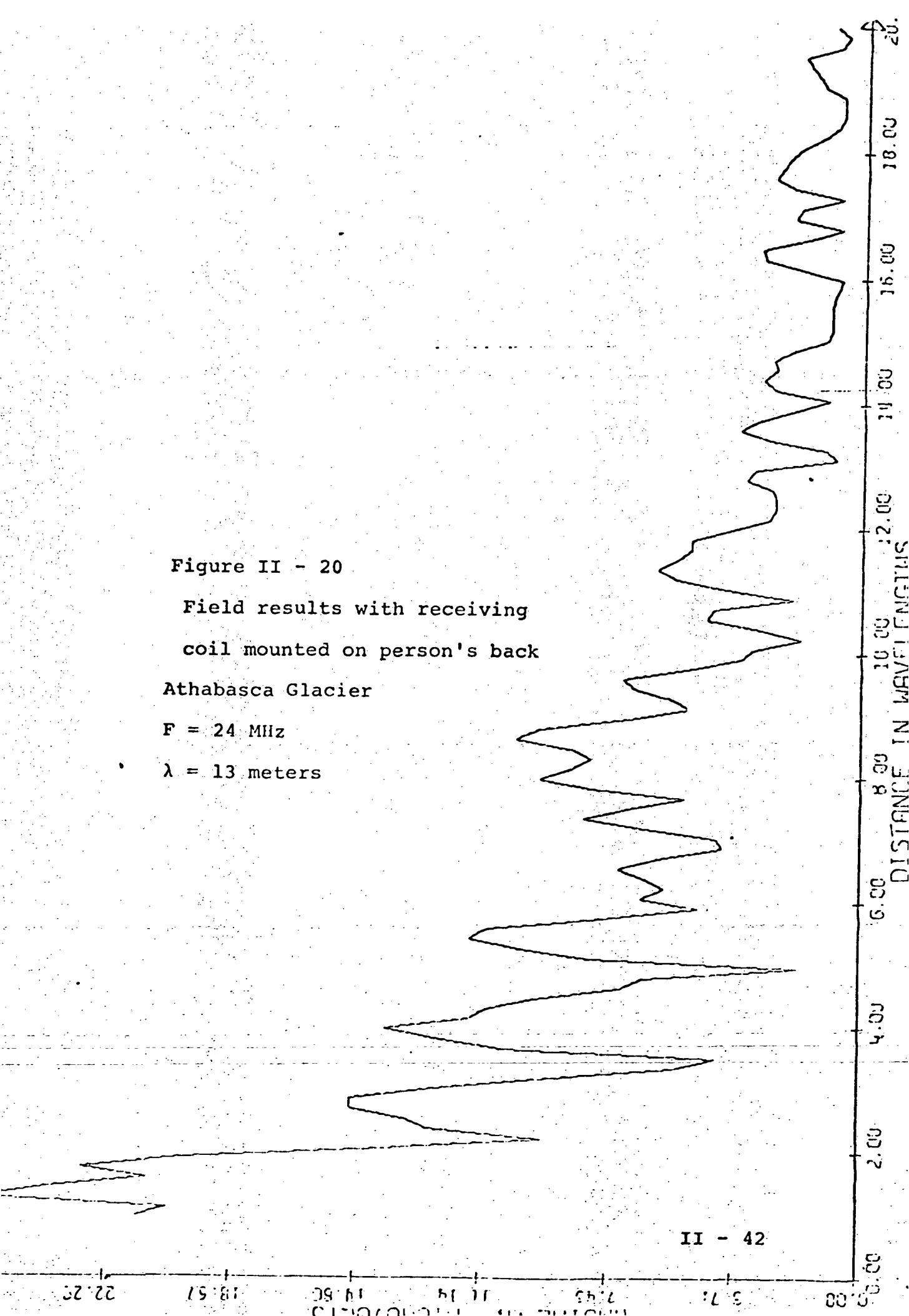

Figure II - 20

Field results with receiving coil mounted on person's back

Athabasca Glacier

F = 24 MHz

λ = 13 meters

Although this trip gave satisfactory results, much remains to be done. Only by field trips can the optimum procedure for taking measurements be determined. Moreover, the problem of scattering requires more study. As prototype instruments are developed, they must be tested in the field without any significant delay.

c. Quantitative range of the measurements

During the traverse, various measurements will be made continuously and recorded automatically on tape. The basic data are the strengths of two independent components of the horizontal magnetic field, and the vertical field. Eight frequencies between 0.5 and 32 MHz will be monitored for the duration of the traverse, with a complete sequence of the eight discrete frequencies repeating once per second. Time also will be recorded on the magnetic tape.

The dynamic range of possible values for the field strengths is quite large, due to the large oscillations imposed by the interference technique. Moreover, some of the most useful information can be obtained when the received signal is relatively small, and the values depend on the electrical properties of the lunar subsurface. Field measurements made over glaciers indicate that the probable range of values of interest at the receiving antenna is from 10 to 0.01 microvolts/meter. This should be measured with an accuracy of about 1%.

The distance between the receiver and the transmitter will range from zero to about 3000 meters, or more if the Rover vehicle is used. For all signal frequencies, it is necessary to know the position to approximately one-fifth of a wavelength. However, the higher frequencies are only useful nearer the transmitter,while the lower frequencies are of principal interest further away. Therefore the ranging measurement will have to be more accurate near the transmitter than it will at a large distance. A good estimate of the accuracy needed is about 1% of the actual distance.

For example, the 32 MHz. signal has a wavelength of approximately 10 meters. It will yield useful information to about 20 wavelengths from the source, or 200 meters. A position accuracy of one-fifth of a wavelength is 2 meters, or about 1% of the maximum useful range at this frequency. The same relative scale applies to the other frequencies.

Therefore, although precise position information is necessary for the first few hundred meters, this requirement relaxes with distance. Near the source, the astronaut can use the distance indicators marked on the antenna arms and read his distance into the voice record. For the remainder of the traverse, azimuth and distance information will be provided by the data itself.

d. Method for analysis and interpretation of data

Analysis of the data will take several steps. First, the receiver location data must be translated from a bearing measurement and range to position versus time information. It is anticipated that this will require combining data from the voice record and photographs, as well as from the experiment itself. The field strengths which will already be in a measurement versus time format then can be converted to field strength versus position. The vertical component will be complete, and the radial component will be the vector sum of the two horizontal components.

Once the information is in this form, it can be compared to standard curves computed for a large number of expected conditions. The problem of a horizontal electric dipole on the surface of a dielectric layer has been tackled theoretically for several cases of interest. The half-space case (i.e. virtually no reflected energy from depth) still gives an interference pattern, and this has been worked out rigorously for both the H_z and H_ρ components. The layered case is not so simple. Approximate solutions have been obtained, for both components, for the case of a dielectric layer underlain by a horizontal reflecting layer. Families of solutions are being computed for arbitrary losses, dielectric constant, and depth of the first layer. A few

examples of these curves have been shown previously in Figures II-3 to II-10.

Many important cases remain unsolved; they must be studied before satisfactory interpretation of the data from the moon can be assured. Examples are the cases of sloping interfaces, arbitrary changes in dielectric properties, more than two layers, etc. The effect of curvature of the moon's surface also is important for the longer wavelengths and distances. Some of these problems are presently being tackled theoretically.

However, it is likely that few of these problems will yield even approximate theoretical solutions. For this reason scale-model studies must be an essential part of the interpretation program. A model already has been used successfully to confirm theoretical studies, and to aid interpretation of field results. A new model is being constructed which will overcome some of the limitations of the previous one.

The new model will consist of a large bath of transformer oil of carefully controlled dielectric properties, and a 5 cm. wavelength electric dipole source. The tank will be anechoic for microwave frequencies, and will allow easy measurement of many different subsurface configurations. Im addition, the radiation pattern of the antenna can be measured in the dielectric medium, which will aid in theoretical studies.

One of the most interesting problems to be modelled in the tank will be the effect of scattering bodies in the subsurface. Scattering effects have been seen in field data, and lunar seismic data indicate that they could be very important on the moon. Therefore, any information on position, surface topography, and coil orientation that the astronaut can supply will be useful in interpreting these effects.

Another aspect of interpretation is the possibility of computerizing the procedure. This may be accomplished by evaluating several critical parameters, such as the dielectric constant, from a set of data, and then allowing the computer to search for the best fit from many theoretical models. Another approach will be to harmonically analyze, then to digitally filter the data looking for characteristic frequencies. This might be essential if a large amount of scattered energy is present.

Further studies of the dielectric properties of lunar samples also should be made. This is important to determine the range of likely cases that may be encountered on the moon.

Above all, the various methods of interpretation must be evaluated on real data. This can come only from field measurements using the types of apparatus that will be used on the moon. As prototypes become available, they must be evaluated without delay. Field work must proceed in

conjunction with all other aspects of the project.

e. Prime obstacles or uncertainties which can be anticipated

The experiment is conceptually simple and uses electronic equipment that is scarcely more complicated than a conventional FM transmitter and receiver. The chief uncertainties are associated with an adequate determination of the astronaut's position during the traverse, and interpretation of the effects of subsurface inhomogeneities.

Most ranging systems on earth use electromagnetic radiation of some nature to monitor location. However, there are drawbacks to this type of system on the moon. If high frequency radiation such as a laser beam is used, the astronaut will soon get out of line of sight, due to the curvature of the lunar surface, or due to surface obstacles such as craters. On the other hand, lower frequencies, which will propagate along the surface, also will propagate downward, and suffer reflection from the subsurface. Thus the traditional problem of multipath is inherent in the lunar surface.

To compensate for these problems, position determination will be done using all eight transmitted frequencies to give an azimuthal bearing and a range. The lower frequencies should give satisfactory operation beyond the line of sight, and the use of many widely spaced frequencies should permit an evaluation of the multipath problems.

Not only the ranging system is affected by inhomogeneities. The experiment itself, like virtually all geophysical techniques, is inherently ambiguous. Although good interpretation of the data is of course possible, the large number of unknown parameters may lead to several possible solutions for a given set of data. This problem will be complicated by random scattering from surface, interface, or subsurface irregularities. Because of this, any information that the astronaut can give on surface features or receiving coil orientation will be useful.

The fact that the experiment uses a large range of discrete frequencies is a beneficial factor. It is not expected that scattering bodies very much larger, or very much smaller, than a particular wavelength will affect that frequency unpredictably. Therefore, although a few frequencies may be adversely affected by random scatter, it is unlikely that they will all be affected simultaneously. And the very fact that a certain wavelength is prone to scatter itself gives useful information on the nature of the subsurface.

Neither of these problems is trivial; both are being studied intensively at the present time. These studies must continue in conjunction with the construction of apparatus. Prototype apparatus must be tested in the field to obtain additional data. Scale-model studies, in which conditions

can be carefully controlled, will yield important clues to the effects of scattering.

f. Significance of the astronaut

The astronaut has several important duties in this experiment. He must choose the optimum site for deployment of the transmitter and transmitting antennas, avoiding large obstacles such as rocks or craters. He must transport the receiver and tape recorder along one arm of the antenna to give accurate position information at the beginning of the traverse. He must then mount the receiver on the MET or Rover before starting on the long traverse.

It would be very desirable to deploy the transmitting antennas so that the long traverse is constrained to a sector of about 20 degrees normal to either one of the crossed dipoles. Also, if the astronaut occasionally could orient the receiving coils with respect to the transmitting antenna, and record that he is doing so, additional useful information on the subsurface inhomogeneities would be obtained. Of course any information on surface topography would aid in interpreting scatter and in checking the receiver location.

Apart from these considerations, the experiment requires minimal attention from the astronaut and will leave him free to perform any other duties.

II-5. BASELINE OR CONTROL DATA

The major support that will be needed during the post-flight data analysis is all available data on the position of the receiver during the traverse. This information may come from a variety of sources. Although the experiment inherently includes a position determining capability, this information may be incomplete or ambiguous due to the nature of the lunar surface. Therefore, any information the astronaut can put on the voice record will be useful. This is particularly true during the initial stages of the traverse. It is expected that surface photographs also will yield helpful position information.

A knowledge of the surface topography along the traverse also would be useful. This information will come from surface photographs that can be tied in with orbital photographic work. Again, any information on the voice record will be helpful. Once the position and surface information during the EVA have been calculated, they will be available to all other experimenters, of course.

SECTION III - ENGINEERING INFORMATION

III - 1. EQUIPMENT DESCRIPTION

a. Summary description

A schematic diagram of the experiment is shown in Figure III-1. A small, low power, transmitter radiates through a crossed dipole antenna laid on the lunar surface. A small receiving unit consisting of three orthogonal loop antennas, some electronics for amplifying and timing the signals, and a magnetic tape recorder, is transported by the astronaut, either on the Mobile Equipment Transport (MET) or on the Lunar Roving Vehicle (LRV). The experimental data is the complex interference pattern between the surface wave and the subsurface and reflected waves; this interference pattern causes a variation in the received field strength as a function of range and frequency. The magnitude of the field components received by each of the three orthogonal loops is detected separately by the receiver and recorded on the tape recorder. The magnetic tape is to be returned to Earth for data analysis and interpretation.

Both the transmitter and receiver are relatively simple. This simplicity is inherent for several reasons.

First, the signal path loss is small because the maximum distance between transmitter and receiver is

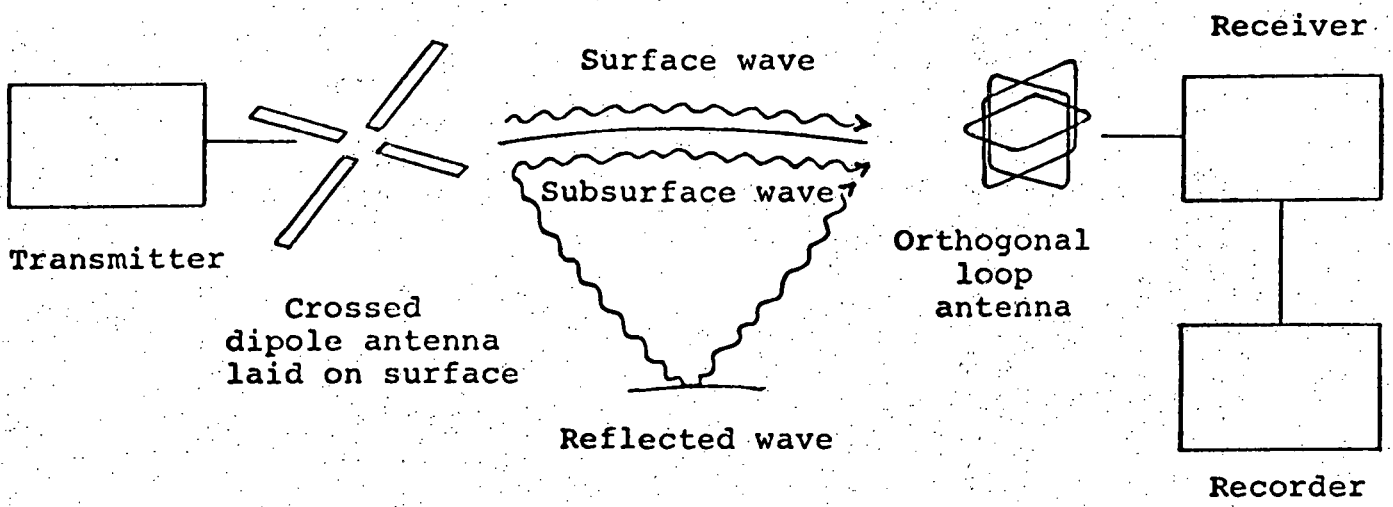

Figure III - 1 Schematic Diagram of Experiment

limited by the astronaut's traverse to a few Kilometers. With this low path loss, a transmitted power of one to two watts is sufficient to create a high field strength at the receiver.

Second, the relatively low frequencies required by the experiment, in the range from 0.5 to 32 Megahertz, can be generated and manipulated easily in high efficiency circuits.

Third, the amount of auxiliary electronics required for timing, formatting, and the like is minimal because the data is recorded on magnetic tape in analog form.

Fourth, the duration of the experiment is limited to the few hours in which the astronaut will operate on the lunar surface. This means that the thermal design does not have to accomodate the temperature extremes of both lunar day and night, and also means that both the transmitter and receiver can use internal power supplies.

The radio frequencies employed range from 0.5 to 32 Megahertz, with corresponding free space wavelengths ranging from 600 to 9.4 meters. Eight discrete frequencies are used, with sequential one-tenth second bursts at 0.5, 1, 2, 4, 8, 16, 24, 32 MHz; this timing is illustrated by Figure III-2. A complete cycle lasts for one second, with two 100 millisecond intervals reserved for receiver calibration.

The transmitted signal is amplitude modulated so that

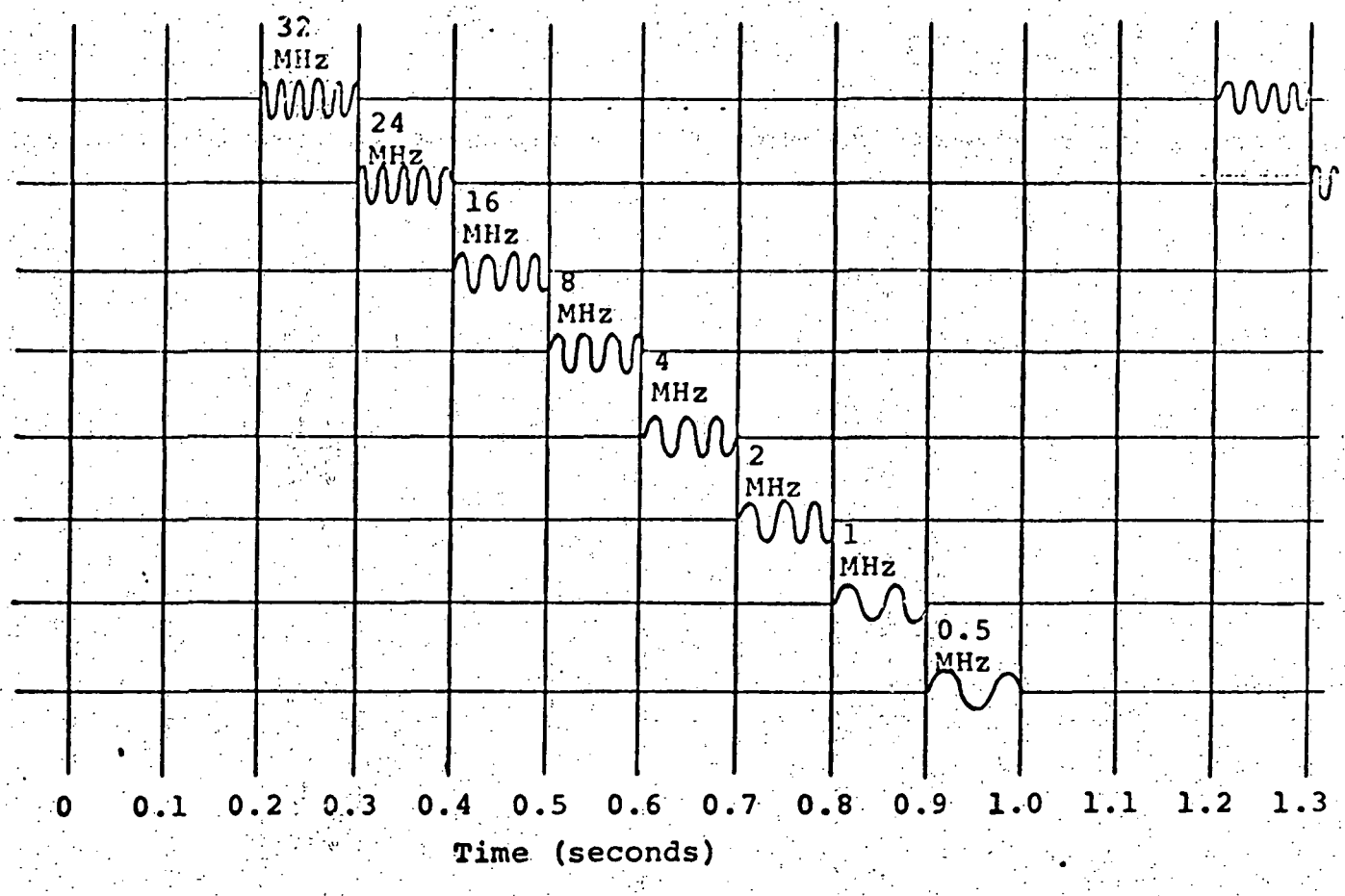

Figure III - 2 Frequency Sequence, Timing Diagram

the radiation pattern of the transmitting antenna rotates at at rate of 15 revolutions per second. The mechanism by which the rotating beam is achieved is discussed in detail in the antenna section of this report. Fundamentally, the technique, which is illustrated here by Figure III-3, uses two crossed dipoles as the transmitting source. One dipole, arbitrarily designated as a North-South antenna, is used to radiate a signal which is amplitude modulated with a cosine function, while an orthogonal, East-West, antenna radiates a signal at the same carrier frequency which is amplitude modulated with a sine function. Superposition of the radiation patterns of these two antennas then creates a composite radiation pattern which rotates in sympathy with the variations of the modulating function.

Because the radiation pattern from a single dipole is a symmetrical figure of eight, the chosen pattern rotation rate causes the field strength seen by any observer to fluctuate at a 30 Hertz rate: that is, the receiver will record three peaks in each 100 millisecond interval devoted to a specific radio frequency. This rate is chosen to be compatible with the antenna loop switching procedure in the receiver. In each 0.1 second interval the receiver sequentially records the received field

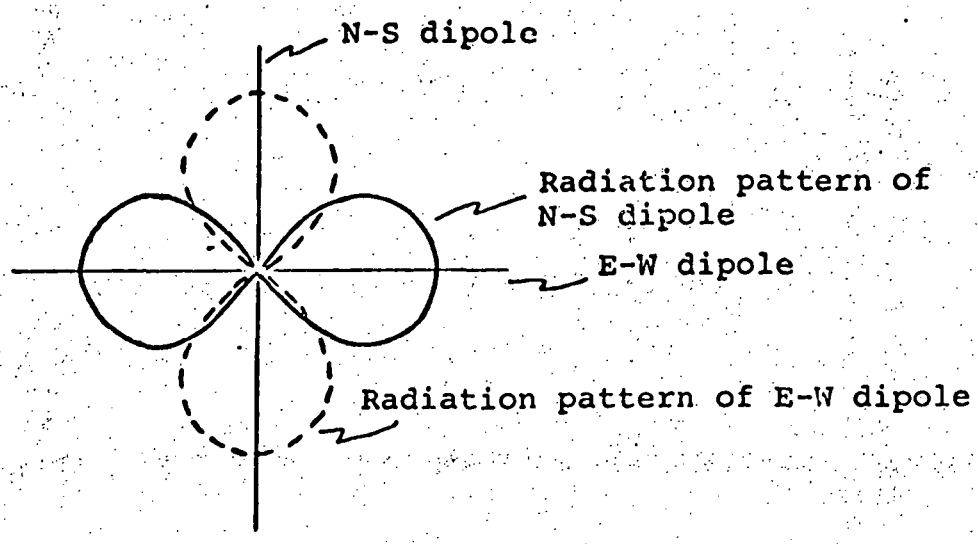

a) Arrangement of orthogonal dipoles

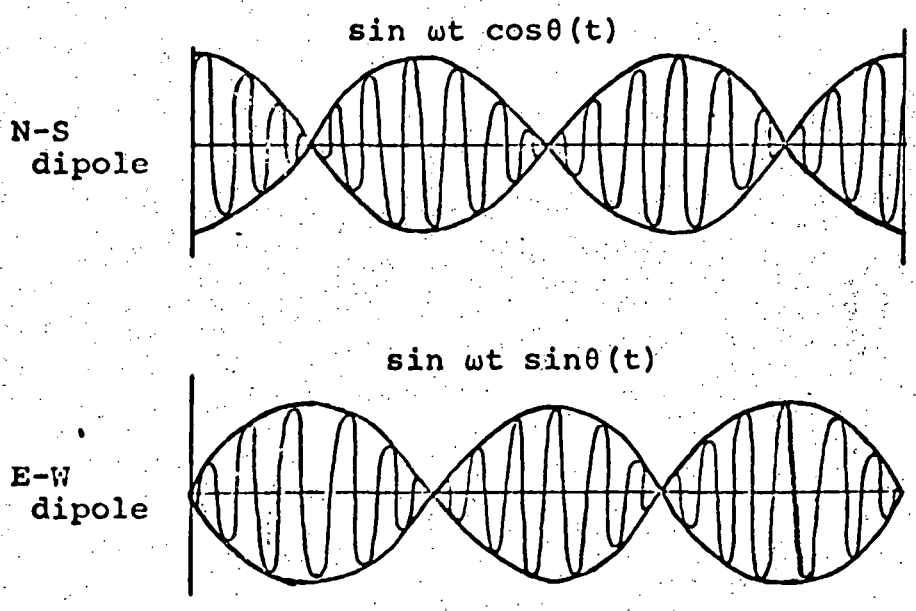

b) Transmitted signals

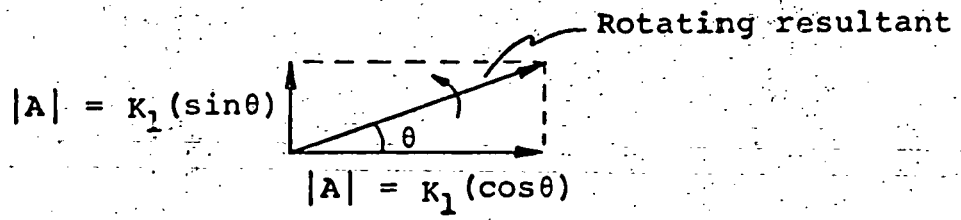

c) Spatial relation of transmitted fields

igure III-3 ROTATING BEAM CONCEPT

strength as seen by each of the three orthogonal receiving loops so each loop in turn will observe one full cycle of variation in the received field strength. This timing relation is illustrated by Figure III-4.

This rotating beam system represents a change from the original hardware proposal, formulated in September 1969, which included some system components not required for the main experiment but designed solely to provide the range and azimuth information needed for proper interpretation of the experimental data. The prior system included three transmitters: a main transmitter radiating through a single dipole laid on the lunar surface, and two subsidiary transmitters located at the ends of the dipole to provide position determining information by fairly conventional range difference, or hyperbolic, navigation techniques.

The revised system described here has three notable advantages. First, because the crossed dipoles used for the main transmitter provide an essentially omni-directional radiation pattern, the experiment is even less sensitive to the exact path followed by the astronaut during a lunar surface traverse. Second, additional scientific data becomes available because with the new system it is possible to obtain a measure of the apparent lateral distortion of the radio beam due to multipath reflections associated

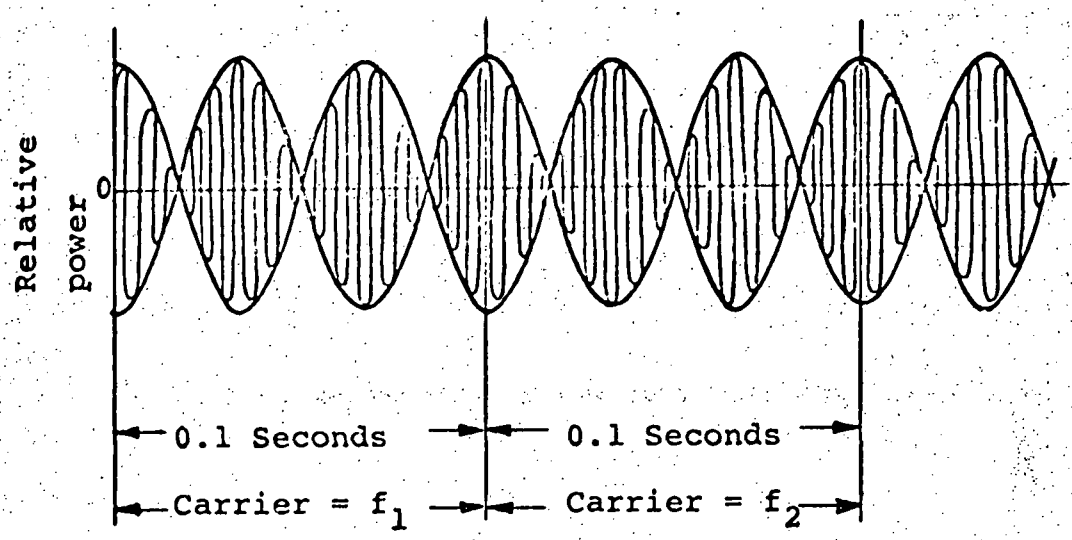

a) Signal transmitted by N-S dipole

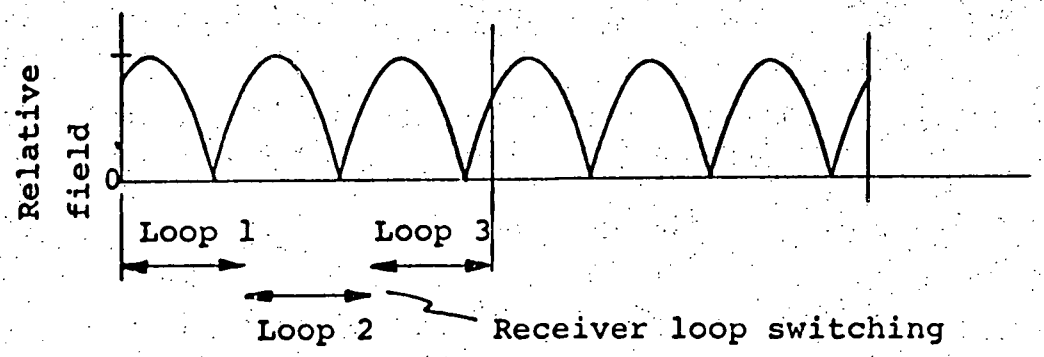

b) Received field strength as seen by observer located N-E of transmitter

Figure III-4 ROTATING BEAM TIMING DIAGRAM

with inhomogeneities close to the lunar surface. And, third, the total weight of the system is reduced by the elimination of the subsidiary transmitters.

The rationale for the new position-determining scheme is discussed below.

Consider, first, the derivation of ranging information. As discussed elsewhere, the experimental data shows the effect of interference fringes as typified by the solid curve of Figure III-5. Examination of actual data obtained during field trials on the Athabasca Glacier in April 1970 has confirmed that when this data is smoothed by a simple integration, the mean received field strength, in itself, provides a range measure which is compatible with the purpose of the experiment provided that at least one calibration point is available to determine the range scale; that is, to determine the attenuation constant of the transmission medium.

It is proposed to obtain many such calibration points simply by marking one of the main dipoles at intervals of say, 5 meters. The astronaut then will be asked to make one short traverse along one limb of the marked dipole, pausing for approximately two seconds at each mark, so that the magnitude of the field received from the other dipole will be known accurately at each of the marked distances. These points alone will provide the needed

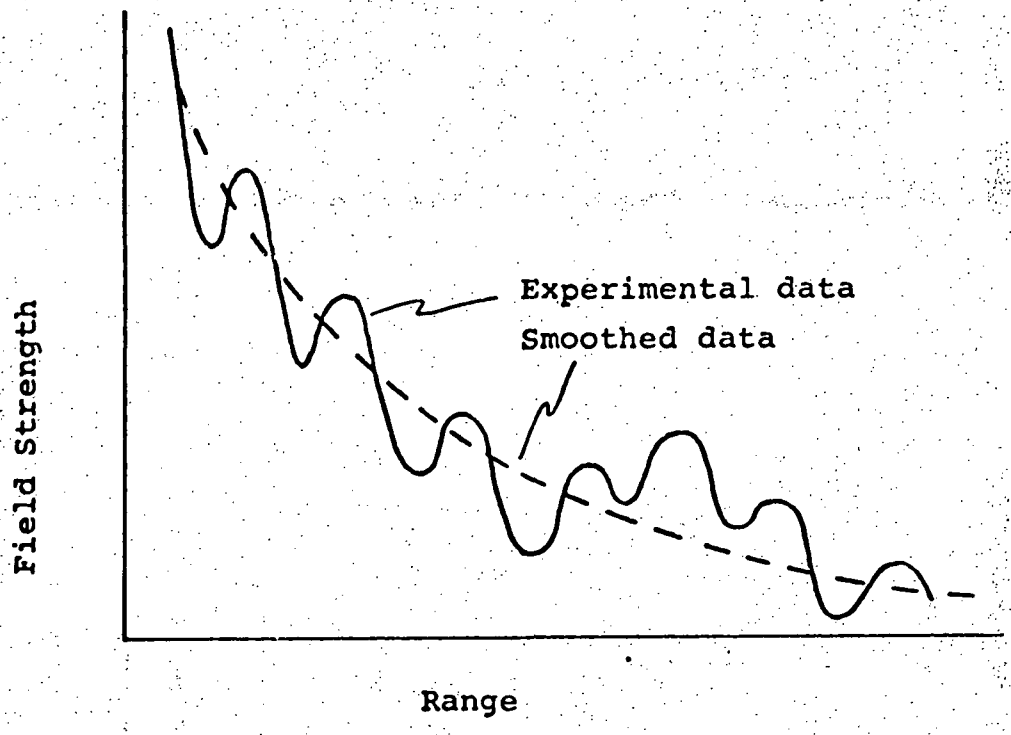

Figure III-5 ILLUSTRATIVE RECEIVED FIELD STRENGTH

measure of the attenuation constant of the transmission medium. As a backup, of course, the data also can be fitted to other, longer range, calibration points if the precise distance between the astronaut and the main transmitter happens to be known from other sources such as photographic correlations.

Azimuth, or direction, data, by contrast, could not be derived solely from the central transmitter in the system proposed previously. Although the received field strength will vary in sympathy with the radiation pattern as the observer departs from a line that is normal to a dipole, the rate of change of field strength as a function of angular displacement is too small to provide a meaningful measure of the relative direction of the observer and, in any case, could not be distinguished easily from a change in received field strength caused by a change in range. For this reason, two subsidiary transmitters were used previously to provide intersecting sets of hyperbolic lines so that a pair of range difference measurements could be used to determine the angular location of the observer with respect to the main transmitter.

The need for the subsidiary transmitters is eliminated by the use of a main antenna feed system which causes the antenna beam to rotate slowly. Conceptually, the

arrangement may be thought of as being analogous to a lighthouse, or a rotating beacon. Given a knowledge of the rotation rate of the beam, and a time reference marker which is synchronous with the time at which the beam is pointing in an arbitrarily designated direction (say, North), the direction of an observer with respect to the transmitter can be determined simply by noting the time at which the beam is pointing toward the observer, that is, the time during the rotation when the maximum field strength is observed by the receiver.

The necessary reference time marker is derived through a simple stratagem. The low frequency signals used to amplitude modulate the transmissions from the crossed dipoles are derived from the same basic timing circuits that are used to determine the 0.1 second intervals to be devoted to each successive radio frequency. Thus, at the start of each 0.1 second interval the phase of the modulating functions is known and, further, is controlled so that the transmitted beam is pointed in a known direction (due North) at that instant. Since the receiver already is required to maintain synchronization in order to tune successively to the different radio frequencies employed in the main experiment, it is a simple matter to utilize this known receiver reference time to permit a measure of the relative time of occurence of the peak received

signal with respect to the time when the radio frequency last changed. This, of course, is the desired measure of the direction of the observer with respect to the transmitter.

As with any radio navigation scheme subject to multipath interference, any individual measurement of direction may be in error due to apparent lateral bending of the radio beam. Fortuitously, however, this turns out to be an advantage in the present experiment rather than a disadvantage as in most navigation systems.

A different set of multipath effects will be associated with each of the different radio frequencies used in the experiment. As in some other radio navigation schemes, the indicated directions may be averaged to compensate for the multipath problem and allow the true direction to be ascertained. But, more importantly in this application, the multipath effect will be dependent upon the relation between the wavelength of the signal and the scale size of the inhomogeneities causing reflections. Thus the observed apparent deflections of the rotating radio beam will be different at each of the experiment frequencies and the recorded data therefore will permit some additional inferences to be made concerning the scale size of the lunar inhomogeneities.

b. Transmitter

Figure III-6 shows a functional diagram of the transmitter. A 32 Megahertz crystal controlled oscillator provides a stable reference frequency from which all other frequencies and timing signals are derived. Output of the oscillator is counted down through a chain of integrated circuit flip-flops to define the eight signal frequencies used in the experiment. Count down is continued through another chain of integrated circuit flip-flops to provide timing signals T_1 through T_8 which actuate gates G_1 through G_8 sequentially so that the input to the power divider is composed of successive 100 millisecond bursts of each of the eight RF signals. Output of the power divider provides a carrier frequency input to each of two balanced modulators. Sine and cosine components of a 15 Hertz signal derived from the count down chain also provide an input to these modulators. The modulated signals are amplified by separate linear amplifiers and connected through impedance matching baluns to the two elements of the crossed dipole transmitting antenna.

Detail of the transmitter circuits is discussed in the following paragraphs.

(i) Reference oscillator

This is a transistor implemented, crystal controlled oscillator which provides one milliwatt output power at a

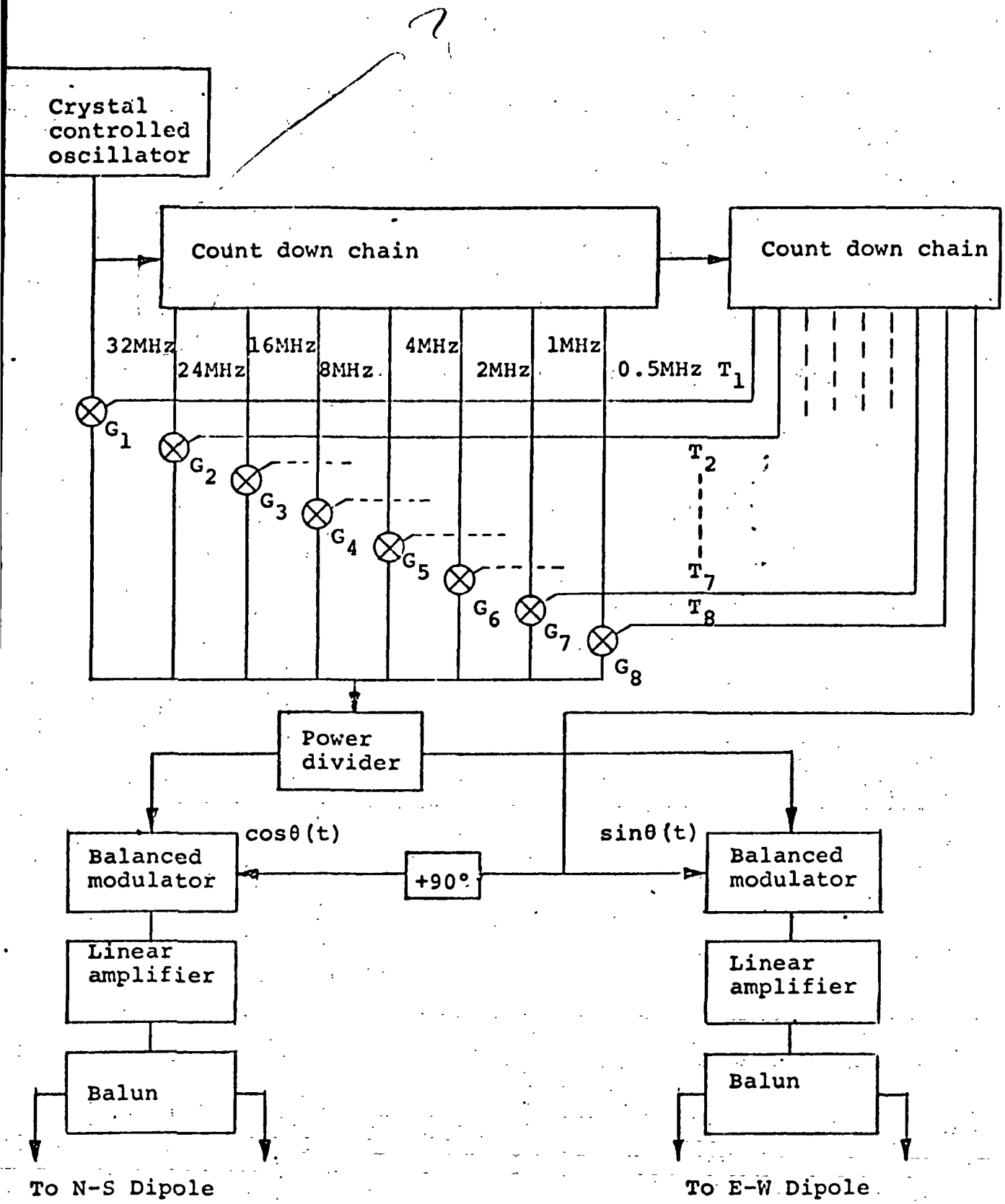

Figure III - 6 Transmitter Functional Diagram

frequency of 32 Megahertz. The crystal is chosen to have a low temperature coefficient so that thermostatic control is not required. The frequency stability is in the order of three parts in 10^9 over a period of one day, and better than one part in 10^{10} over a period of one second.

(ii) Count down chain

This is implemented with conventional monolithic integrated circuit flip-flops and gates. The total chain accepts an input signal with a frequency of 32 Megahertz from the basic oscillator and provides all necessary lower frequencies ranging down to the 100 millisecond timing signals used to define the transmission intervals.

(iii) Power divider

RF power at frequencies of 0.5, 1, 2, 4, 8, 16, 24, and 32 MHz is fed into the power divider which performs an equal phase, 3dB, power split to provide inputs to the balanced modulators. The power divider is a passive, lumped element, network with broad band frequency characteristics. The divider maintains a phase balance within 1° and an amplitude balance better than 2 dB over the full frequency range of the experiment. Isolation between the output ports is better than 30 dB; the insertion loss is less than 0.3 dB

(iv) Balanced modulators

The output signal of an amplitude modulator can be described as a summation of various terms such as:

$$i(t) = k_1 \sin\omega_c t + k_2 \sin(\omega_c-\omega_m)t + k_2 \sin(\omega_c+\omega_m) + f_n(t)$$

where

$i(t)$ is the output signal current

k_1, k_2 are constants

ω_c is the carrier frequency

$(\omega_c+\omega_m)$ is the upper side band (ω_u)

$(\omega_c-\omega_m)$ is the lower side band (ω_l)

$f_n(t)$ are small amplitude higher order products caused by nonlinearity of the modulating device.

Two frequency components, the upper sideband ω_u, and the lower sideband ω_l, are needed to drive the crossed dipole transmitting antenna so as to generate a rotating radiation pattern. Accordingly, a linear balanced modulator is used to suppress the carrier frequency and other harmonic components.

Several options for balanced modulator circuits are available. A simple diode bridge, illustrated by Figure III-7, has been demonstrated to provide adequate performance for this system. It has good isolation between the ports, wide dynamic range, and low distortion. The output

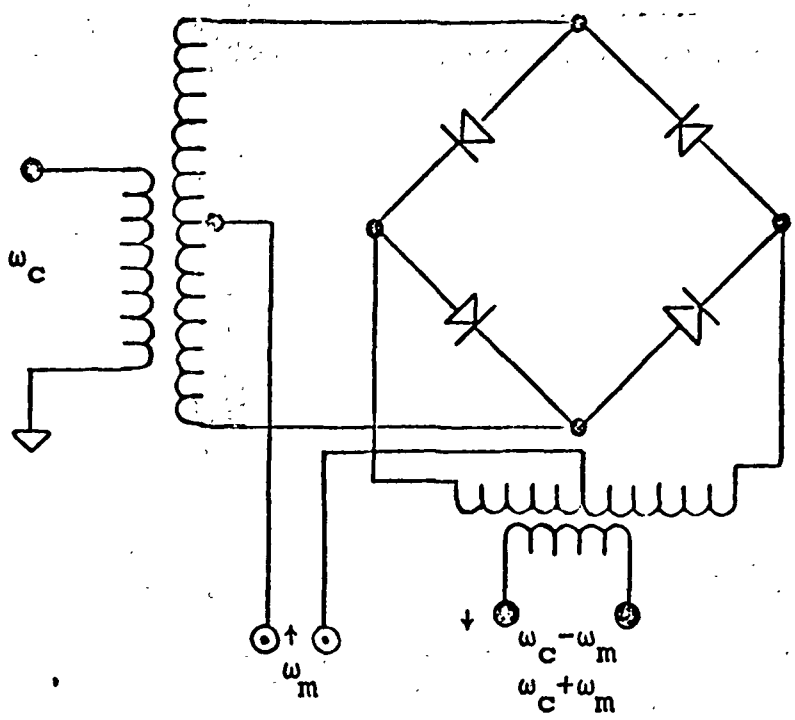

Figure III - 7 Balanced Modulator

carrier suppression exceeds 40 dB. The experimental circuit uses a matched pair of ultrafast switching hot carrier diodes having a forward resistance of less than 5 ohms and a reverse-bias resistance greater than 10^9 ohms. This large resistance ratio is responsible for the relatively good performance quoted above.

(v) Linear amplifiers

For this experiment, the linear amplifiers must be capable of providing an output power of the order of 2 watts in the frequency range from 0.5 to 32 Megahertz. Other important design characteristics include a differential phase error of less than $\pm$ 5° and a gain error of less than $\pm$ 1 dB over the frequency and temperature range of interest.

Experimental circuits have substantially exceeded these requirements, providing a differential phase error of less than 2° and a differential gain error of less than 0.2 dB.

(vi) Baluns

These are broadband, 180° phase shift, lumped circuit hybrids which connect the coaxial output of the linear amplifiers to the feeder lines of the dipole antennas. Commercial elements used in an engineering model provide an amplitude balance better than 0.2 dB, a phase balance better than 1°, an insertion loss of less than 0.5 dB, and isolation exceeding 30 dB. These commercial units,

which have a power handling capability of 5 watts, weigh 1.4 ounces each.

c. Transmitting antenna

The configuration of this antenna is shown by Figure III-8. The identical and orthogonal 'North-South' and 'East-West' dipoles are each composed of eight separate elements. Seven of these are used as standard half-wave dipoles at the experiment frequencies ranging from 1 to 32 Megahertz. A loaded quarter-wave dipole is used for the lowest, 0.5 MHz, experiment frequency in order to keep the antenna weight and deployment time within reasonable limits.

With the exception of the 24 MHz signal, which will be discussed separately, the wavelengths of the RF signals used in the experiment are related by successive factors of two. So, when the shortest dipole element is fed at 32 MHz, the 16 MHz dipole antenna and all successively longer elements are even multiples of the wavelength of the transmitted signal. These "parasitic dipoles" therefore appear as large value inductors across their respective feed lines. This is true as each successively longer dipole is fed with its resonant frequency. Conversely, when the longest antenna is fed at its resonant frequency, each of the shorter antennas appears as a small capacitor across its respective feed lines. In either case, there is a large reactance in series with the antenna and, consequently, a very poor impedance match (with a VSWR of the order of 40) so that essentially no signal current flows

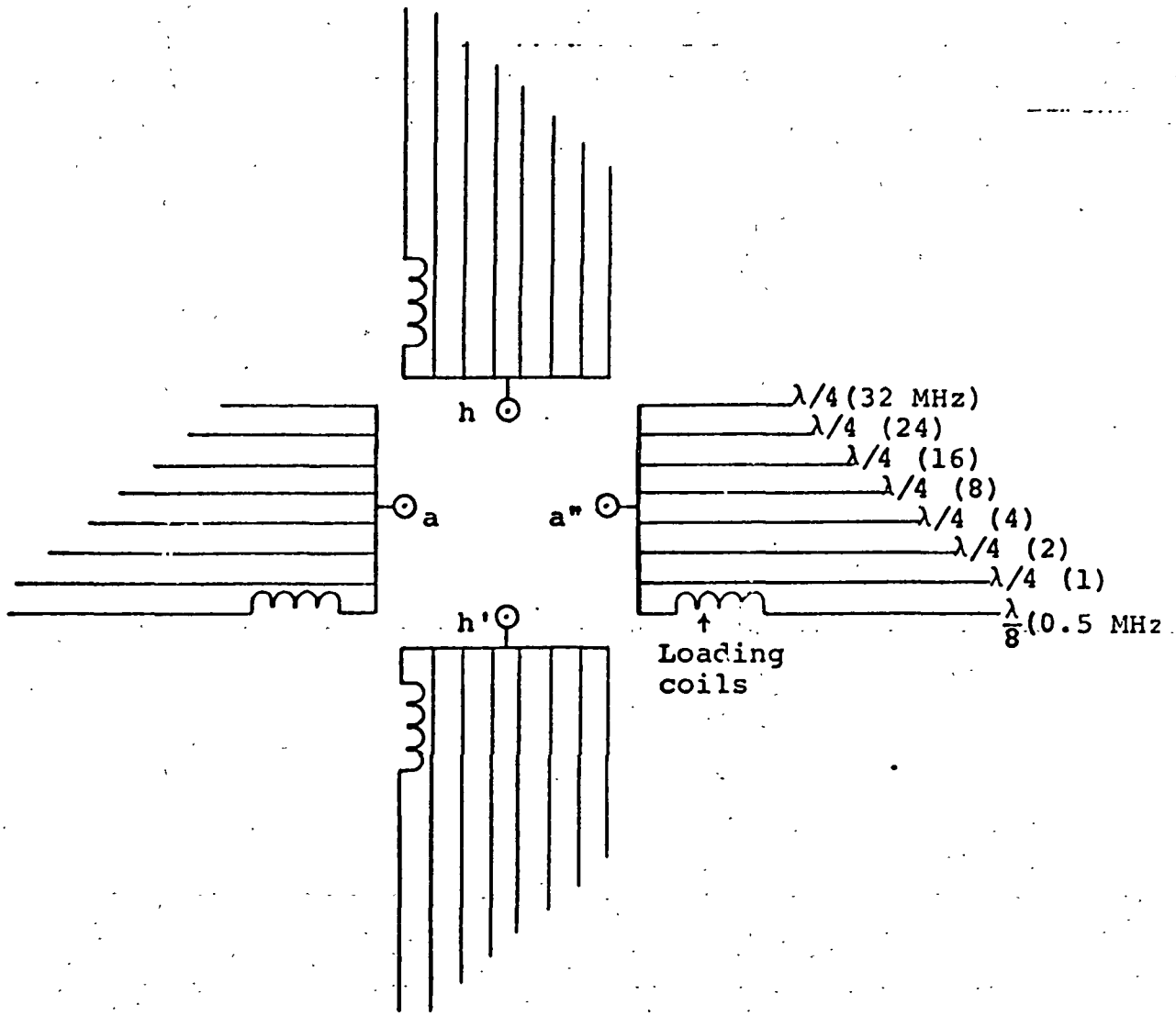

Figure III - 8 Transmitting Antenna Configuration

in any dipole except the one that is resonant to the signal. In other words, each antenna functions as a simple dipole and the signal free elements can be placed very close to the active element with negligible effect on either the feed line impedance or the radiation pattern. For ease of deployment, therefore, each of the four limbs of the antenna can be formed with a multiple conductor flat ribbon wire.

There is one exception to the above condition. When the 24 MHz antenna is excited at its resonant frequency, the 8 MHz antenna becomes a $3\lambda/2$ dipole. Current will flow in this antenna and the 8 MHz antenna will radiate with the pattern of a $3\lambda/2$ dipole in addition to the 24 MHz antenna radiating as a $\lambda/2$ dipole. The result is a six-lobed pattern with nulls existing between about 10° and 30° from the axis perpendicular to the dipoles. This condition might cause the 24 MHz signal data to be marginal at maximum range. However, inasmuch as the higher frequencies are for short ranges anyway, this problem is not considered to be serious.

d. Signal/noise Analysis and Receiver

(i) Introduction

The basic idea of the SEP experiment receiver is to record the local magnetic field strength at each frequency radiated by the transmitter as a function of the receiver position on the lunar surface.

If the signal were strong enough, then in principle all that would be required for the receiver would be an antenna, a diode-resistor-capacitor combination (detector), plus a recorder as indicated by Figure III-9. Because this experiment derives data from interference patterns, however, the signals strength are necessarily faint at certain intervals and strong at others. This along with assumptions related to the properties of the lunar subsurface and the unknown noise environment of the lunar rover vehicle dictate receiver design concepts that will not only accommodate wide signal excursions (large dynamic range) and handle very low

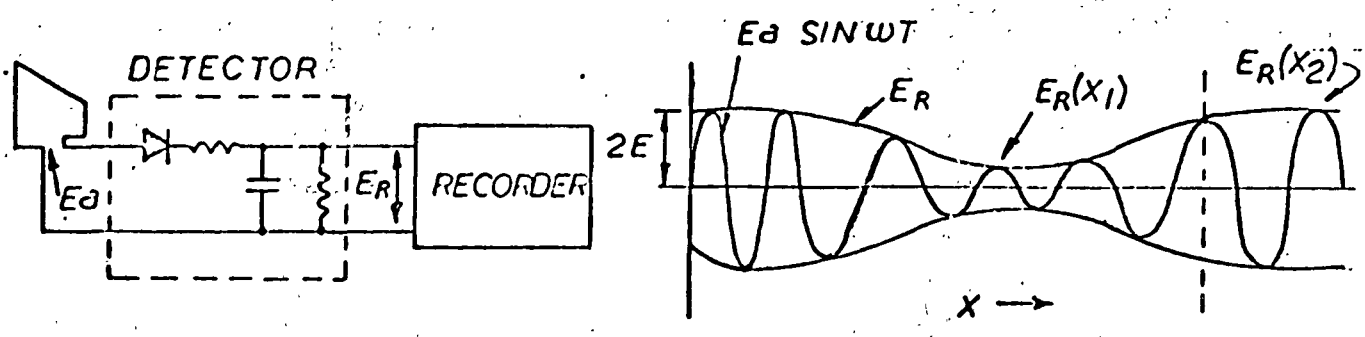

Figure III-9 Receiver

signals levels (low noise design) but will as, well, remain time synchronized with the transmitter in the event of complete loss of signals for extended time intervals. In addition, the SEP receiver must be designed to meet the following constraints: (1) three orthogonal electrostatically shielded circular loop antennas are required to eliminate receiver directionality; (2) because the receiver is to be mobile, the three antennas must be physically small (approximately 1 ft. diameter), and therefore, only a small fraction of a wavelength in diameter and, consequently, are very inefficient; (3) in order to minimize the required storage capacity, the three orthogonal signal components are time multiplexed onto one tape track; and (4) interpretation of the experiment data requires an approximate knowledge of the relative range and azimuth between the transmitter and receiver.

Fron an electrical viewpoint, the receiver functional requirements are fairly standard. The signal sequence following the loop antennas is: (1) wideband, low noise gain, followed by, (2) pre-detection narrowband filtering, (3) detection, (4) signal compression, and finally (5) storage on magnetic tape.

There are, of course, several different detailed design configurations that would meet the SEP requirements. For example, we have studied two alternative methods to accomplish the pre-detection filtering, namely using individual crystal filters or a phase locked loop to accomplish the narrowband filtering. We also have considered different compression

techniques. (1) Low frequency (base band) compression techniques have been successfully used to obtain wide dynamic range ($>10^8$) at a carrier frequency of 1 KHz in several plasma probes[1] (Pioneer 6 and 7; Mariners 4 and 5; IMP A, B, C, D, E, H and J). These techniques are directly applicable and flight proven and can be utilized in a post-detection compression configurations. (2) The compression function can also be accomplished in a pre-detection configuration at high carrier frequencies. The standard implementations of this is to use an intermediate frequency logarithmic amplifier as described in a recent discussion with RCA. (3) The post-detection compression may also be accomplished at direct current utilizing operational amplifier in a piece wise linear configuration as described in our original proposal.[2]

The low noise wideband front end amplifiers are readily available in integrated circuits form. The noise figure should be less than 6 db, and the gain should be constant ($\pm\frac{1}{4}$db) over a (.3 to 35) MHz band.

Some of the receiver design details and relevant performance figures depend on the input signal characteristics and noise environment as well as the output tape recorder performance. The tape unit as you know is a special problem

---

[1] "Mariner A Plasma Probe," Lincoln Laboratory, Technical Report No. 337, 5 December 1963, Pg. 12, Figures 13, 14, 15, and 16.

[2] "Surface Electrical Properties Proposal", October 23, 1969, Pages 18-20, Figure III-9.

area that has been much discussed (L.H. Bannister's memorandum August 28, 1970), and therefore, will not be covered here except in as much as its performance limits the receiver design. The input signal discussion follows.

(ii) Signal/noise Analysis

Three different received signal powers are of interest in this experiment.

First, a plane wave will propagate through free space and will be received over the line of sight, that is to a range of the order of 1.5 Kilometers.

Second, a collinear wave will propagate through the lunar subsurface at a velocity different from that of the free space wave. It is the interference between the subsurface and free space waves which provides a measure of the dielectric constant of the medium. The subsurface wave will suffer additional attenuation due to the finite losses of the medium. The range of interest of the experiment necessarily will be restricted to those distances at which the excess attenuation is less than about 15 db: beyond this point the interference will be too weak to yield meaningful data.

Third, a wave propagating obliquely through the regolith will be reflected to the receiver. It is the interference between this wave and the surface and subsurface waves which provides a measure of the depth of the reflecting interface. Again, this wave will suffer additional attenuation, and the range of interest of the experiment necessarily will be restricted to those situations in which the excess attenuation of the reflected wave is less than about 15 db with respect to

the wave with which it interferes: within the line of sight this will be the free space wave, while beyond the line of sign this will be the collinear subsurface wave.

To define the design limitations for the receiver, these three components of the received signal will be evaluated.

Consider, first, the line of sight, or free space, signal. For a conventional radio communication system operating in a lossless medium, available signal power at a receiving antenna is given by:

$$P_a = \frac{P_t G_t A_e}{4 \pi R^2} \qquad (1)$$

where:

P_a is the available power, in watts

P_t is the power radiated by the transmitting antenna, in watts

G_t is the directional gain of the transmitting antenna

A_e is the effective capture area of the receiving antenna, in meters^2

R is the range, or distance, from the transmitter to the receiver, in meters.

The effective capture area of a receiving antenna is given by:

$$A_e = \frac{G_r \lambda^2}{4 \pi} \qquad (2)$$

where G_r is the directional gain of the antenna

λ is the signal wavelength, in meters

So, substituting (2) in (1):

$$P_a = \frac{P_t G_t G_r \lambda^2}{(4 \pi R)^2} \qquad (3)$$

Power delivered to a load, that is to the input terminals of a receiver, is given by:

$$P_r = P_a \eta \qquad (4)$$

where P_r is the power in the load, in watts

η is the efficiency of the receiving antenna

So, substituting (3) in (4):

$$P_r = \frac{P_t G_t G_r \lambda^2 \eta}{(4 \pi R)^2}$$

or, setting $G_t = G_r = \frac{3}{2}$ which is appropriate for both the transmitting dipole and the receiving loop:

$$P_r = 0.142\ 10^{-1}\ \frac{P_t \lambda^2 \eta}{R^2} \qquad (5)$$

This result will be used later.

The efficiency of an untuned receiving antenna may be evaluated using the following equivalent circuit:

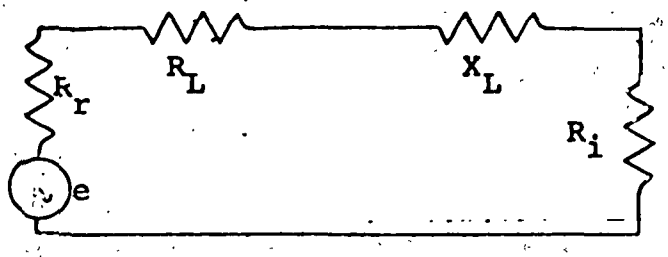

where e is the open circuit voltage at the antenna terminals

R_r is the radiation resistance of the antenna

R_L is the loss resistance of the antenna

X_L is the reactive impedance of the antenna

R_i is the resistive component of the receiver input impedance.

The small magnetic loop receiving antenna to be used in this experiment is formed with one turn of wire with a loop diameter of about 0.3 meters which is much smaller than any signal wavelength used in this system. For this configuration, the loss resistance is primarily the wire resistance, corrected for skin effect, and is given by:

$$R_L = \pi D \rho S$$

where R_L is the loss resistance, in ohms

D is the loop diameter, in meters

ρ is the wire resistance, in ohms per meter

S is a skin effect correction factor

Using AWG #10 wire at the lowest frequency of 500 KHz, the loss resistance is:

$$P_L \approx \pi \; 0.3 \;\; 3.3 \;\; 10^{-3} \;\; 7 \approx 0.02 \text{ ohms}$$

The inductance of the receiving loop is given by:

$$L_o \approx \frac{\mu_o D}{2} \left[\log_e \frac{8D}{d} - 2\right]$$

where L_o is the inductance, in Henrys

D is the loop diameter, in meters

d is the wire diameter, in meters

Again using AWG #10 wire, this yields:

$$L_o \approx \frac{1.257 \; 10^{-6} \; 0.3}{2} \left[\log_e \left(\frac{8 \;\; 0.3}{2.59 \;\; 10^{-3}}\right) - 2\right]$$

$$\approx 0.9 \; 10^{-6} \text{ Hys}$$

So, at the lowest system frequency of 500 KHz, the reactive impedance is:

$$X_L = 2 \pi f L_o$$
$$= 2 \pi 5 \;\; 10^5 \;\; 0.9 \;\; 10^{-6}$$
$$\approx 2.8 \text{ ohms}$$

It may be noted that, at the lowest system frequency:

$$\frac{|X_L|}{R_L} \approx \frac{2.8}{0.02} \approx 140$$

that is, the loss resistance is much smaller than the reactive impedance and can be neglected. This will also be true at the higher system frequencies because the reactive impedance is proportional to f while the skin correction factor, in the range of interest, is proportional to $\sqrt{f}$.

With this simplification, the equivalent circuit of interest is:

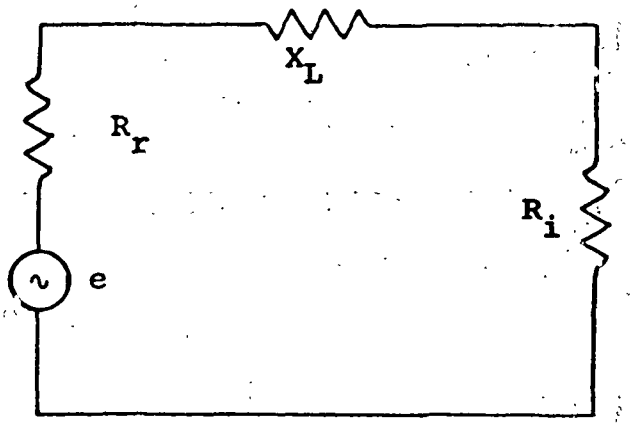

Now, the radiation resistance for the small loop receiving antenna is given by:

$$R_r = 20\ \pi^2 \left(\frac{\pi D}{\lambda}\right)^4$$

which yields:

$$R_r = \frac{20\ \pi^6\ (0.3)^4}{(600)^4} \approx 1.2\ 10^{-9} \text{ ohms } [f = 500 \text{ KHz}]$$

and

$$R_r = \frac{20\ \pi^6\ (0.3)^4}{(9.375)^4} \approx 2.04\ 10^{-2} \text{ ohms } [f = 32 \text{ MHz}]$$

So, at all system frequencies, the radiation resistance is much smaller than the reactive impedance of the antenna, and this, also, can be neglected when computing the power delivered to the load.

The efficiency of the receiving antenna is defined by:

$$\eta = \frac{\text{Power delivered to load}}{\text{Available power}}$$

and with the foregoing restrictions and simplifications is given, approximately, by:

$$\eta \approx \frac{\left(\frac{|e|}{\sqrt{R_i^2 + X_L^2}}\right)^2 R_i}{\frac{|e|^2}{4\ R_r}} = \frac{4\ R_i\ R_r}{(R_i^2 + X_L^2)} \qquad (6)$$

The resistive component of the receiver input impedance will be set equal to the magnitude of the antenna reactance at the lowest system frequency of 500 KHz. That is:

$$R_i = |X_L|_{[500\ KHz]} = 2.8 \text{ ohms}$$

Using this value and substituting (6) in (5) yields the values shown in Table 1, which defines the power received over the free space path in terms of carrier frequency, transmitter power, and range.

f (MHz)	λ (meters)	R_r (ohms)	$\|X_L\|$ (ohms)	η	P_r (watts)
0.5	600	$0.12\ 10^{-8}$	2.8	$0.85\ 10^{-9}$	$0.43\ 10^{-5}\ (P_t/R^2)$
1	300	$0.19\ 10^{-7}$	5.6	$0.54\ 10^{-8}$	$0.69\ 10^{-5}$ "
2	150	$0.31\ 10^{-6}$	11.2	$0.25\ 10^{-7}$	$0.79\ 10^{-5}$ "
4	75	$0.50\ 10^{-5}$	22.4	$0.11\ 10^{-6}$	$0.89\ 10^{-5}$ "
8	37.5	$0.80\ 10^{-4}$	44.8	$0.45\ 10^{-6}$	$0.90\ 10^{-5}$ "
16	18.75	$0.13\ 10^{-2}$	89.6	$0.18\ 10^{-5}$	$0.90\ 10^{-5}$ "
24	12.5	$0.65\ 10^{-2}$	134.4	$0.40\ 10^{-5}$	$0.90\ 10^{-5}$ "
32	9.375	$0.30\ 10^{-1}$	179.2	$0.70\ 10^{-5}$	$0.90\ 10^{-5}$ "

Table 1

Frequency Dependence of Receiver Signal Input Power for Free Space Path.

We must also consider the relative magnitudes of the collinear and reflected subsurface waves. It is these two signal components that yield data regarding the lunar subsurface through the nature of the dielectric losses and dissipative attenuation of RF waves in the lossy medium.

NATURE OF DIELECTRIC LOSSES

When an electric field is incident on a dielectric medium, it can cause three types of polarizations, i.e.,

(i) Electronic polarization due to displacement of orbital electrons

(ii) Atomic polarization

(iii) Molecular polarization

The end result is that electric flux density D (also called displacement) in the dielectric medium is different from the incident electric field. For the static electric case, it is known that

$$D_s = E_s + 4\pi P = k_e E_s \qquad (7)$$

where:

D_s is the displacement or electric flux density in the medium

E_s is the static electric field

K_e is a constant (characteristic of the medium)

P is the total polarization of medium, i.e. electric dipole moment/unit volume

When an RF time harmonic field E is incident on a dielectric medium, the polarization P also varies with time and so does the displacement D. However, at higher frequencies P and D may lag behind in phase relative to E and this hysteresis factor accounts for losses in a dielectric medium as shown below.

Let $E = E_o e^{j\omega t}$ (8)

such that displacement D is given by

$D = \varepsilon E e^{-j\delta}$ (9)

where:

δ is the lag angle between the incident field and displacement D.

ε is the permitivity of the medium.

E_o is the maximum amplitude of the incident RF wave

From (9),

$D = (\varepsilon \cos \delta - j \varepsilon \sin\delta) E$

$D = (\varepsilon' - j\varepsilon'') E$ (10)

such that $\tan \delta = \frac{\varepsilon''}{\varepsilon'}$ (11)

The energy dissipated per unit volume per second in the medium in form of heat is

$$W \triangleq \frac{1}{T} \int_0^T R_e(VI)\, dt \quad (12)$$

where $R_e(V)$ is the real part of rf voltage across unit distance $\triangleq \int_o^1 R_e(E) \cdot dx = E_o \cos \omega t$ (13)

$T = \frac{\omega}{\pi}$ is the time period of the incident wave

$R_e(I)$ is the real part of the displacement current

$$\triangleq \frac{dq}{dt} = \frac{1}{4\pi}\frac{dD}{dt} = \frac{\omega E_o}{4\pi} \quad (\varepsilon''\cos\omega t - \varepsilon'\sin\omega t) \qquad (14)$$

From (12), (13), and (14), the energy dissipation in the dielectric media is given by:

$$W = \frac{1}{T}\int_0^T \frac{\omega E_o^2}{4\pi} \quad (\varepsilon'' \cos\omega t - \varepsilon'\sin\omega t)\cos\omega t \, dt$$

$$W = \frac{\omega E_o^2}{8\pi}\varepsilon'' \qquad (15)$$

Thus losses in the dielectric medium are dependent on ε'', the imaginary part of the dielectric constant. The loss tangent ($\tan\delta$) is a measure of the energy dissipated to the energy stored in the medium. Furthermore, it can be said that both $\varepsilon'(\omega,\theta)$ and $\varepsilon''(\omega,\theta)$ are frequency and temperature dependent. Physical explanation is that frequency and temperature variations create disalignment and lag of polarized dipoles. For a non-polar medium $\varepsilon'(\omega)$ remains practically constant over a wide frequency range and $\varepsilon''(\omega)$ is of relatively small magnitude. The losses in the dielectric medium are ohmic in nature and can be associated with the conductivity, σ, of the medium.

DISSIPATIVE ATTENUATION OF RF WAVES IN A LOSSY MEDIUM

A plane R.F. wave propagating in a lossy medium in the positive z direction is represented as

$$E(z) = E_o e^{-jKz} \qquad (16)$$

where:

E_o is the electric field amplitude at z = 0

K is the propagation constant; a complex number

For a simple case, it can be assumed that the medium is homogeneous, isotropic, linear and non-magnetic. The propagation constant K is given by

$$K \triangleq \omega\sqrt{\mu\varepsilon} \tag{17}$$

where:

$\mu = \mu' - j\mu'' = \mu o$ for a lossless, non-magnetic medium

$\varepsilon = \varepsilon' - j\varepsilon''$ is the complex permitivity of the lossy dielectric medium (18)

From (17) and (18),

$$K = \omega\sqrt{\mu o(\varepsilon'-j\varepsilon'')} = \omega\sqrt{\mu o\varepsilon'}\left[1-j\frac{\varepsilon''}{\varepsilon'}\right]^{\frac{1}{2}}$$

$$= \omega\sqrt{\mu o\varepsilon'} - j\omega\frac{\sqrt{\mu\varepsilon'}}{2}\tan\delta \tag{19}$$

where:

$\tan\delta$ = loss tangent of medium $\triangleq \frac{\varepsilon''}{\varepsilon'}$

and $\varepsilon'' << \varepsilon'$

Substituting $\sqrt{\varepsilon'} = \sqrt{k_e\varepsilon_o}$ in (19),

$$K = \frac{2\pi}{\lambda}\sqrt{k_e} - j\frac{\pi}{\lambda}\sqrt{k_e}\tan\delta \tag{20}$$

where:

k_e is the dielectric constant of medium

λ is the free space wavelength

$\frac{2\pi}{\lambda}\sqrt{k_e}$ is the phase constant of the medium

$\frac{\pi}{\lambda}\sqrt{k_e}\tan\delta$ is the attenuation constant of the medium

From (20) and (16), the propagating electric field E(z) at distance z is given by

$$E(z) = E_o\, e^{-\frac{\pi}{\lambda}\sqrt{k_e}\,\tan\delta\, z\, j\,\frac{2\pi}{\lambda}\sqrt{k_e}\, z} \qquad (21)$$

At distances $z = 0$ and z_1, from (21)

$$|E(0)| = E_o \qquad (22)$$

$$|E(z_1)| = E_o\, e^{-\frac{\pi}{\lambda}\sqrt{k_e}\,\tan\delta z_1} \qquad (23)$$

Therefore, the dissipative attenuation α_D in db at distance z_1, from (22) and (23) is,

$$\alpha_D(z_1) \triangleq 20 \log \frac{|E(0)|}{|E(z_1)|} \simeq 27.26\, \frac{\sqrt{k_e}\,\tan\delta}{\lambda}\, z_1 \text{ db} \qquad (24)$$

Equation (24) is the basic equation used to compute dissipative attenuation (α_D) for varying parameters. It also indicates that a linear relationship exists between the loss tangent and the dissipative attenuation for the considered medium.

For ready reference attenuation calculations for various cases are listed below.

Case (1): For $z_1 = \lambda$; $\tan\delta = 0.01$; $k_e = 9$,

$$\alpha_D(\lambda) = 0.818 \text{ db}/\lambda \qquad (25)$$

Case (2): for $z_1 = \lambda$; $\tan\delta = 0.05$, $k_e = 9$,

$$\alpha_D(\lambda) = 4.09 \text{ db}/\lambda \qquad (26)$$

Case (3): for 0.5 MHz $\leq f_o \leq$ 32 MHz; $0.01 \leq \tan\delta \leq 0.05$ z_1 = 1 Kilometer; $k_e = 9$

FREQUENCY (MHz)	ATTENUATION	
	Tan δ = 0.01 $\alpha_D(\lambda)$=.818db/λ	Tan δ = 0.05 $\alpha_D(\lambda)$=4.09db/λ
0.5 MHz	1.35 db/kilometer	6.82 db/kilometer
1 "	2.73 "	13.63 "
2 "	5.45 "	27.26 "
4 "	10.9 "	54.52 "
8 "	21.81 "	109.04 "
16 "	43.62 "	218.08 "
24 "	65.42 "	327.12 "
32 "	87.23 "	436.16 "

To conclude, the excess attenuation suffered by a wave propagating in a lossy medium is given by:

$$\alpha = 81.8 \frac{L_t}{\lambda} \tan\delta \qquad (27)$$

where α is the excess attenuation, in decibels

L_t is the length of the transmission path, in meters

λ is the free space signal wavelength, in meters

tan δ is the loss tangent characteristic of the transmission medium

It is expected that the loss tangent for the lunar material, in situ, will range from 0.01 to 0.05; accordingly, the excess attenuation will be:

$$0.818 \leq \alpha \leq 4.09 \text{ db/wavelength} \qquad (28)$$

From Figure III-10 one can guess that the received field strength which is the complex interference pattern of the surface, subsurface and reflected waves will vary as a function of frequency, range, depth dielectric properties of the lunar material (both electrical and mechanical), etc. Even the surface wave (air wave component of the field will most likely be dependent upon the surface terrain. Accordingly, the signal levels shown in Figures III-11 through III-19 are only typical of what might be expected. It is on these calculated results, however, that the experiment configuration is based. We are currently working to verify these theoretical results with quantitative experimental data from glacier trials.

SUMMARY OF INPUT SIGNALS

Figure III-10 gives some pertinent experimental geometry and gives an idealized view of the signal paths.

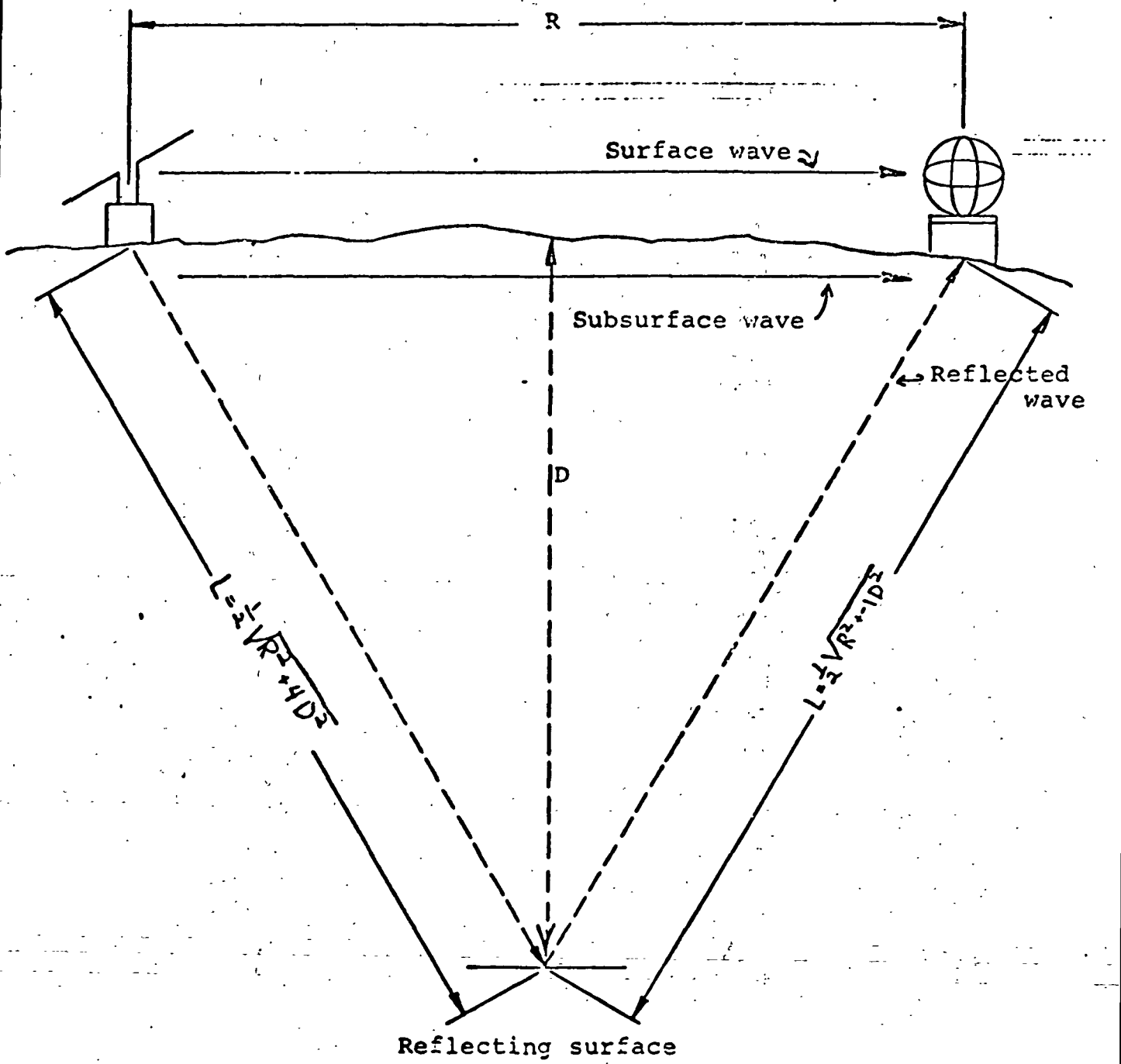

$$P_{surface} \propto K\frac{1}{4\pi R^2}$$

$$P_{reflected} \propto K[\frac{1}{4\pi R^2}] - \alpha L$$

$$P_{subsurface} \propto K[\frac{1}{4\pi R^2}] - \alpha R$$

Figure III-10

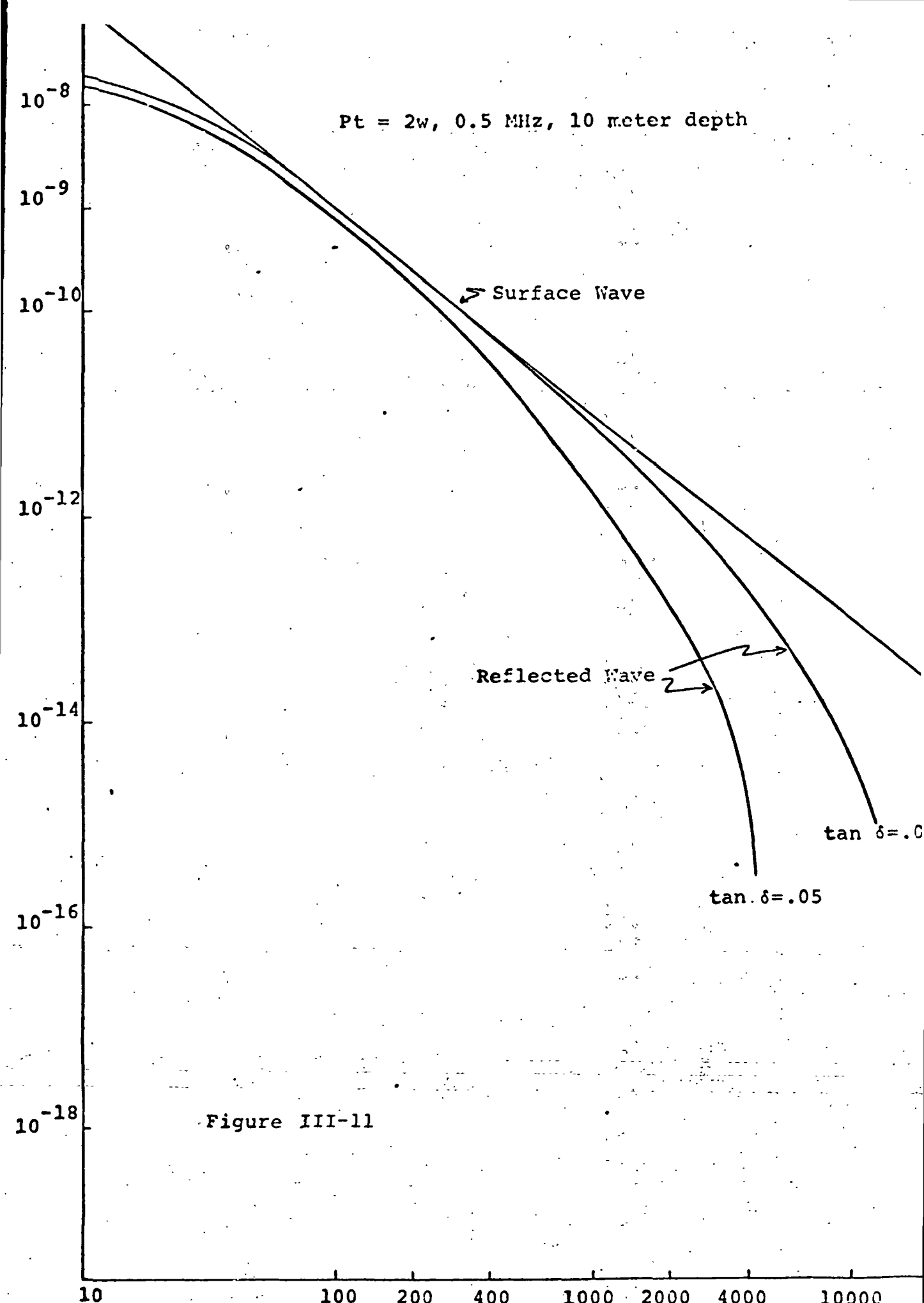

Figure III-11

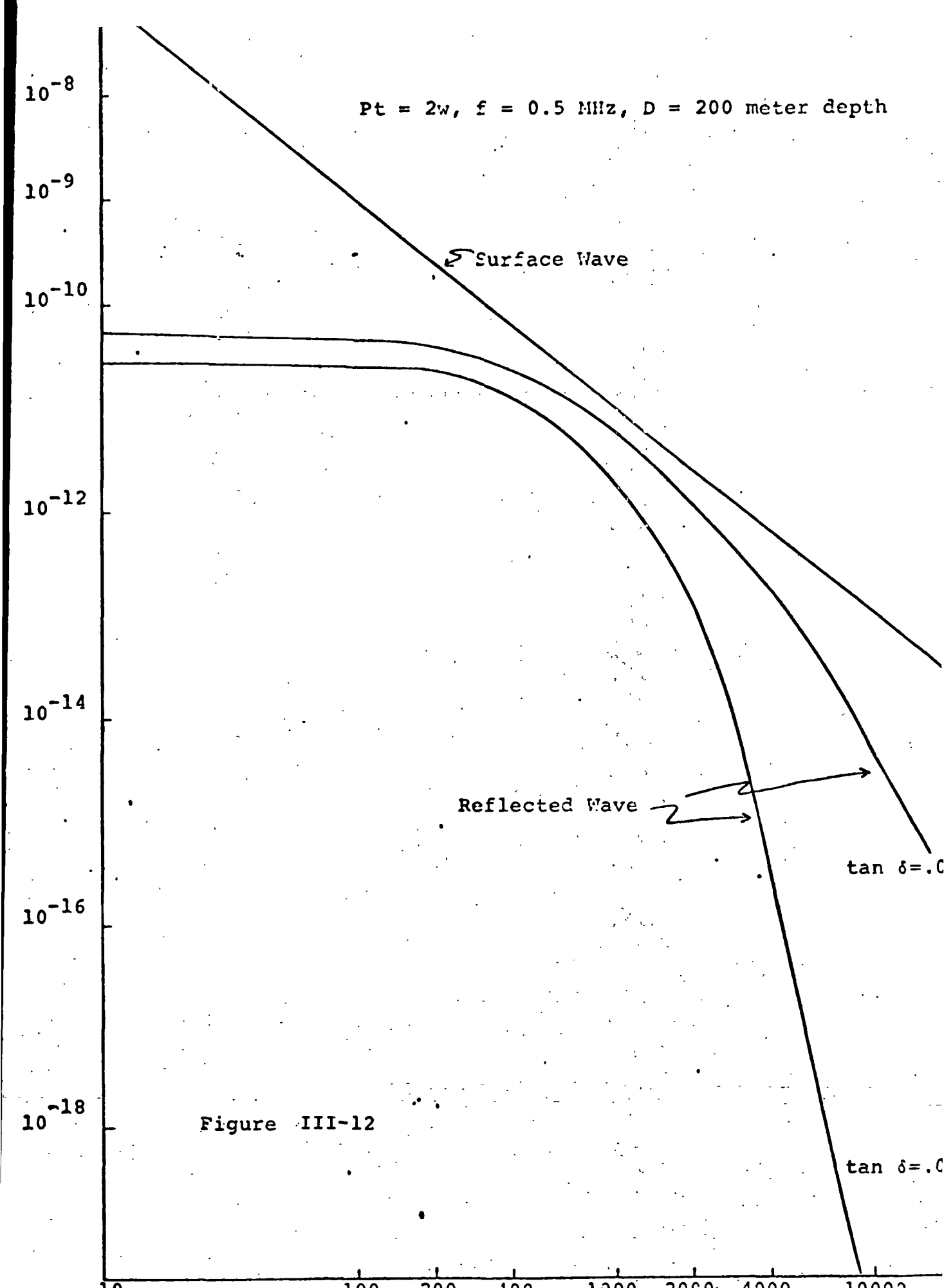

Figure III-12

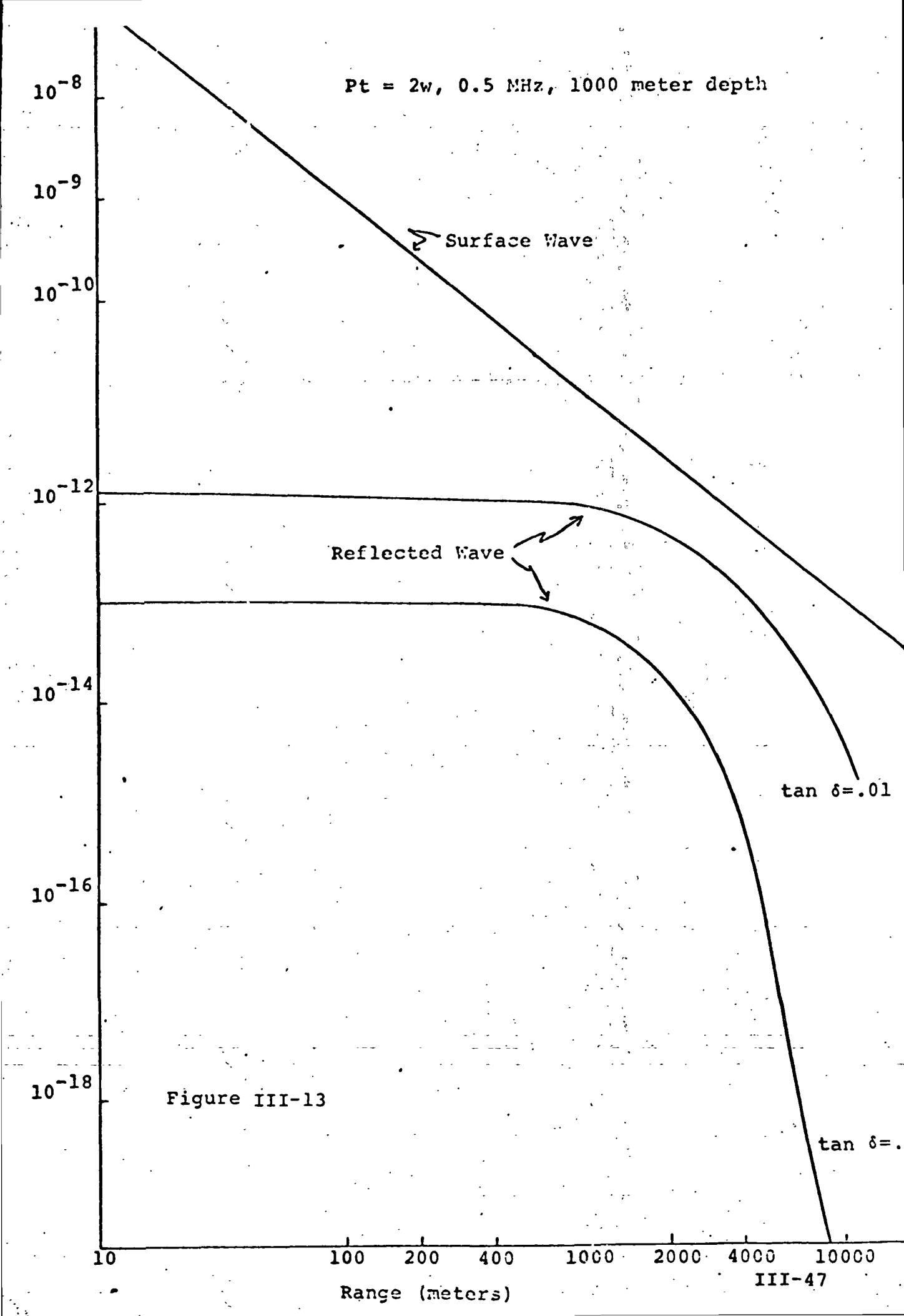

Figure III-13

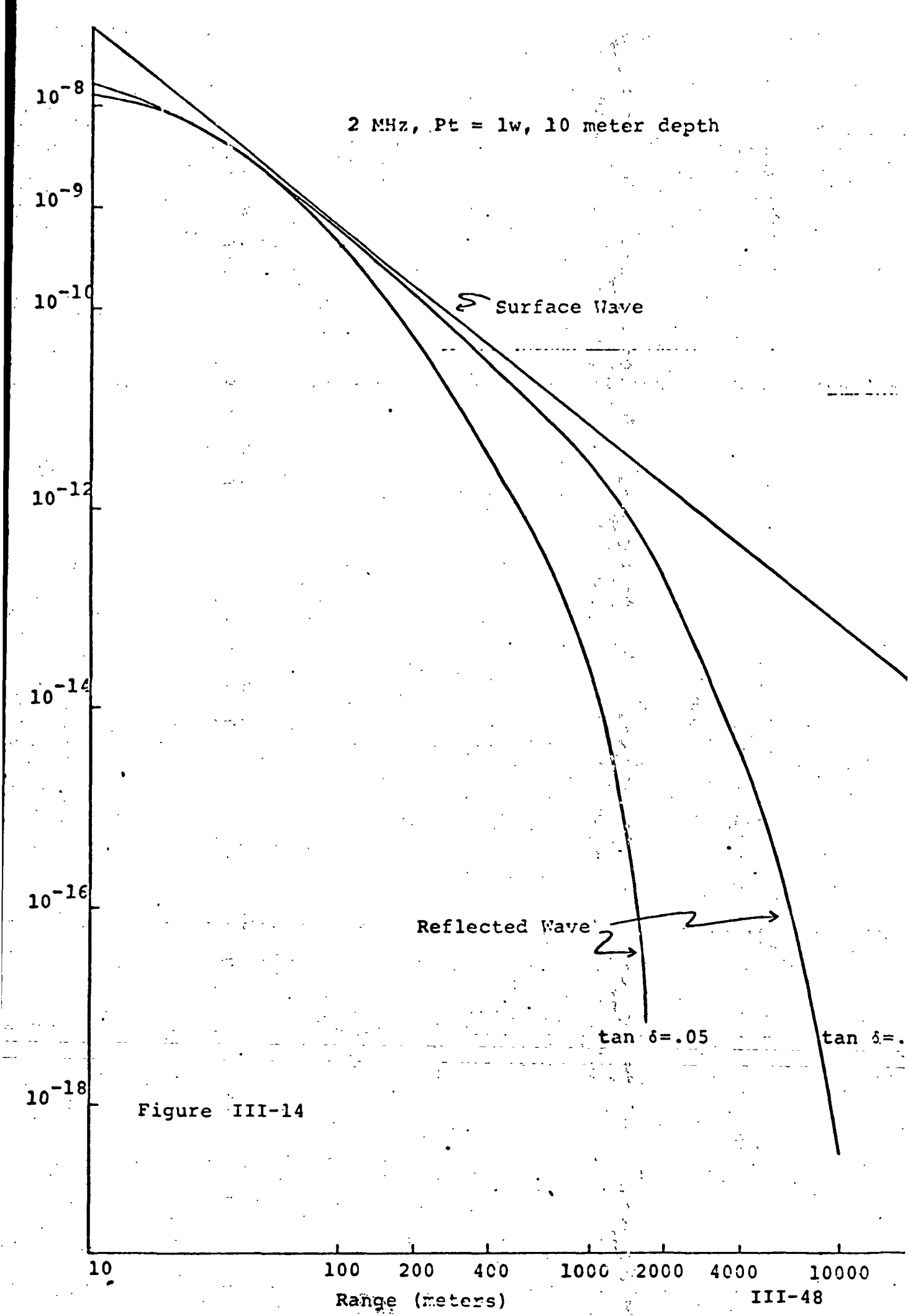

Figure III-14

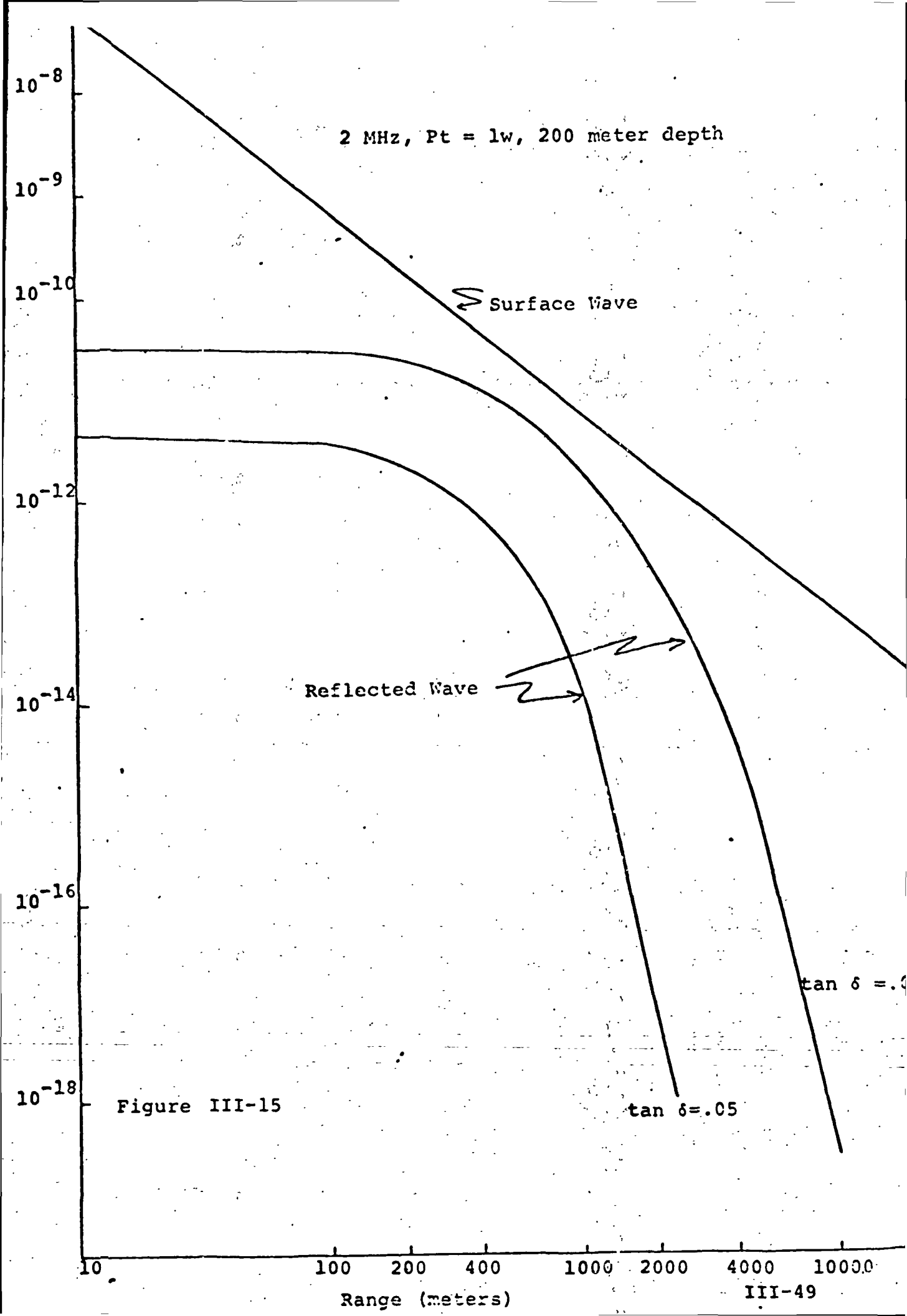

Figure III-15

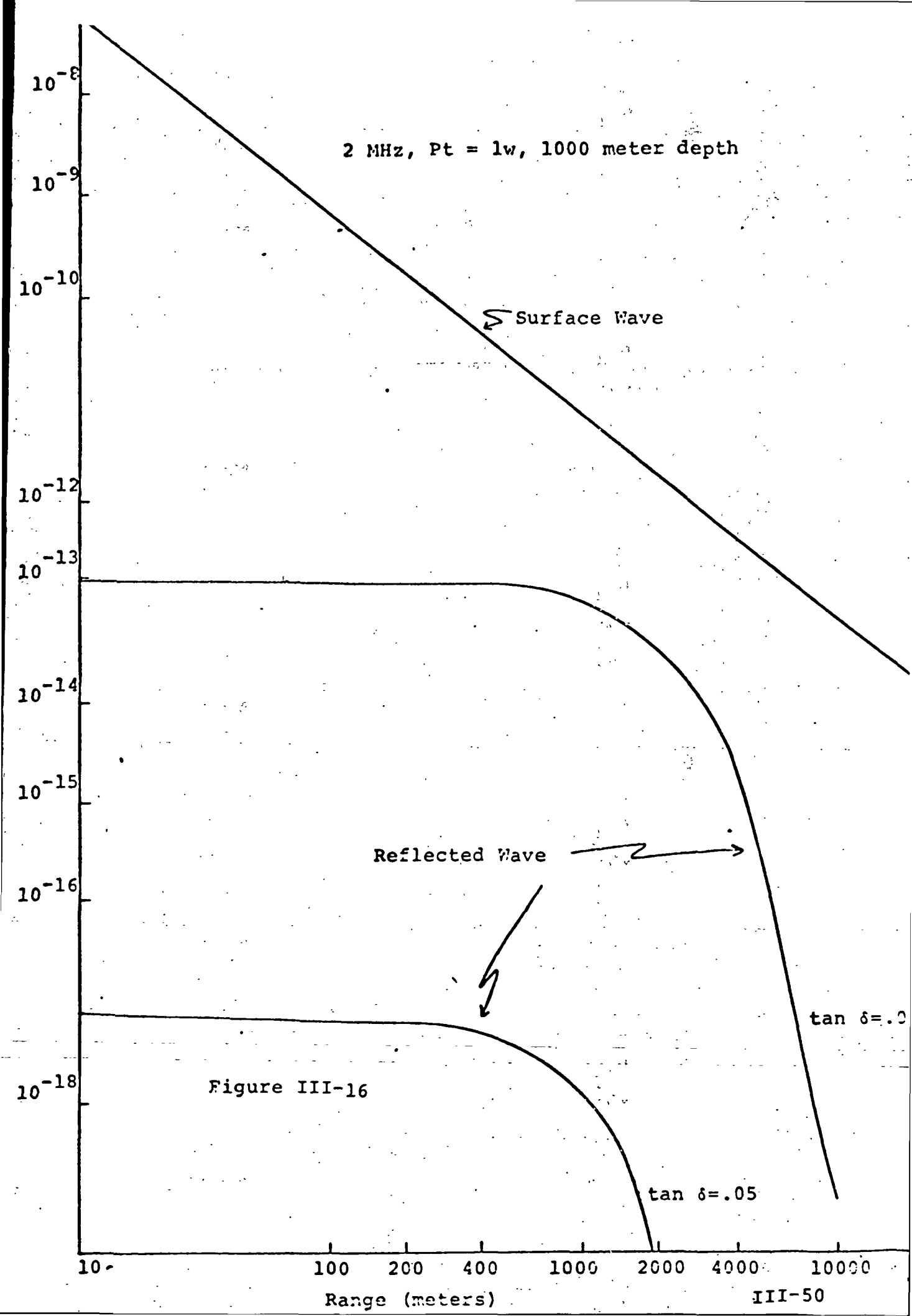

Figure III-16

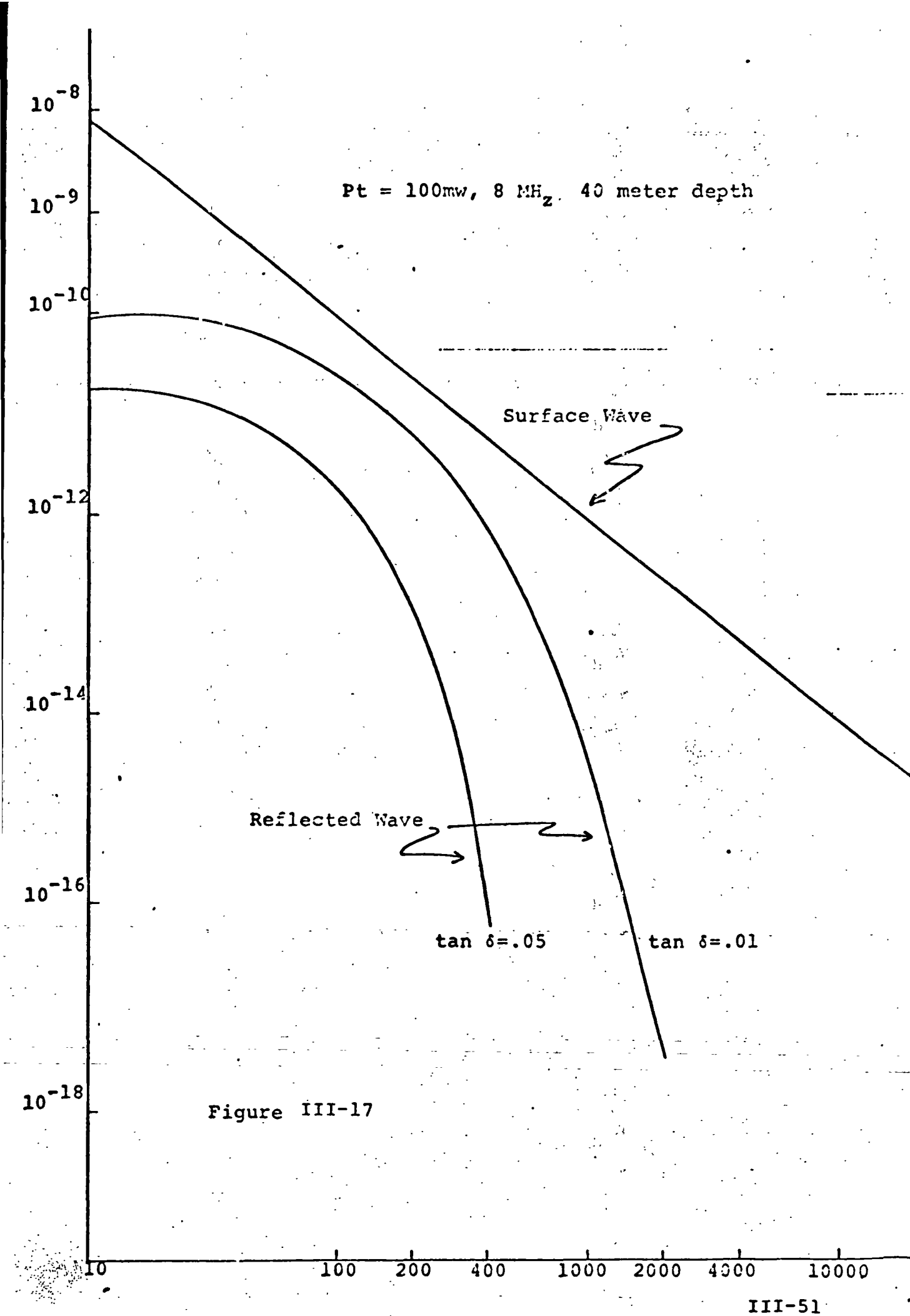

Figure III-17

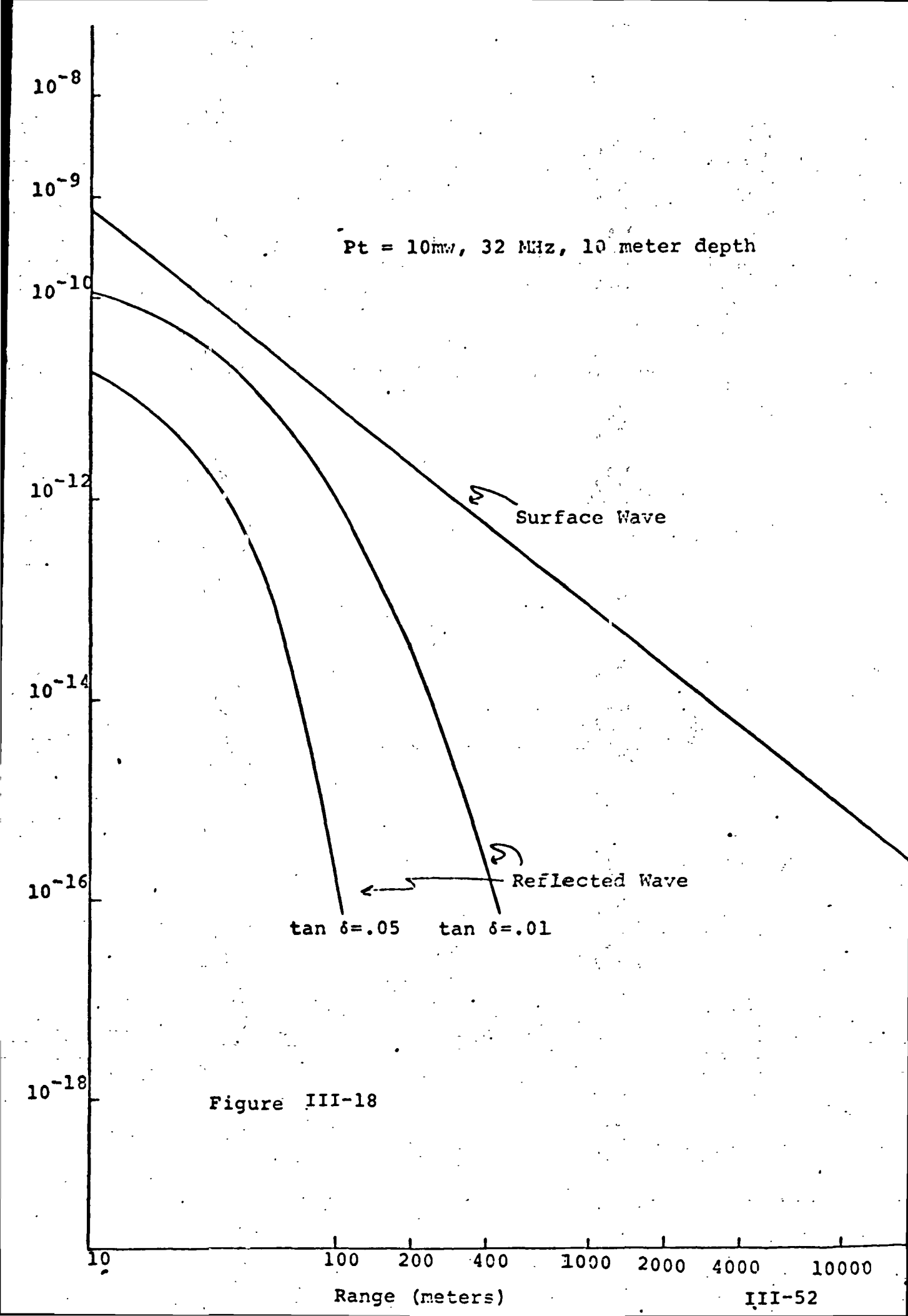

Figure III-18

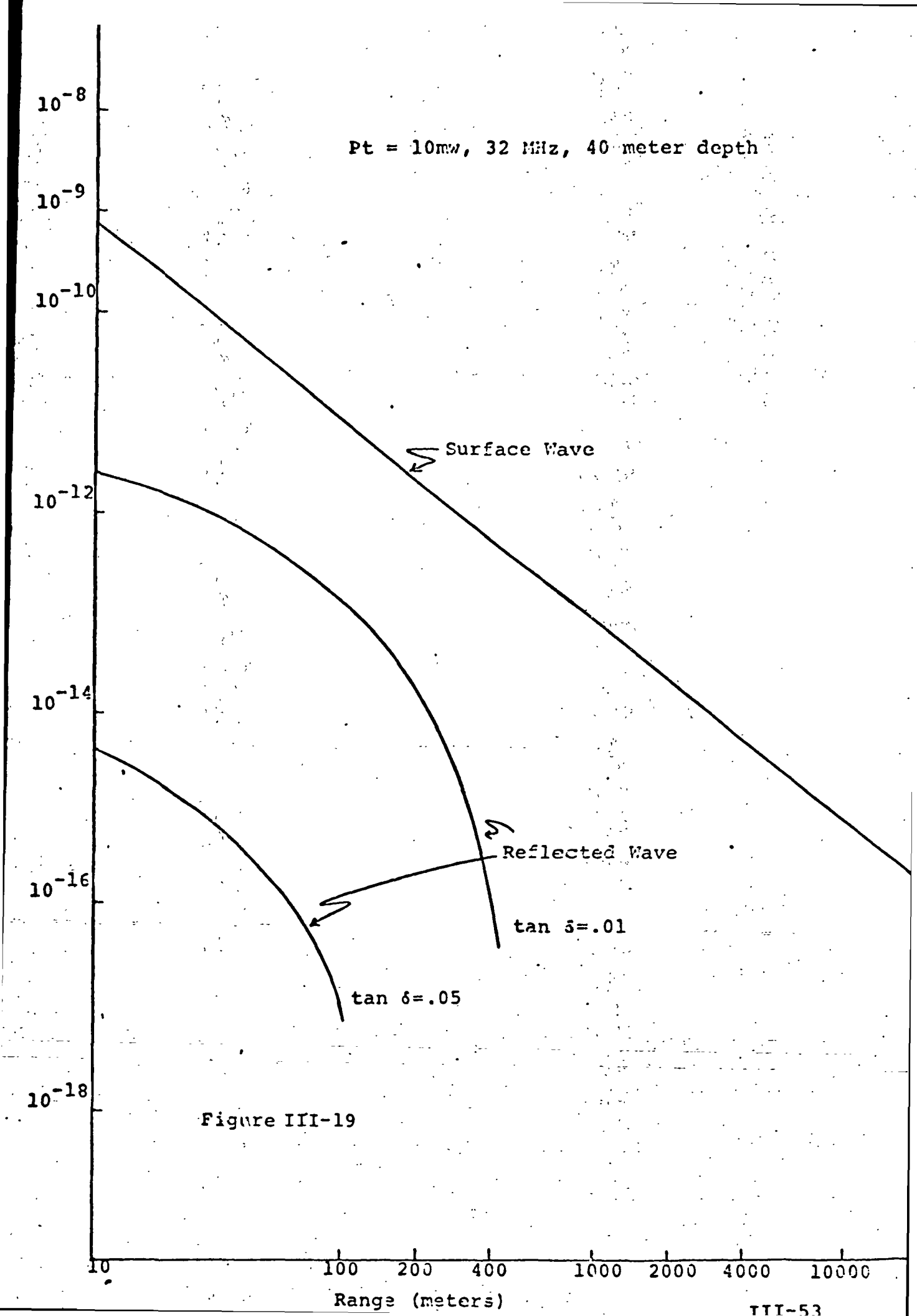

Figure III-19

(iii) Receiver

The basic electrical functions that the SEP receiver must accomplish (see Figure III-20) are: gain, timing, loop selection (to obtain the individual components of the local field), signal filtering to surpress the effect of noise, detection, and because of the wide amplitude range of the input signal, signal amplitude compression.

The wideband (.3 MHz to 35 MHz) low noise (NF_{max} = 6 db) amplifiers performance is nominal and, therefore, designs are readily available. The timing function which is discussed later can be accomplished in a variety of ways and is non-critical. The loop selection or RF switch is also a standard item and a number of good designs exist. (For example, a four diode-bridge with both plus and minus voltages bases.) With the loop selection switches placed as shown in Figure III-20 the summation function is just a node. The last three functions of Figure III-20, namely the filtering, compression/detection and tape unit are judged to be the more difficult and, therefore, critical. Indeed, the tape unit is so critical that to date only one method (unit) has been identified that appears to be applicable to the SEP receiver. Both the filtering and compression functions are now discussed in more detail.

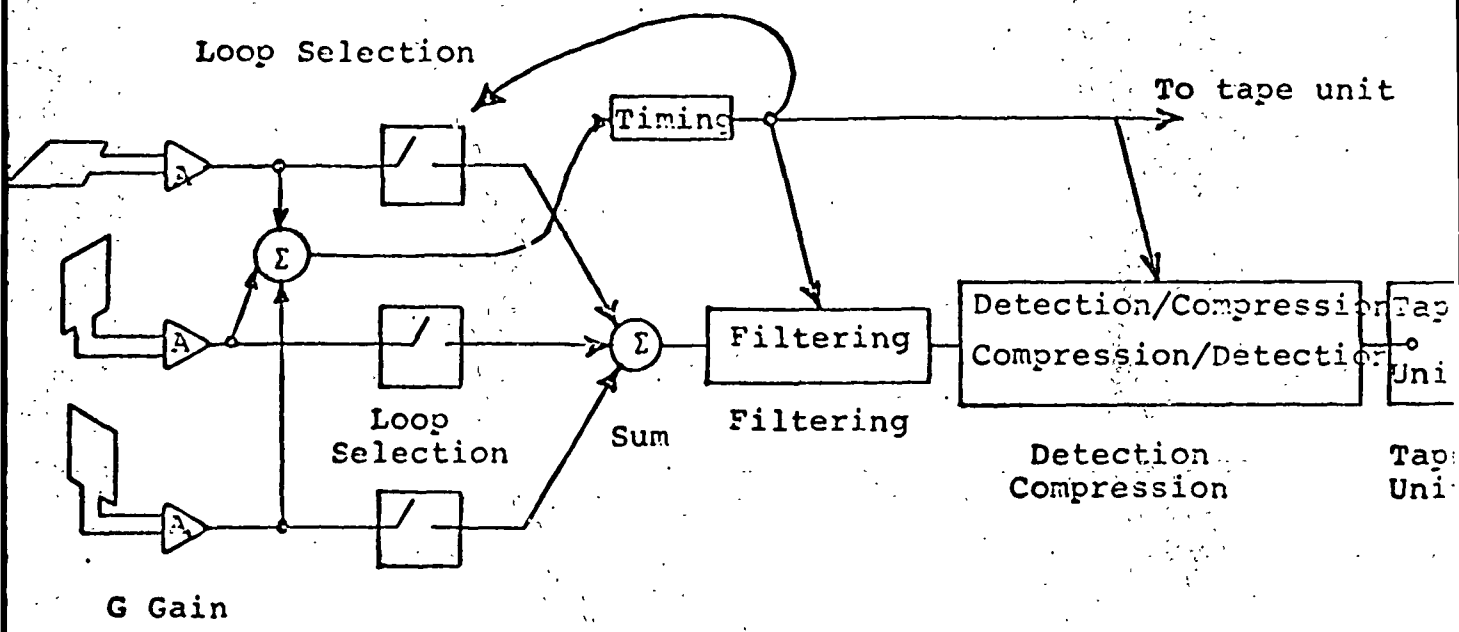

Figure III-20

FILTERING:

It is prudent, in view of the lack of definitive information regarding the LRV noise spectrum to limit as much as practicable the in-band noise. Fortunately, the experiment signals are discrete frequencies transmitted in time sequence, and the experimental configuration has been defined such that the various modulating (amplitude and frequency) phenomena are shown varying so that the receiver signals may be processed through very narrowband filters (≈300 Hz).

There are two (known to me) ways of obtaining very narrowband pass filtering with low insertion loss: either use crystal filters or a phase lock loop. In our original proposal, we chose the crystal filters because phase locked loop tend to become rather complex when dealing (as we are) with a multi-frequency signal that is widely varying in amplitude. We have, by now, studied both systems in some detail and conclude that the crystal filter is the best solution considering the tight time schedule with which we are now constrained.

Figure III-21 shows three methods of connecting the crystal filters. The connection of III-21a represents the simplest hence more reliable. The connection of III-21b has superior noise performance because the signal of the connected filter is not degraded by the noise content in the pass bands of the other seven. At higher signal levels the connection of

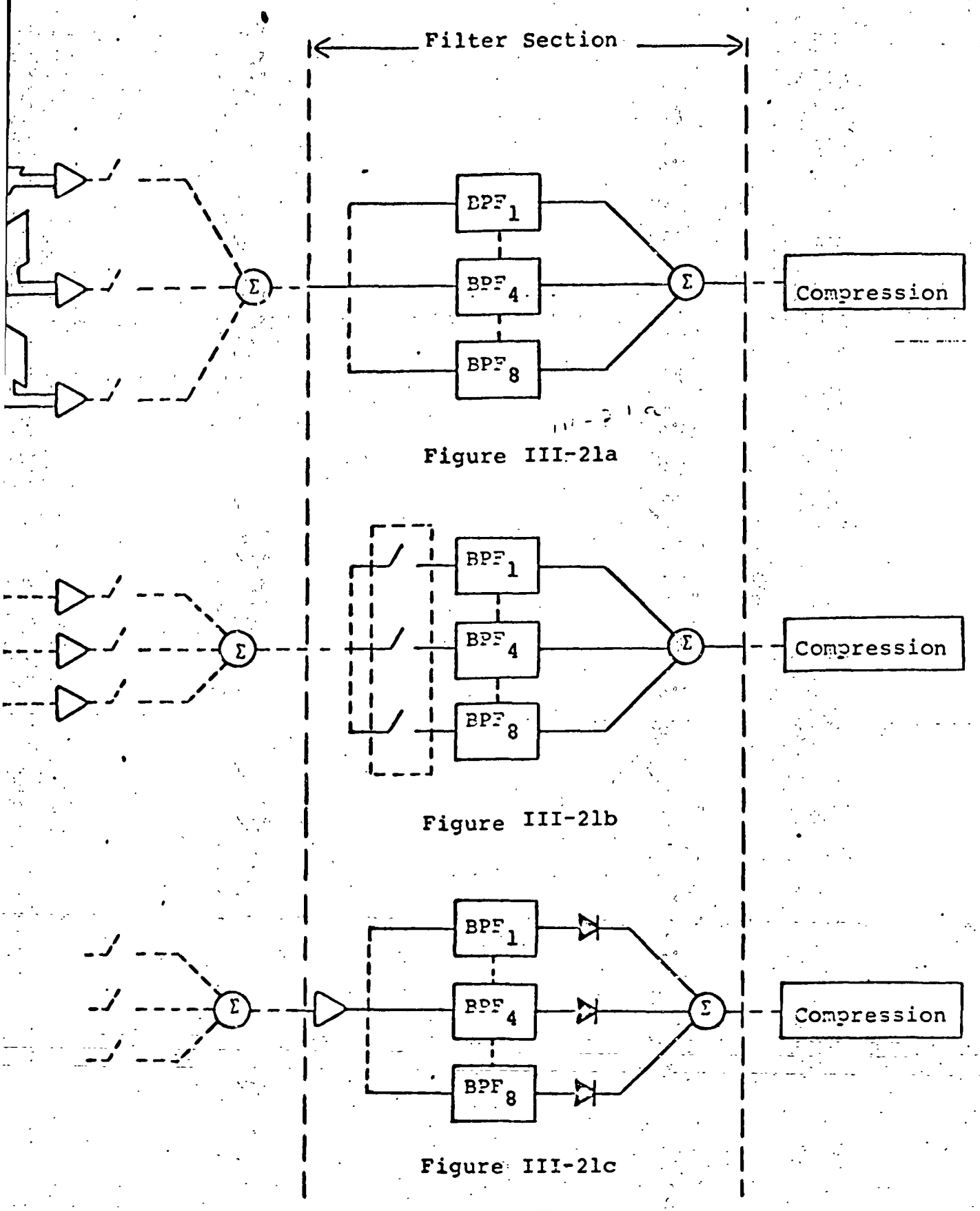

Figure III-21a

Figure III-21b

Figure III-21c

III-21c has equal performance to III-21b because the filter with the largest signal automatically back biases the diodes to the companion filters giving noise (small signal) supression. This connection which gives better performance than III-21a was selected in the original proposal because the diode can also serve as the detector and the configuration tends to minimize the inherent intermodulation distortion when using only one detector.

Results of subsequent studies, however, indicate that the system signal to noise ratio may not be as high as originally hoped and, therefore, the connector of Figure III-21b is recommended.

Typical crystal filter pass band characteristics are shown in Figure III-22. It is desirable to hold the in-band ripple to less than $\frac{1}{2}$ db with the 3 db filter width of 450 Hz and the 30 db skirts width equal to about 1500 Hz. However, the skirt width can be increased if necessary.

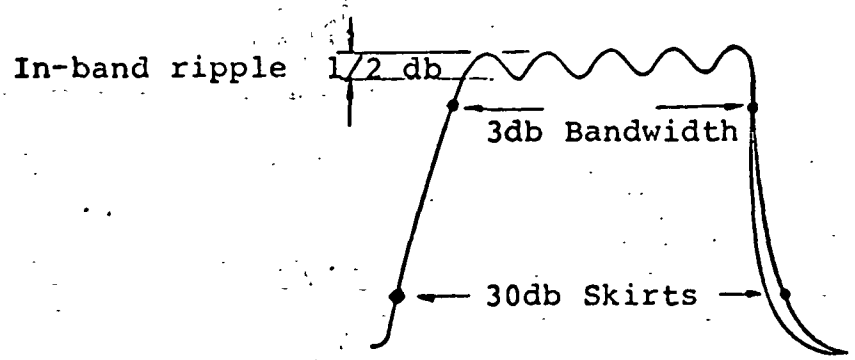

Figure III-22
Crystal Filter Pass Band Characteristics

COMPRESSION TECHNIQUES:

Basically what is to be accomplished in a compression amplifier is to design a transfer function that will compress the input signal range of about 10^8 to some small range say 1 to 5 volts or for the SEP receiver cause the VCO in the tape unit to vary from approximately 300 Hz to 3000 Hz. Figure III-23 gives the mathematical relationship. Incidentally, the results of Figure III-23 show that a one percent reading in a 10^8 range requires the results from the tape recorder to be read to a precision of 1.458 Hz which would seem to be incompatible with the presently contemplated tape unit. However, this difficulty can be overcome somewhat by coding the information into several 300 Hz to 3000 Hz bands where each band is recorded at a different amplitude.

In general, the three methods (systems) for accomplishing logarithmic compression are: (1) a DC or base band system using operational amplifiers; (2) a low frequency carrier system, and (3) a high frequency carrier system. For the SEP receiver application, each system has some merit so each are now briefly discussed.

DIRECT COUPLED SYSTEM:

This system was used in the original proposal in the form of a low frequency amplifier (DC to 3000 Hz) system

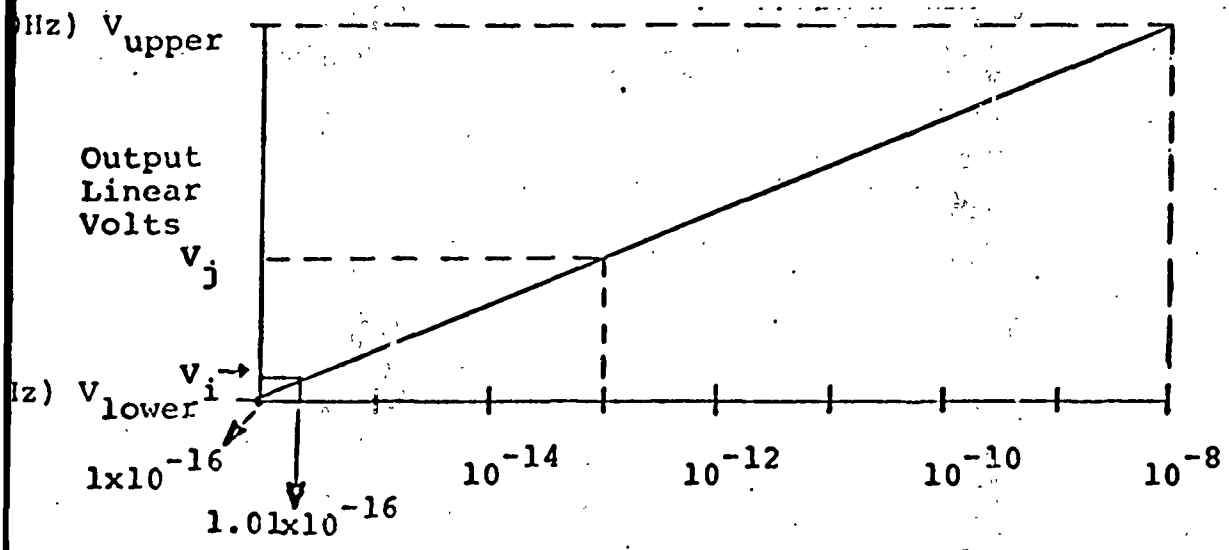

$$\frac{V_i - V_{lower}}{V_{upper} - V_{lower}} = \frac{\text{Log } 1.01x10^{-16} - \text{Log } 10^{-16}}{\text{Log } 10^{-8} - \text{Log } 10^{-16}}$$

$$\frac{V_i - 300}{3000 - 300} = \frac{\text{Log } 1.01 - 0}{\text{Log } 10^{8}} = \frac{.00432}{8}$$

$$V_i = 300 + \frac{2700(4.32)10^{-3}}{8} = 301.458 \text{ Hz}$$

$$\Delta V_i \, (\Delta F)/_{1\%} = 1.458 \text{ Hz}$$

Figure III-23

using operational amplifier and resistor feedback in a piece-wise linear approach.* This technique is standard when a non-linear transfer function is needed with operational amplifier. Diodes are required, however, and, therefore, the break points are difficult to temperature compensate. One way of getting around this difficulty is to make the output swing so large that the diode threshold is negligible by comparison. However, for this application where the required compression range (10^8) is larger than we had originally thought necessary and low power drain is more important due to the longer EVA duration, we now recommend that the carrier scheme be used.

LOW FREQUENCY CARRIER SYSTEM:

Figure III-24 shows one method of implementing a low frequency AC (carrier) compression amplifier. If the input signal is very small, only the last amplifier in the chain is saturated. As the signal increases in amplitude successively earlier state saturate (limit) and the output is formed from each stage properly "weighted" with a ladder network to give a logarthmic response. This concept is valid over a range of frequencies limited by the value of the coupling capacitor at the low end

* "Electrical Surface Properties Proposal," October 23, 1969, Figure III-9.

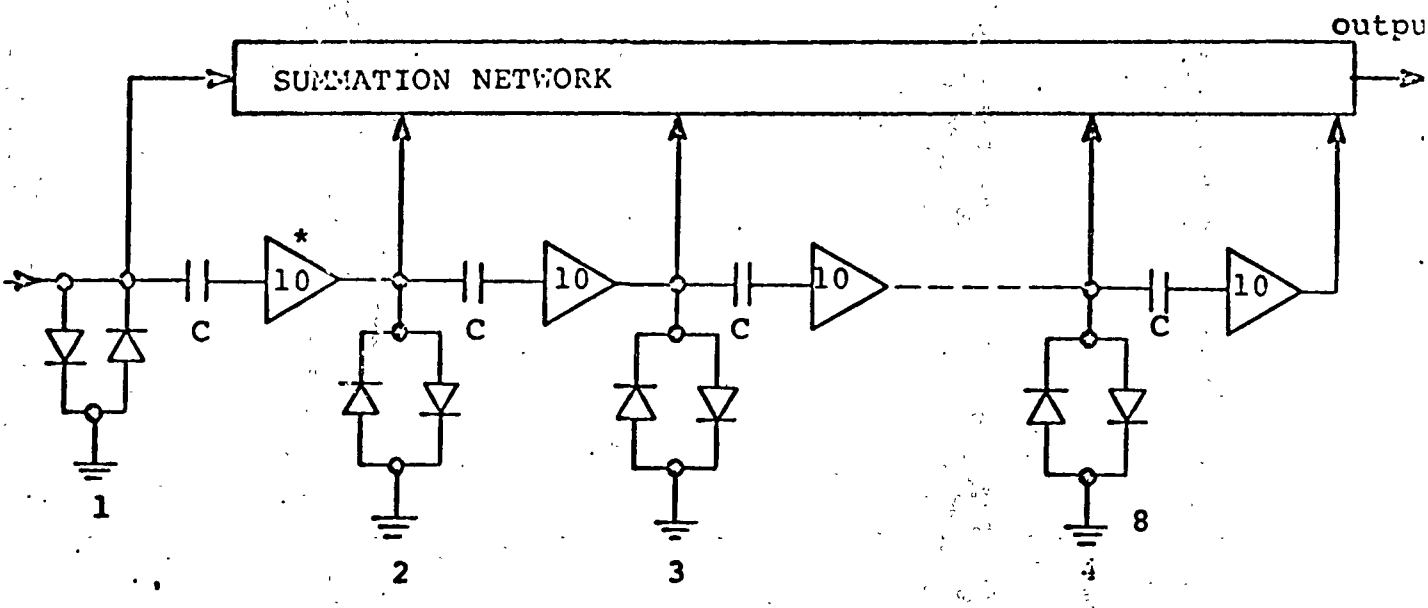

*each amplifier has a gain of 10

AC Logarithmic Amplifier

Figure III-24

of the band and by the phase delay (shift) at high frequencies.

As previously mentioned, this system has been extensively used in several scientific probes.[3] One general difficulty is that this implementation tends to be unstable and requires not only high frequency components to minimize phase shift but also a great deal of decoupling, stiff biases, etc., which increases both the complexity and power drain.

LOGARITHMIC AMPLIFIERS:

An amplifier circuit in which an incremental gain is inversely proportional to the input signal voltage has the characteristics of logarithmic mode of operation. With reference to Figure III-25a, the incremental gain ΔG is related to the input signal V_i as

$$\Delta G \triangleq \frac{\Delta V_o}{\Delta V_i} = \frac{m}{V_i} \qquad (29)$$

integrating, we obtain

$$V_o = m \log V_i + c$$

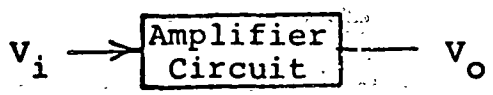

Figure III-25a

[3] Ibid footnote #1.

where c = constant of integration

V_i and V_o = are input and output voltages respectively

m = slope of the curve

Three main circuit design approaches are available to correlate the input and output voltages logarithmically in order to achieve high dynamic range capability. These approaches are,

(1) Non-linear feedback circuits (piece-wise linear)

(2) Circuits using non-linear loads (Reference #1)

(3) Successive detection circuits

The first two which have been discussed and the successive detection method is commonly used for high frequency logarithmic compression amplifiers.

DESCRIPTION OF SUCCESSIVE DETECTION METHOD:

Figure III-25b describes the typical functional diagram of a logarithmic amplifier circuit using a successive detection approach wherein A's are the amplifier stages, D's are the detector stages feeding the delay line.

The individual output of each detector stage is shown in the lower portion of Figure III-25c. Since the time delays in each delay section are the same as those of amplifier stage, the output sun is as shown in upper portion of Figure III-25c, whereby the input and output voltage bear a logarithmic relationship.

SUCCESSIVE DETECTION METHOD

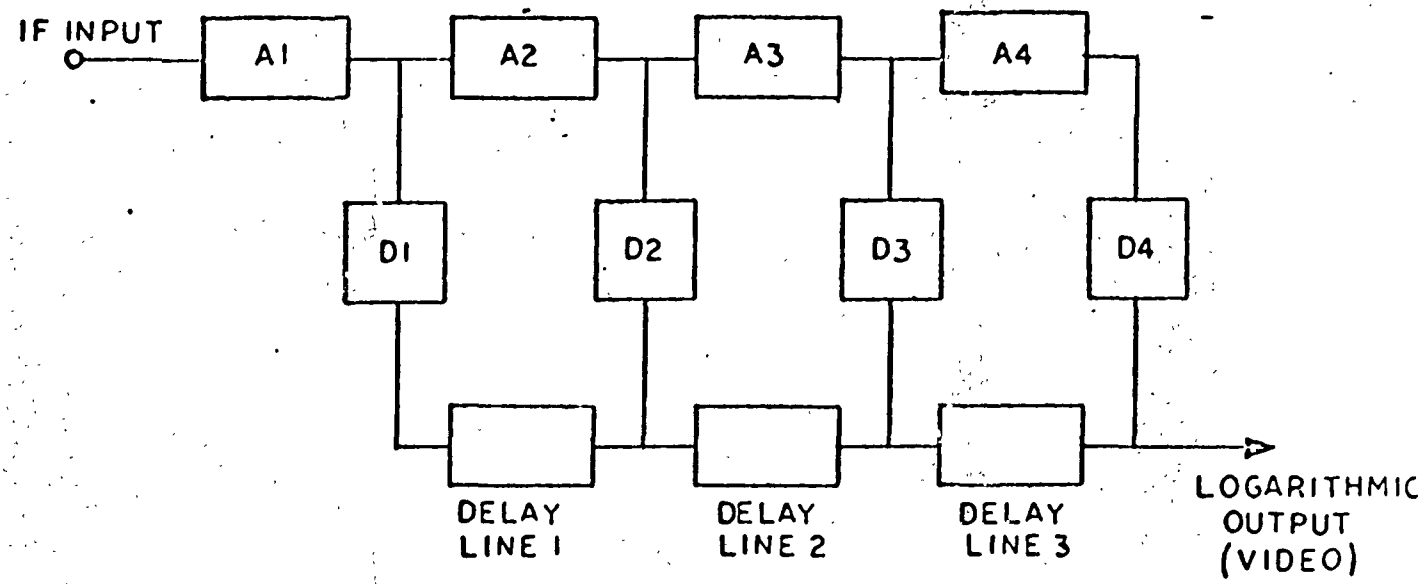

FIGURE III-25b

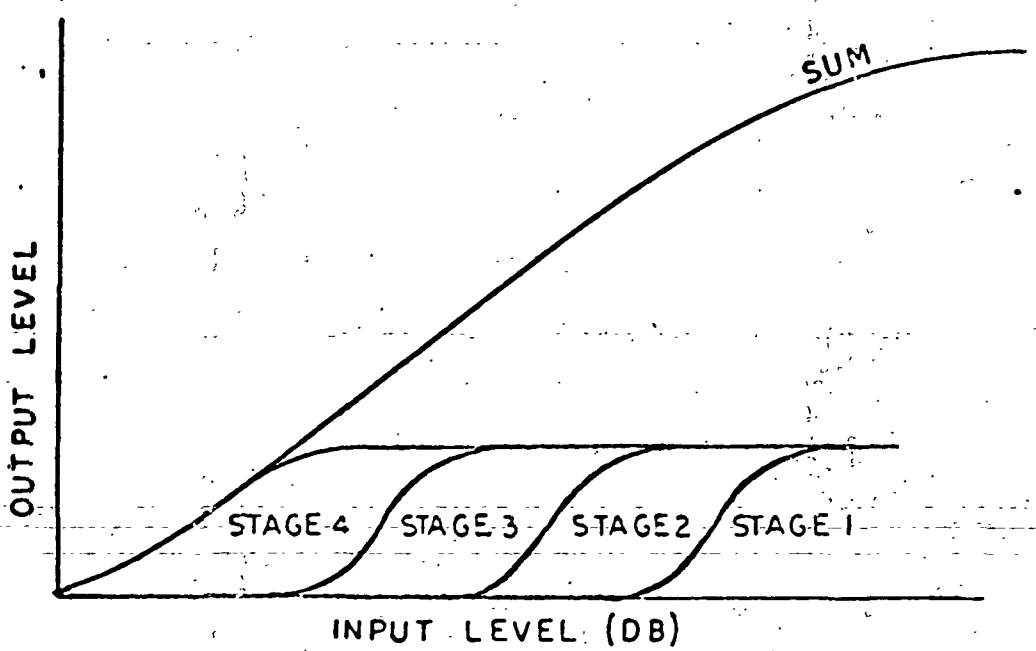

FIGURE III-25c

Logarithmic IF amplifiers using this technique are available at various frequencies and, therefore, can be considered.

THE RECEIVER BLOCK DIAGRAM:

Based on technical considerations that were outlined in the previous sections, the receiver configurations shown in Figure III-26 is recommended. This system which is very similar to the original proposal may be implemented using standard electronic designs.

The front end amplifiers should have a maximum noise figure of 6 db with a gain of 20 db $\pm\frac{1}{2}$ db per stage over the expected temperature range in a frequency band from .3 MHz to 35 MHz.

The preamp is made up from the same stages as the front end amp.

The RF switches are 4 diode quads made with HP hot carrier diodes.

The band pass filters are standard crystal filters with 450 Hz BW (3db) and about 1500 Hz 30 db skirts. The in-band ripple should be loss than $\frac{1}{2}$ db peak to peak. The insertion loss is not critical but should be specified less than 6db.

The mixer preamp is a one stage amplifier and serves to isolate the mixer from the crystal filters.

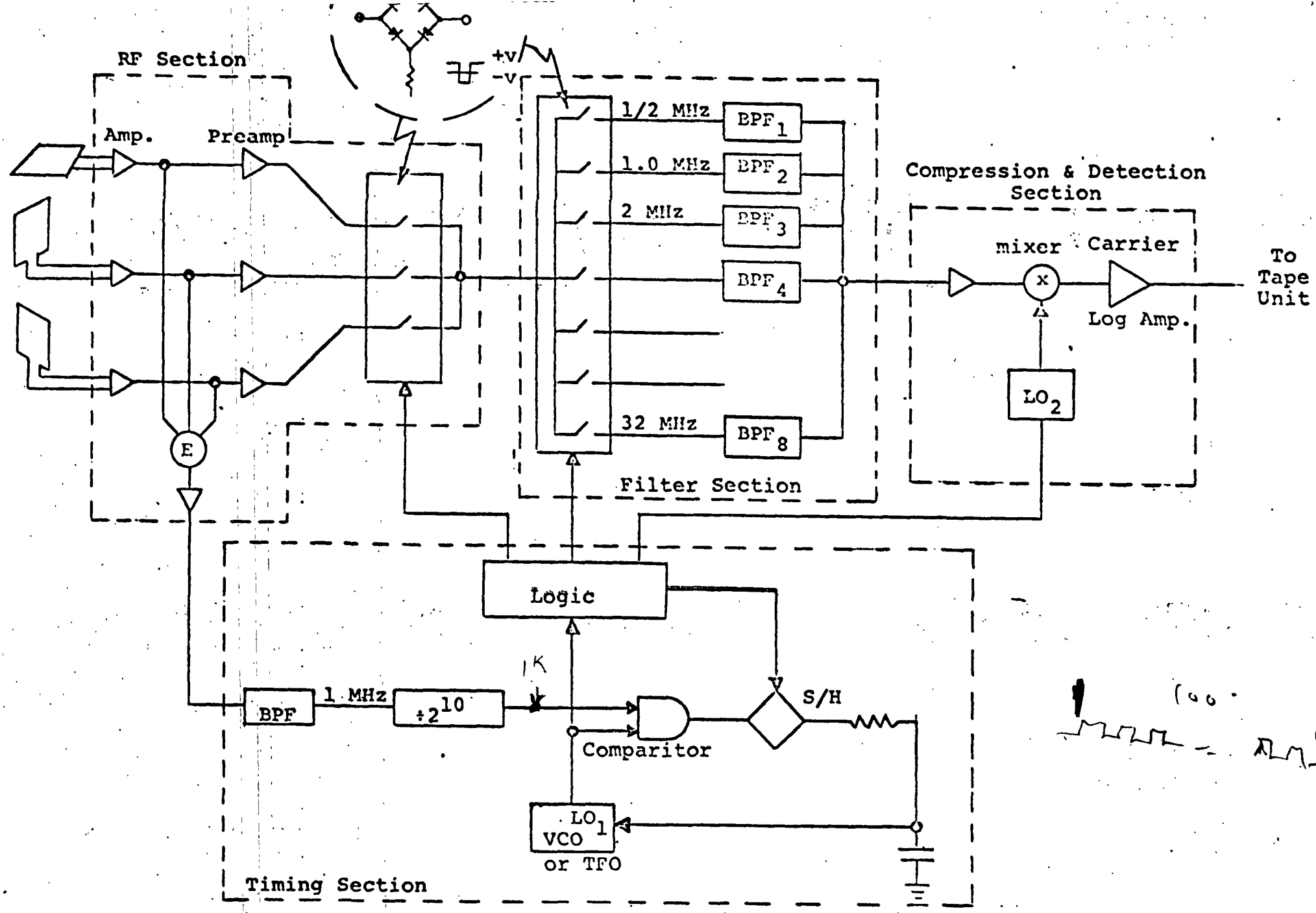
RF Section
+v
-v
Amp.
Preamp
1/2 MHz
BPF 1
1.0 MHz
BPF 2
2 MHz
BPF 3
BPF 4
32 MHz
BPF 8
Compression & Detection Section
mixer
Carrier
To Tape Unit
Log Amp.
LO 2
E
Filter Section
Logic
1K
BPF
1 MHz
÷2 10
S/H
Comparitor
LO 1
VCO
or TFO
Timing Section

The operating frequency of the logarithmic amplifier and its companion local oscillator is not critical and the choice should be governed by performance and delivery of qualified commerical designs.

The receiver timing may be accomplished in a number of ways the exact system choice should be based on simplicity of components. The RCS proposed timing system would appear to be overly complex, but it would certainly suffice. I believe the system indicated in Figure III-26 is simpler. Functionally, the timing section must generate the necessary control signals to sequencially switch the three loop antennas, the band pass filters and the proper local oscillator synchronously with the transmitter. Analysis of the timing error analysis indicated that without resynchronization in the required stability of the local oscillator (LO#1) would be one part in 10^6 per day with a frequency offset of one part in 10^7. We believe that to obtain this offset would require a crystal oven and should be, therefore, avoided. The feedback loop shown allows direct frequency comparison with the transmitter one per second and should suffice.

e. Tape Recorder

A typical late Apollo mission could involve three EVA's, each of six-hour duration, with traverses lasting four or five hours. A minimum of ten hours of recording time is desired to allow the receiver to operate without attention during two traverses.

For this application, power consumption and operating time directly affect battery weight. Since a relatively long operating time is desired, power consumption should be small. Additionally the recorder should be small and light-weight, it should contain enough tape so that tapes need not be changed, and it should be sealed to maintain a proper environment for the mechanical parts and lubricants.

Provisionally, the tape recorder selected to meet these requirements is the Leach 11-14000 Data Storage Electronics Assembly (DSEA). This unit was designed as a voice recorder for use aboard the LM, and has been qualified for use in the LM and for return to earth in the CM cabin environment. The unit is used in the Lunar Module to record voice-keyed audio with superimposed time information. A reference frequency is recorded for operating the speed-control servo in the reproduce transport.

(i) Specifications

Specifications for the existing, qualified, tape

recorder are listed below:

Size: 6.22 x 2.05 x 4.0 inches

Weight: 2.3 pounds

Power: 2.4 watts

Channels: One. (The DSEA uses 4 tracks with track switching to realize the recording time)

Recording Time: 10 hours

Tape Speed: 0.6 inches per second

Tape: 450 ft. of 1/4 inch, 1/2 mil tape.

Frequency Response: 300Hz to 5.2KHz, with audio compressed into 300Hz to 3KHz, a time-code modulated FM carrier at 4.4KHz ± 5%, and a reference at 5.2KHz.

Signal to Noise Ratio: 35dB.

Operational Environment: Temperature: 0° to 160°F.

Pressure: Atmospheric to hard vacuum

Acceleration: 15g

Random Vibration: 9g rms for 3% p-p flutter

Shock: 52g for 11ms, 1/2-sine shock (survival only)

Non-Operational Temperature: -20°F to 160°F

Start Time: 50 milliseconds

Track Switching and Reversal Time: 100 milliseconds

Life: 5000 hours.

Storage: 5 years, provided recorder is operated at least once every 120 days for a minimum of one minute.

Survival Probability for 10-hr. mission: 0.9998

(ii) Operation

Once loaded and initialized for operation, the DSEA operates automatically for up to 10 hours, with track switching and tape motion reversal accomplished by logic circuitry using latching relays. Track switching at the end of each of the 2.5 hour passes occurs in less than 100 milliseconds. The latching relays provide a memory function and ensure that recording will resume on the same track in the same direction after a power interruption so that no special attention need be given the tape unit before or after the shut-down between traverses.

An indication of recorder operation is given by a tape motion amplifier which provides a relay closure when signals are sensed on the tape in the range of 300Hz to 3KHz; this signal may be used to drive a go/no-go indicator, since the VCO will continuously supply a signal to the recorder regardless of the received signal strength.

(iii) Data Retrieval

Following the final traverse, the recorder is removed from the receiver package and returned to earth. No attempt at handling the tape magazine need be made and the seal need not be opened, alleviating the problems of dust and mishandling. The weight of the recorder is small (2.3 lb.) and the recorder itself serves as a protective carrying case for the return trip. This procedure is essentially the same as that used to return the LM's DSEA, and experience has indicated that the tape is suitably protected by the recorder.

(iv) Preflight and Postflight

The DSEA is intended for use as a recorder only, although a monitoring signal is available for each tape track. Playback after recording is done with a reproduce transport in a test set provided by the manufacturer; Leach, NASA/MSC and KSC have playback equipment for the DSEA as configured for the LM, so it is obviously desirable to maintain interface compatibility.

The DSEA is tested by recording a test tape magazine for playback in the reproduce transport. Following test, a clean tape magazine is installed, the head shield realigned, and the DSEA is sealed using a fresh O-ring and a coat of sealant. A 'reset' pulse is applied to set the control logic to track 1 forward (this need be done

only on the ground) to prepare the recorder for operation. After the fourth pass is completed the DSEA will stop until another reset is applied; thus preventing overwriting of data.

(v) Modifications

The DSEA will work in this application with minimal modification; indeed it will operate satisfactorily with no modification at all, although a few simple changes may be desirable.

Since the voice operated keying feature of the DSEA is not required in this application, it may be desirable to eliminate this feature to save some weight and power consumption.

The input power level required for the existing DSEA is 115 volts, 400 Hertz; this is transformed down to 26 volts to operate the drive motor. Since this input power must be provided by a battery driven inverter in the experiment, it may be desirable to modify the DSEA to accept 26 volts, 400 Hertz directly.

Discussions with the manufacturer of the DSEA are continuing to define the desirability of these and other minor modifications which can be accomplished without requiring extensive requalification.

III-2. Envelope Description

The experiment package consists of two assemblies, a transmitter (assembly I) and a receiver (assembly II). Before deployment the transmitter assembly contains the transmitting antennas on four reels, and the receiver assembly contains the receiving loops folded in a flat configuration. The transmitter is to be deployed a short distance from the LM and the receiver may be mounted on the Mobile Equipment Transport, on the Lunar Roving Vehicle, or may be hand carried for a walking traverse.

a. Transmitter Mechanical

The transmitter assembly contains the transmitter electronics, the antennas reels, and a solar panel for a power source. The transmitter case is a cylinder of 6-inch diameter mounted on a 9x9 inch base which serves as a protective cover for the solar panel before deployment, and as a foot for the assembly after deployment.

The four elements of the transmitting antennas mount on four reels stowed around the transmitter. Each reel measures 6.25 in ID, 8.5 in OD, and 1 inch thick, and weighs less than 1/3-lb without wire. Handling of the reels may be done using a universal handling tool or a special tool may be supplied to interface conveniently with the reel hubs.

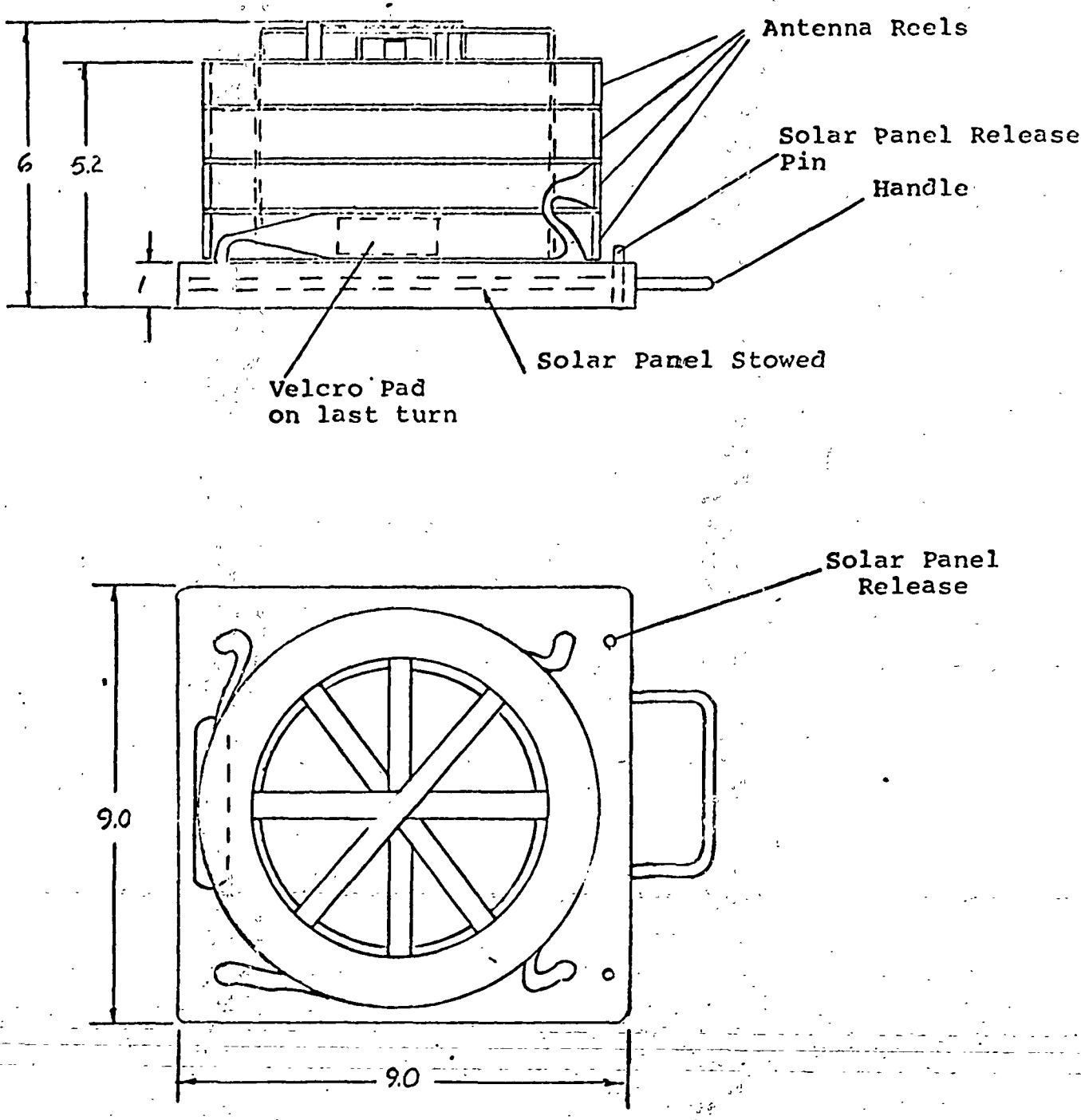

Figure III-2.7 Transmitter Stowed

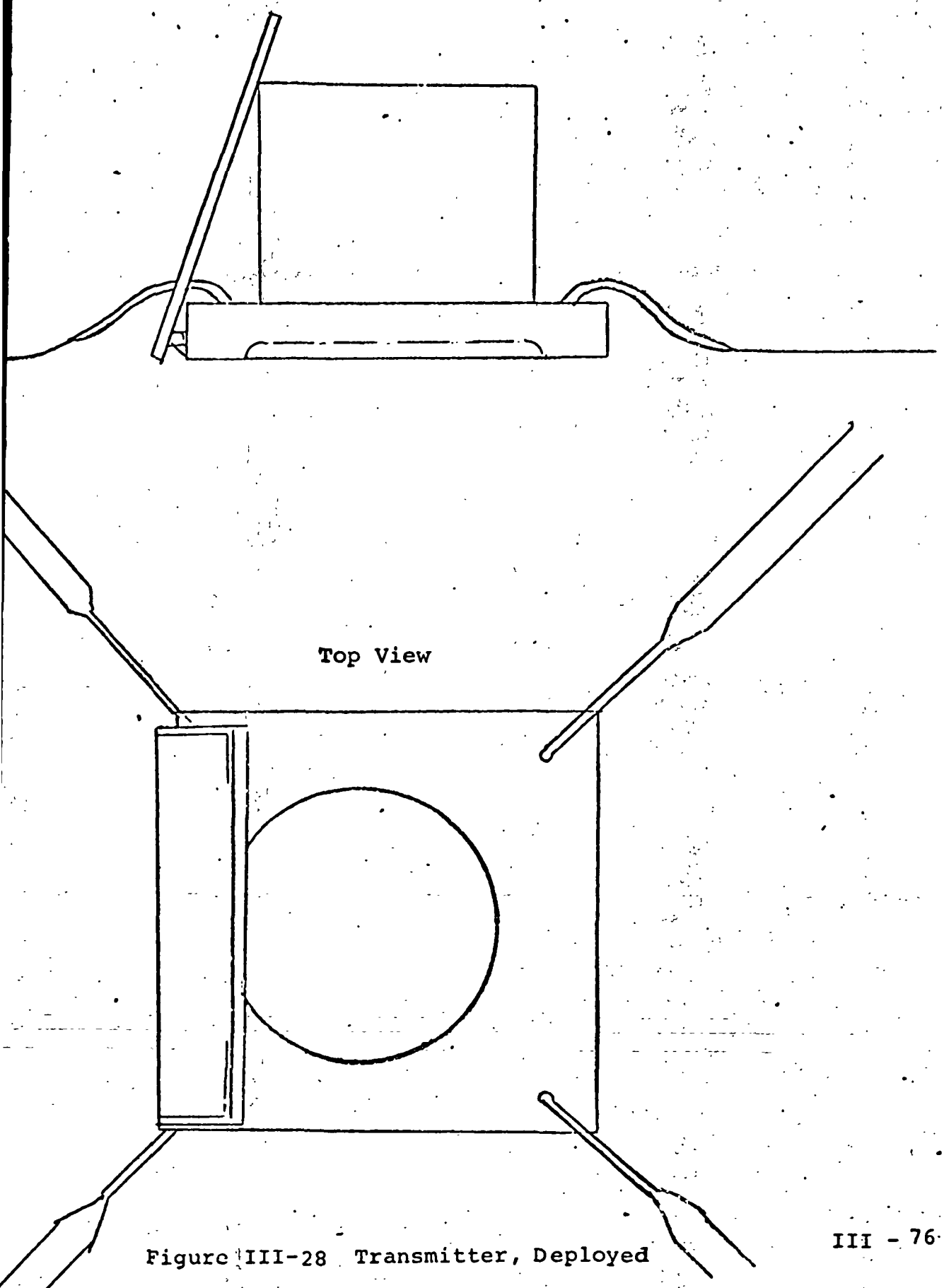

Figure III-28 Transmitter, Deployed

The solar panel provides continuous power to the transmitter and also serves as a sun screen for the transmitter's radiating (top) surface. The panel measures 9x9 inches and weighs approximately 1 lb with its fixtures.

Essentially all the volume in the transmitter case is allotted for the transmitter electronics. The interior dimensions, after thermal blanketing, are 5.5 dia x 4.5 inches high or 107 in^3.

b. Receiver Mechanical

The major features of the receiver assembly are the case (a), containing the electronics, tape recorder, and batteries, the antenna assembly (b), and an extendable mast (c) for Rover use. The antennas and mast will be sufficiently strong to permit handling of the package by the antennas.

The space remaining in the receiver case after the thermal blanketing is 4.5 x 8 x 8 in. (256 in^3). The allocation of this volume is as follows:

Recorder with interconnect block:	2.1x5x7	(73.5 in^3)
Energy source (Silver-Zinc battery):	2x4x7	(56 in^3)
Receiver Electronics:	2x5x7	(70 in^3)

Within the case, a central web serves as the medium for conducting heat from the subassemblies to the heat switch. The tape recorder is mounted by means of slide

fasteners, and is released after the last traverse by opening a door and pulling a lanyard.

A three-position lever-type control and an indicator are located on the side of the receiver case (mounting on the top of the case would increase the possibility of contaminating the radiator with dust). Position 1 of the control turns the receiver off; position 2 places the receiver in the semi-active thermal control mode between traverses, and position 3 turns the receiver on. When the receiver is on, the indicator is illuminated when there is satisfactory output from the tape motion sensor. When the receiver is placed in the semi-active thermal control mode, the indicator remains lit for several seconds after the switch is thrown, and then is extinguished; and when the receiver is shut off, the indicator goes off immediately.

c. Stowed Configuration

In the stowed configuration, the complete package occupies a volume of less than one cubic foot. The transmitting antennas occupy four reels, the receiving loops are folded flat, and the solar panel for the transmitter is stowed beneath the transmitter foot. To prevent dust contamination, the solar panel and the radiating surfaces for both the transmitter and receiver are covered by protective sheets until deployment is complete.

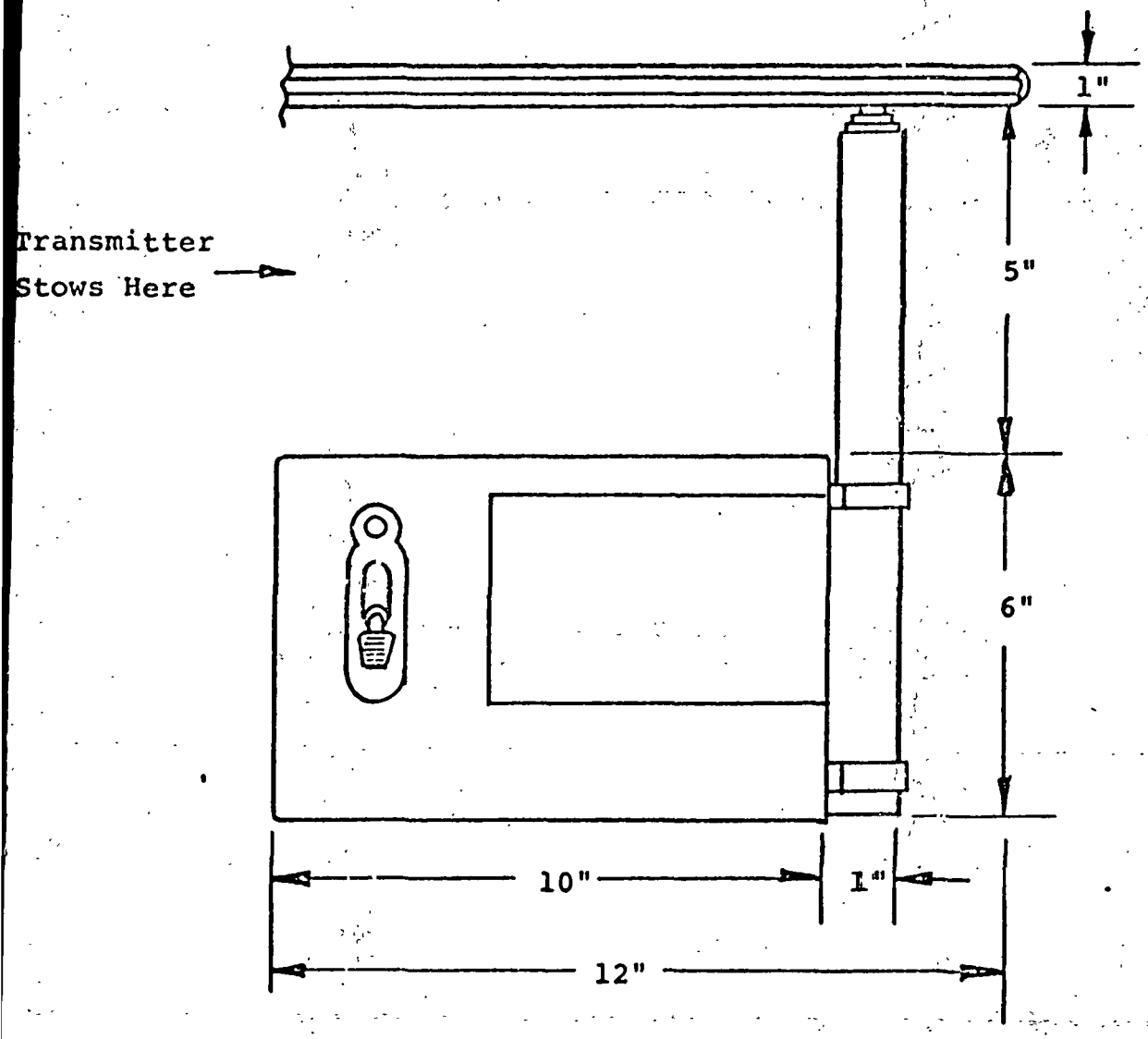

Figure III-29 Receiver, Stowed

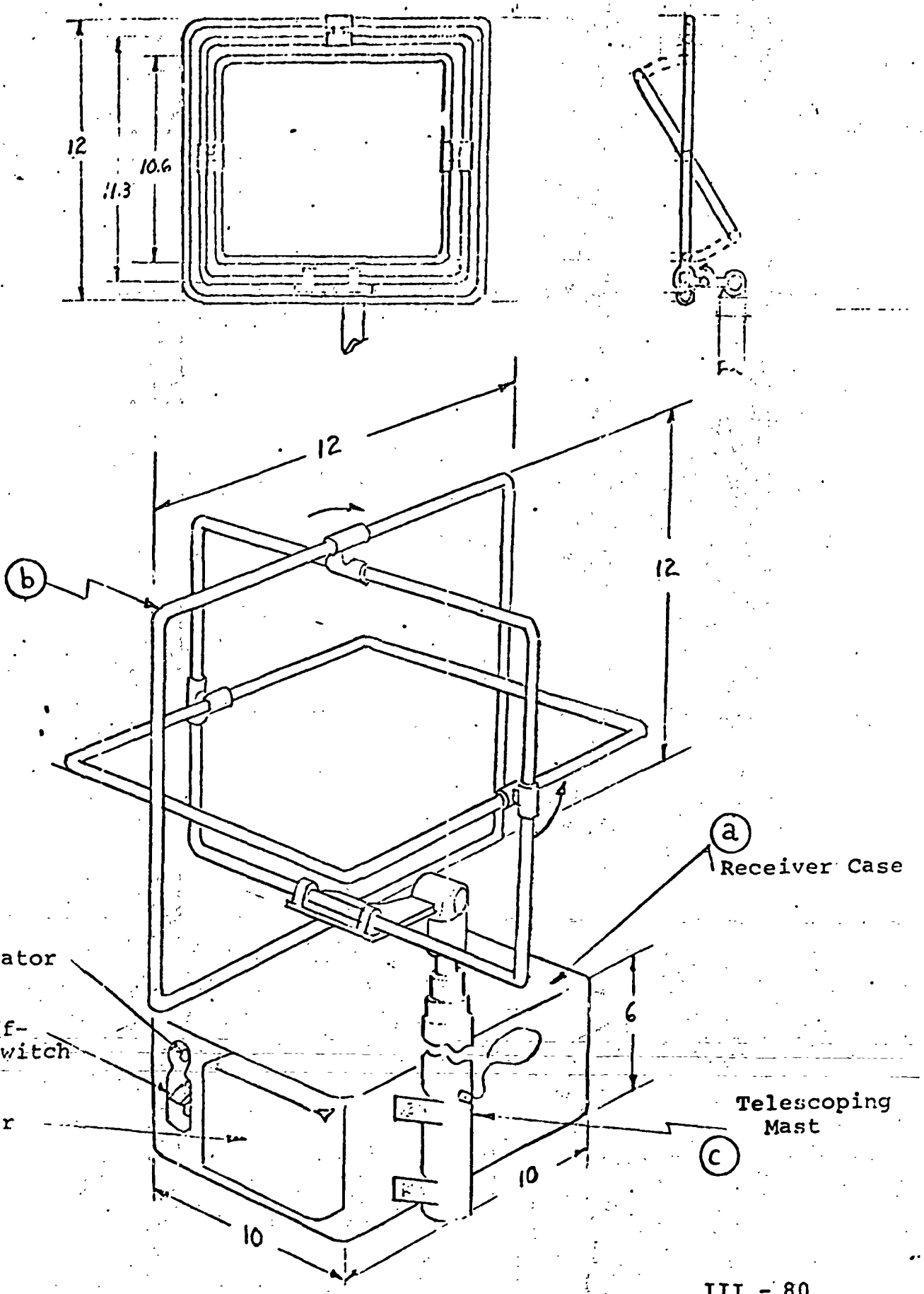

Figure III-30 Receiver, Deployed

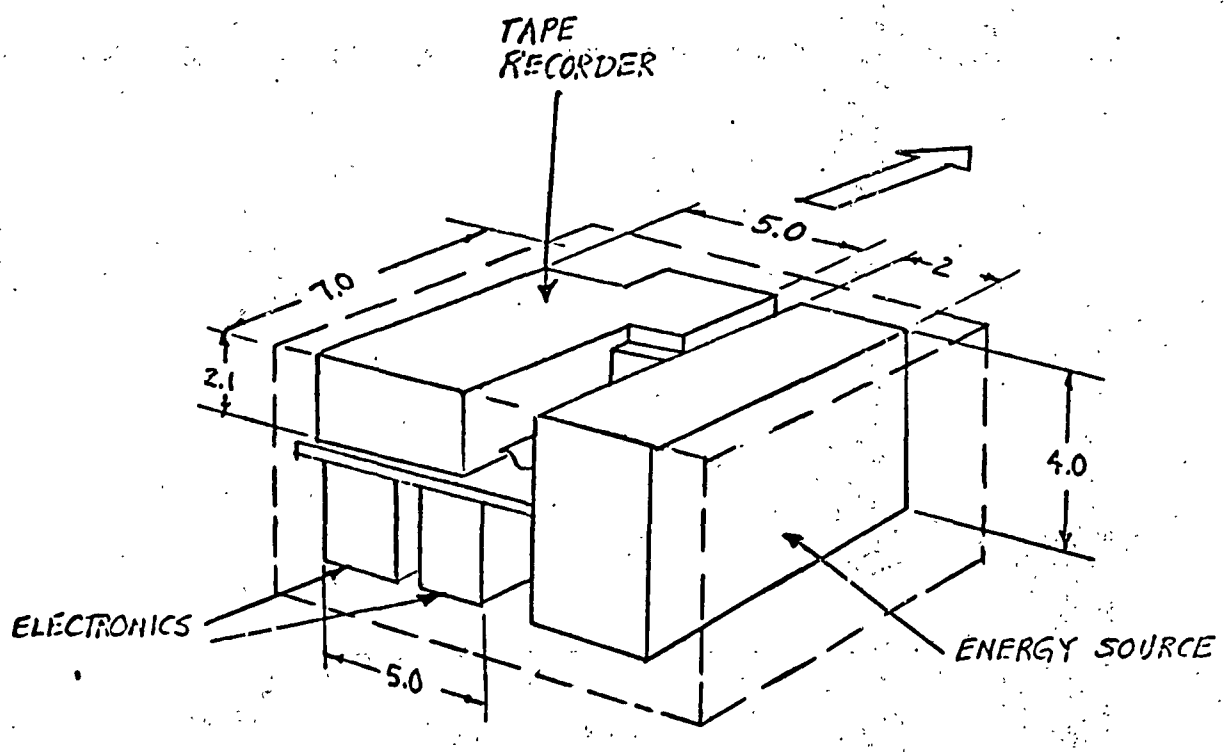

Figure III-31 Receiver Electronic Subassemblies

III-3. Thermal design

In writing a heat balance equation for an object on the lunar surface it is necessary to consider:

1. Heat generated in the equipment;
2. Heat absorbed by direct radiation from the Sun;
3. Heat absorbed from reflected radiation from the lunar surface;
4. Heat absorbed from IR radiation from the lunar surface;
5. Heat conducted to or from the lunar surface;
6. Heat transferred to or from man-placed objects on the lunar surface;
7. Heat loss from the object by radiation.

The surface temperature of the moon varies between 90° and 310° K for a sun angle variation from 0 to 25° . Since the amount of heat transferred to an object by IR from the moon's surface can be quite high, and is obviously a large variable, the thermal control problem can be reduced if the equipment is insulated from this effect. This will be done by applying insulation to the bottom and sides of the equipment. With adequate insulation, the heat flow through these surfaces can be neglected by comparison with the heat flow through the top surface and it is only necessary to examine in detail the top surface of the equipment.

a. Transmitter

The heat balance equation is:

$$\varepsilon A_r \sigma T^4 = Q + \alpha A_i S \sin\phi$$

or:

$$T = \sqrt[4]{\frac{Q + \alpha A_i S \sin\phi}{\varepsilon A_o \sigma}}$$

where:

ε is the emissivity of the radiating surface

A_r is the area of the radiating surface, in meters^2

σ is the Stefan-Boltzmann constant

$= 5.669 \ 10^{-8}$ watts meter^{-2} (deg K)$^{-4}$

T is the surface temperature in degrees Kelvin

Q is the internal power dissipation, in watts

α is the absorbtivity of the surface

A_i is the area of the absorbing surface, in meters^2

S is the solar constant = 1375 watts/meter^2

ϕ is the angle of the sun with respect to the radiating surface

The solar panel actually will serve as a sun shield, but for a preliminary design, the beneficial effect of this shield will be neglected, and the temperature will be calculated for the two extreme conditions marked by a sun angle of 0 and 25 degrees. The transmitter power dissipation is 5 watts, and the top surface is assumed to be painted with an 8-mil thickness of S13-G paint which has an absorption, α, of .20 for sunlight and an emissivity, ε, of .87 for IR. The

surface area is .01825 meters^2. The temperature then is:

$$T = \sqrt[4]{\frac{5 + (0.2)(0.01825)(1375)(0.4266)}{(0.87)(0.01825)(5.669)\ 10^{-8}}}$$

$$= 298^{\circ}K \equiv 25^{\circ}C \quad \left[\phi = 25^{\circ}\right]$$

or:

$$T = \sqrt[4]{\frac{5}{(0.87)(0.01825)(5.669)\ 10^{-8}}}$$

$$= 273^{\circ}K \equiv 0^{\circ}C \quad \left[\phi = 0^{\circ}\right]$$

If α increases to .50 because of dust contaminating the heat transfer surface, then:

$$T = \sqrt[4]{\frac{5 + (0.5)(0.1825)(1375)(0.4226)}{(0.87)(0.01825)(5.669)\ 10^{-8}}}$$

$$= 327^{\circ}K \equiv 54^{\circ}C \quad \left[\phi = 25^{\circ};\ \alpha = 0.5\right]$$

This range of temperatures is reasonable for the heat sink surface. However, some important effects have not yet been taken into account.

1. At what temperature will the electronics stabilize during deployment before the solar cells can supply power to the transmitter?
2. Is there any problem during stowage on the way to the moon if the top surface sees mostly space?

3. What thermal effect can be expected due to thermal paths through the antenna wires? Also, what effect will conductive paths between the radiating surface and the rest of the case have?

The first two problems above may be solved by providing a temporary thermal blanket and dust shield over the top surface which can be removed at the time the transmitter is turned on.

At the 25° sun angle the antennas and other wires will be cooler than the 50°C calculated for a dirty radiating surface and therefore tend to lower the temperature of the transmitter as desired. At the 0° sun angle these wires may be as cold as 100^{0}K. Assuming 30 number 25 gage copper wires conducting heat to the outside with a $\frac{\Delta T}{\Delta X}$ of 20°C per cm., the thermal balance is then:

$$\epsilon \, A_r \, \sigma \, T^4 + K A_c \, \frac{\Delta T}{\Delta X} = 5$$

$$(.87)(.01825)(5.669 \times 10^{-8})T^4 + 3.8\,(.039)(20) = 5$$

and the temperature then is:

$$T = \sqrt[4]{22.5 \;\; 10^8} = 218^{\circ}K \equiv -55^{\circ}C$$

It is apparent that these losses are very significant and will have to be reduced by thermally insulating the cable for some distance (~1 foot).

The conductive paths between the radiating surface and the rest of the case can be minimized by proper insulation and materials selection.

b. Receiver

The receiver poses a different problem in that its orientation is not fixed; it may or may not be shaded; it will be turned off for periods of time, and since it is battery powered, a high-powered heater cannot be used for thermal control. Also, the tape recorder and batteries impose a more limited temperature range than that required by the transmitter: ideally, these elements should be maintained between +20 and +150°F (-7 to +65°C). The number of wires emanating from the receiver is less but the thermal leakage paths provided by them still is signigicant. Assuming 6 wires of 8-mil diameter with a 20°C per centimeter gradient, the loss will be 0.15 watt.

Obviously, the heat transfer surface cannot be allowed to radiate continuously because if the receiver were turned off and then shaded by a part of the transport structure, the battery might become too cold for proper operation. This means that the radiation heat transfer surface must be thermally isolated except for a "thermal switch" which allows heat to flow when the receiver heats up during operation. Either an insulating shutter or a contacting type switch might be used. A preliminary design indicates that a contacting type switch will offer the lowest leakage.

For design purposes it appears that something on the order of 1/4 watt will be required to maintain the receiver thermal environment when it is turned off.

The thermal configuration proposed for the receiver therefore is a semi-active system. The electronics, tape unit, and battery are mounted in a container thermally insulated on all sides and insulated from the radiator. The radiator surface is designed so that its temperature will never exceed 80°F. A thermal switch is used to provide a heat path from the internal heat sink to the radiator whenever the internal temperature approaches 80°F. A preliminary design indicates that it should be possible to build a heat switch with thermal resistance in the "on" state of less than 1 mw/°F.

In the operational state the receiver's thermal system must eliminate approximately 5 watts plus the heat evolved from the batteries; assuming 7 watts total for now, the temperature drop across the closed thermal switch will be 70°F (21°C) for a maximum internal temperature of 150°F (65°C). In the standby state, the internal power is small, and the thermal switch usually will be open.

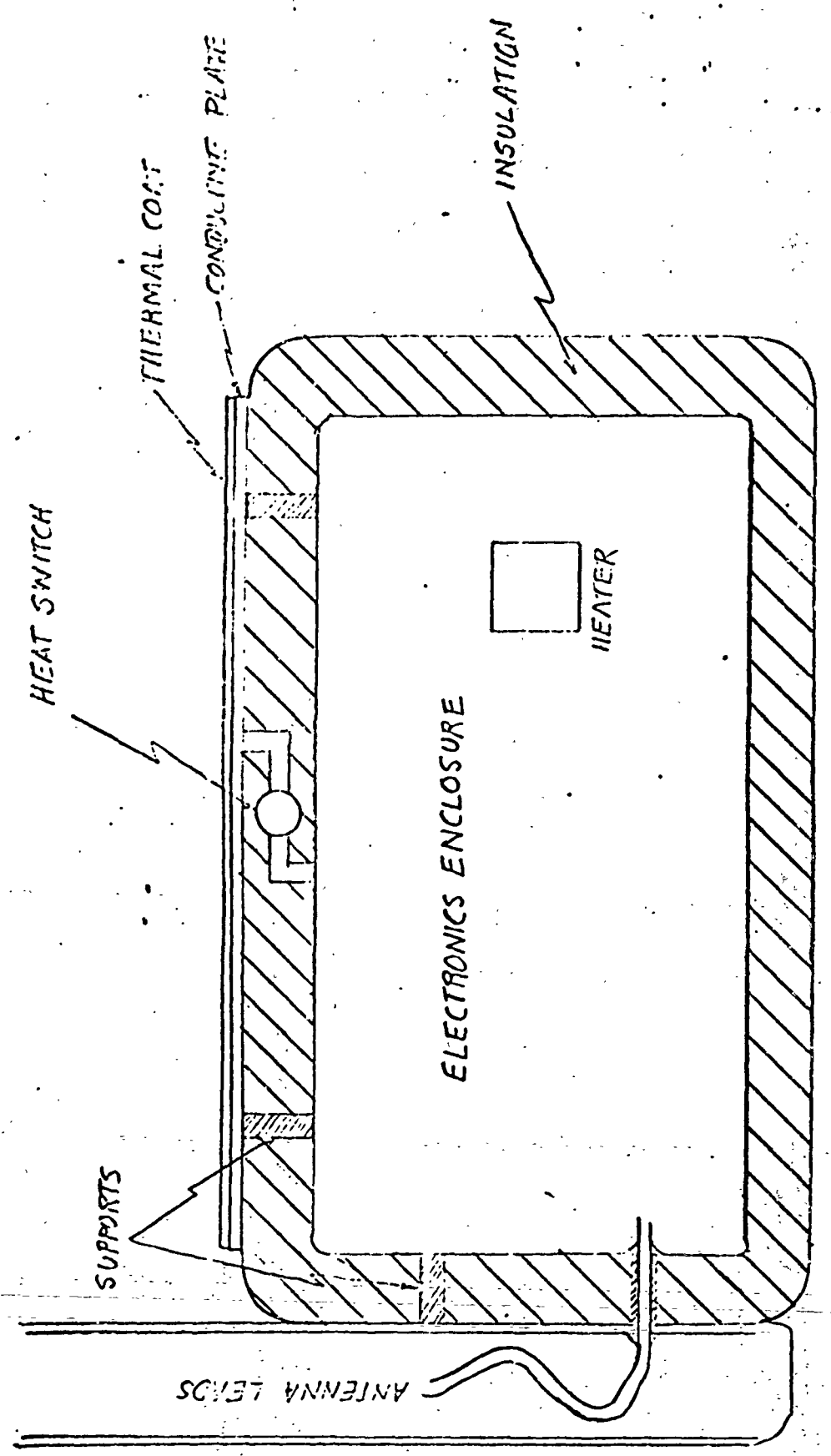

Figure III-32 Receiver, Thermal

III-4. Weight Estimates

a. Transmitter

Antennas: a.) Reels, 4 at 0.3	1.2 lb
b.) Ribbon wire	5.6 lb
Solar Panel with Fixtures	1.0 lb
Case and Thermal	1.4 lb
Electronics	1.9 lb
	11.1 lb

b. Receiver

Loops	0.9 lb
Mast	1.0 lb
Recorder	2.3 lb
Case and Insulation	2.4 lb
Batteries (Silver Zinc, 60 wH @ 40wH/lb)	1.5 lb
Electronics	2.5 lb
	10.8 lb

c. Totals

Launch and Lunar Descent weight:	21.9 lb
Receiver Weight for LRV, MET, or carrying:	10.8 lb
Tape Recorder Weight for Data Retrieval	2.3 lb

III-5. Power Requirements

The SEP equipment contains its own power sources and requires no external power.

a. Transmitter Power

The transmitter power source is a solar panel measuring approximately 9x9 inches. Using a derated (for dust) density of 6.5 watts/ft^2, the power available to the transmitter electronics is 3.66 watts, continuous.

The average power radiated by the transmitter is 0.325 watts so, assuming an efficiency of 50%, the power input to the RF amplifier is 0.65 watts. Additional electronics might require 1.0 watt, and the logic is expected to consume less than 0.5 watt, for a total power dissipation of less than 2.15 watts. There is then 1.5 watts available for operation of a thermostatically-controlled heater if needed for temperature control.

b. Receiver Power

The receiver power source is a silver-zinc battery of the secondary type. Silver-zinc batteries exhibit energy densities from 15 to 60 watt-hours/lb. These batteries are rechargeable and have a cycle life of a few hundred cycles.

The receiver's power budget is as follows:

Operational (10 hours total):

Tape Recorder:	2.4 watts (max)
Tape Recorder Power Supply:	1.2 watts
Receiver Electronics:	1.0 watt
Receiver Logic:	0.4 watts
	5.0 watts, or 50 watt-hours

Non-Operational (heater mode):

Assuming that 0.25 watts average is required to maintain the electronics temperature satisfactorily, and permitting 40 hours of operation in this mode, an additional 10 watt-hours will be required.

Using a typical energy density of 40 watt-hours/lb. and 2.8 watt-hours/in.^{3}, predicted battery weight is 1.5 lb. and predicted volume is 21.5 cubic inches.

A number of available cells fit this application closely. The Eagle-Picher SZLR 20.0 cell is a 20A-hour device at the 10-hour discharge rate with initial energy densities of 60 watt-hours/lb. and 4.05 wH/in^3. Each cell measures 0.89 x 2.20 x 3.75 inches and weighs 8.1 oz. The cell voltage, at a low discharge rate, is fairly constant at 1.5 volts so one such cell will supply 30 watt-hours. Three cells, then, will give a battery with an initial available energy of 90 watt hours, 50% more than required. The additional capacity covers the effects of self-discharge during wet stand, and low temperature.

III-6. Required Equipment

A. Breadboards

To assist in early design efforts and preliminary concept evaluation.

B. Engineering Unit

A non-production electrical equivalent of the SEP apparatus to be used for design verification and evaluation changes.

C. Structural/Thermal Mockups

As required for proof of the mechanical and thermal design. The primary thermal mockup unit is to be used for thermal/vacuum testing, and requires internal heat sources (in lieu of electronics and tape recorder) and sufficient instrumentation (i.e., temperature sensors) to prove the soundness of the thermal design.

D. System Interface Mockups

For simulation and demonstration of S/C and lunar vehicle interfacing. The following are contemplated:

a. A stowed configuration mockup for the LM.

b. A receiver mockup for the LRV or MET.

c. A mockup of the tape recorder.

E. Astronaut Training Mockup

Since the operation of the SEP equipment requires minimal attention and there are no real-time display or operational requirements, the training equipment may be functionally simple and may be made one-sixth the weight

of the flight hardware to simulate lunar gravity. To demonstrate the transmitting antenna deployment, this unit will require reels and ribbons identical to those designed for the flight equipment. The form factor and handling will be exactly that of the flight equipment, although this unit will contain no actual electronics or tape recorder.

F. Prototype Unit

This unit is a non-production prototype fabricated insofar as possible to the flight hardware design. The unit is intended for a glacier test of the experiment concept and design in March, 1971, and will require a tape recorder and full electronics, although not necessarily flyable hardware. The equipment will be identical to the flight equipment as defined by October, 1970.

G. System Compatibility Model

This is the first production equipment; following evaluation it will be delivered for compatibility testing as directed by the Contracting Officer.

H. Qualification Unit

The second production unit is intended for qualification testing, following acceptance testing; this is the first unit requiring all flight-qualified components.

J. Flight Unit

K. Flight Spare

L. Flight Unit

M. Flight Spare

a. Ground Support Equipment

The equipment required to evaluate the transmitter and receiver must perform the following:

a. For the transmitter

1. Provide adjustable metered power to the transmitter electronics.
2. Provide adjustable or switchable dummy loads.
3. Measure and display power output at each frequency as a function of time.
4. Measure transmitter clock frequency.

b. For the receiver

1. Provide adjustable metered power.
2. Measure battery voltage for determination of state of charge.
3. Provide to the antenna terminals adjustable signals simulating those transmitted for evaluation of sensitivity, noise figure, and frequency characteristics. Sufficient adjustment should exist to permit receiver calibration.
4. Provide a battery-charging capability.
5. Display recorder VCO output and input.

6. Provide facilities for evaluating the tape recorder and for reproducing tapes.

The GSE will consist largely of rack-mounted commercial instruments. Specialized hardware will be required for commutating and decommutating signals, simulating loads, and switching among the various functions.

The transmitter and receiver will have test connectors for interfacing with the GSE.

Three sets of GSE are proposed; two for delivery (to MSC and KSC) and one to be used at MIT for acceptance, qualification, and production final testing.

UNIT	DESCRIPTION	ELECTRONICS	MECHANICAL	THERMAL	RECORDER
A	Breadboard	N			
B	Eng'g Unit	N,F			
C	Structural/ Thermal		N	N	
D	Mockups				
E	Training				
F	Prototype	N	N	N	N
G	Compatibility	N,F*	F	F	N,F*
H	Qualification	F	F	F	F
J	Flight	F	F	F	F
K	Flight	F	F	F	F
L	Flight	F	F	F	F
M	Flight	F	F	F	F

N: non-flyable hardware

F: flyable hardware

* Flyable if schedule permits

Table III-6.1 SEP Hardware

SECTION IV - OPERATIONAL REQUIREMENTS

IV-1 Mission requirements

a. Spacecraft orientation requirements

There are no requirements for special landing sites or spacecraft maneuvers.

b. Astronaut participation

The astronaut is required to deploy the transmitter and transmitting antenna, perform a calibration walk, mount the receiver in the MET or LRV before starting a traverse, turn the receiver on or off at the beginning or end of a traverse, and recover the tape unit at the conclusion of the experiment. Detail of these tasks is discussed below.

(i) Deployment

The stowed asembly is taken from the LM descent stage and carried approximately 200 meters from the LM. The transmitter is released from the package by a lanyard pull, the covered solar panel is unfolded and the transmitter assembly placed so that the solar panel is facing in the general direction of the sun ($\pm 15^{\circ}$). The topmost antenna reel is lifted from the transmitter by the handling tool and the antenna limb is extended in a straight line. The antenna wire will be color coded near the end to prevent overstress when the reel is fully unwound. The reel is placed hub down on the surface and may be anchored by stepping on it. This procedure is repeated for the other three antenna sections.

The astronaut then returns to the transmitter, and removes the protective covering on the transmitter radiator surface and solar panel.

Attention then is directed to the receiver. The receiving loops are unfolded, the mast is extended, and the protective cover removed from the radiator. The receiver then is turned on and its operation verified by observing the indicator. The astronaut should indicate when the receiver is turned on over the voice link.

(ii) Calibration

The receiver then is carried along one limb of the antenna, and pauses are made at several points indicated by markings on the antenna. The receiver then is placed in the thermal-control mode until the first traverse.

(iii) Operation

Following the calibration, the receiver is mounted in the MET or on the LRV. When the first traverse is to be made, the receiver is turned on and left on until the traverse is complete. Again, for data correlation purposes, the astronaut should indicate, by voice, the time at which the receiver is turned on. Following the traverse, the receiver is returned to the thermal-control mode.

The above procedure is repeated for each traverse but the last. Following the final traverse, the receiver is turned off and the tape recorder is removed for return to earth.

(iv) Time Estimate for Deployment by One Astronaut

Remove equipment from Descent Stage	60 sec
Carry to deployment site (200m @ 0.8/sec)	250 sec
Separate package and set up transmitter	120 sec
Deploy antennas (see Figure IV-1) 560m @ 0.8m/sec	700 sec
Remove transmitter dust covers	60 sec
Extend receiver mast, remove dust cover, and turn on. Indicate over voice link	60 sec
Verify receiver operation	60 sec
Carry receiver for calibration (70m @ 0.5m/sec + 10 stops @ 2 sec)	160 sec
Set receiver to standby mode	30 sec
Return receiver to vicinity of LM, LRV or MET	250 sec
Install receiver on LRV or MET	120 sec
	1870 sec = 31 min.

(v) Time estimate for other activities

Turn receiver on or off at beginning or end of traverse	30 sec
Remove tape recorder at the end of last traverse	180 sec

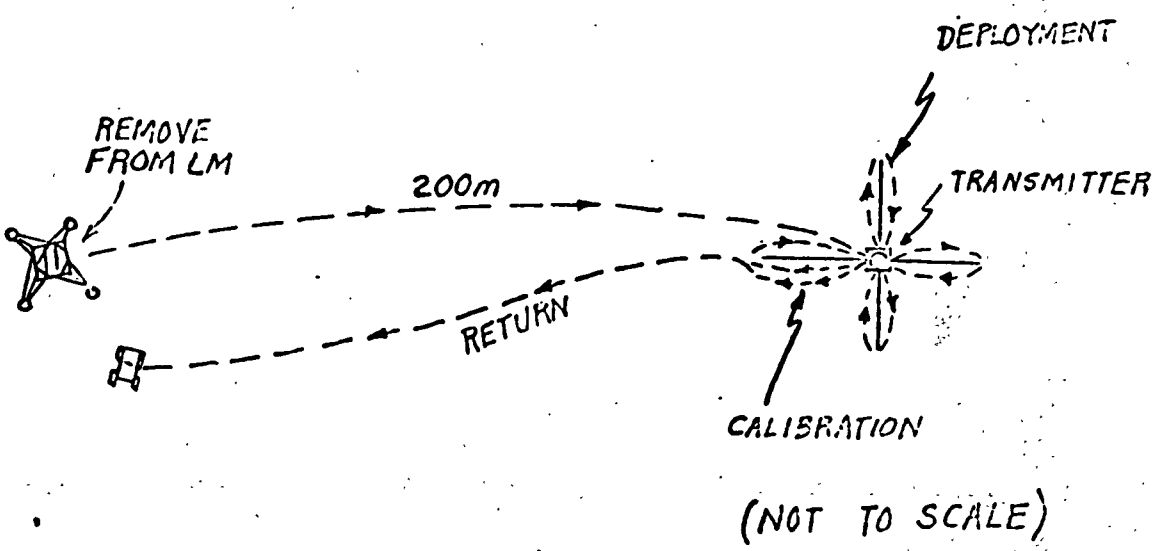

Figure IV-1 Deployment

c. Flight Operational Requirements

With the single exception of voice-link notification when the receiver is turned on, there are no special communication, tracking, or control requirements. There is no requirement for real-time operational support.

d. Possible Interference

The SEP apparatus will radiate RF energy at the following frequencies and levels during the experiment:

Frequency	Power
0.5 MHz	2w
1 MHz	1/2w
2 MHz	1/8w
4 MHz	1/8w
8 MHz	1/8w
16 MHz	1/8w
24 MHz	1/8w
32 MHz	1/8w

Interference generated by the low-level circuitry (logic and switching functions) will be minimal.

The susceptibility of the receiver to noise generated by nearby man-made equipment will be assessed using a curve of overall receiver sensitivity vs. frequency as the engineering information becomes available.

IV-2 Support requirements

a. Prelaunch

(i) Astronaut training

A moderate amount of crew training will be required to successfully perform the SEP operational tasks described above. Crew training will be accomplished through use of a crew training manual and a training mockup.

The training manual will provide a description of all handling and control interfaces with the crew. It will provide step by step details of SEP handling, deployment, activation, calibration, etc. The external features of the training mockup will be sufficiently complete to train the crew in SEP handling and operation.

(ii) Tape recorder storage

To maintain a proper distribution of lubricant in the tape recorder it is necessary that this unit be exercised for a minimum of one minute at least once every 120 days.

b. Data recovery

Following the experiment, the collected data is stored on magnetic tape in the tape recorder. The tape recorder is removed from the receiver assembly as discussed previously, and brought aboard the LM. Preliminary calculations indicate that no special handling will be required during the period that the recorder may be exposed on the lunar surface. Special handling or stowage for the return trip should not be required.

c. Data processing and analysis

For safety reasons, it will be desirable to make copies of the returned magnetic tape as soon as possible. These copies then will be converted in special purpose data processing equipment to conventional digital computer magnetic tape format.

Subsequent analysis will require a good deal of computer examination of the converted data tapes, along with comparison of theoretical and analog scale models as described in Section II of this report.

APPENDIX A

ROTATING FIGURE-OF-EIGHT RADIATION PATTERN

A rotating figure-of-eight pattern can be generated by modulating the excitation currents of two orthogonal dipole antennas. Let i_a, i_b be the excitation currents of such a set of dipole antennas aa and bb, shown in Figure 1, such that,

$$i_a = \cos \alpha \; e^{j\omega t} \tag{1}$$

$$i_b = \sin \alpha \; e^{j(\omega t+\Delta)} \tag{2}$$

where:

ω is the carrier frequency

Δ is the relative phase shift at the carrier frequency

α is the modulating angle; $|\alpha(t) << \omega t|$

The corresponding normalized far electric-field components E_a and E_b will be,

$$E_a(t,\theta) = \cos \alpha \sin \theta \; e^{j\omega t} \tag{3}$$

$$E_b(t,\theta) = -\sin \alpha \cos \theta \; e^{j(\omega t+\Delta)} \tag{4}$$

where: θ is the azimuthal angle defined in Figure 1.

From (3) and (4), the resultant field pattern E_T is,

$$E_T = E_a + E_b = \left[\cos \alpha \sin\theta - \sin\alpha \cos \theta \; e^{j\Delta}\right] e^{j\omega t}$$

where $e^{j\omega t}$ is a common time dependence factor which can be dropped for analysis purposes, resulting in:

$$E_T = [\cos\alpha \sin\theta - \sin\alpha \cos\theta \cos\Delta] - j \sin\alpha \cos\theta \sin\Delta = X - jY \quad (5)$$

where X, Y are the real and imaginary terms of E_T.

The maxima (or minima) of the pattern can be determined by taking a derivative of the radiated power with respect to the azimuthal angle (θ) and solving it for θ. The roots of θ determined thereby define the maximum and minimum of the pattern as described below.

$$\frac{\partial |E_T|^2}{\partial \theta} = \frac{\partial [E_T \cdot E_T^*]}{\partial \theta} = E_T \frac{\partial E_T^*}{\partial \theta} + E_T^* \frac{\partial E_T}{\partial \theta} = 0 \quad (6)$$

where:

$|E_T|^2 \triangleq E_T \cdot E_T^*$ is the radiated power

$$E_T^* = X + jY = [\cos\alpha \sin\theta - \sin\alpha \cos\theta \cos\Delta] + j\sin\alpha \cos\theta \sin\Delta \quad (7)$$

is the conjugate of E_T.

From (5),

$$\frac{\partial E_T}{\partial \theta} = [\cos\alpha \cos\theta + \sin\alpha \sin\theta \cos\Delta] + j\sin\alpha \sin\theta \sin\Delta = M + jN \quad (8)$$

where M, N are the real and imaginary parts of $\frac{\partial E_T}{\partial \theta}$

From (7),

$$\frac{\partial E_T^*}{\partial \theta} = [\cos\alpha \cos\theta + \sin\alpha \sin\theta \cos\Delta] - j\sin\alpha \sin\theta \sin\Delta = M - jN \quad (9)$$

From Equations (5) thru (9),

$$\frac{\partial |E_T|^2}{\partial \theta} = [X-jY][M-jN] + [X+jY][M+jN] = 0$$

$$XM - YN = 0 \qquad (10)$$

Substituting values of X, M, Y, N in (10),

$$[\cos\alpha \sin\theta - \sin\alpha \cos\theta \cos\Delta][\cos\alpha \cos\theta + \sin\alpha \sin\theta \cos\Delta]$$

$$-[\sin\alpha \cos\theta \sin\Delta]X[\sin\alpha \sin\theta \sin\Delta] = 0 \qquad (11)$$

which can be simplified to yield:

$$\tan 2\theta = \cos\Delta \frac{\sin 2\alpha}{\cos 2\alpha} = \cos\Delta \tan 2\alpha \qquad (12)$$

The roots of θ from (12) are given as,

$$\theta_\eta = \frac{1}{2} \tan^{-1} [\cos\Delta \tan 2\alpha] + \frac{\eta\pi}{2} \qquad (13)$$

For $\eta=0$, $\theta_o = \frac{1}{2} \tan^{-1} [\cos\Delta \tan 2\alpha]$ (14)

For $\eta=1$, $\theta_1 = \frac{1}{2} \tan^{-1} [\cos\Delta \tan 2\alpha] + \frac{\pi}{2} = \theta_o + \frac{\pi}{2}$ (15)

Field values at the two roots θ_o, θ_1 from (5), (14) and (15) are,

$$E_T(\theta_o) = [\cos\alpha \sin\theta_o - \sin\alpha \cos\theta_o \cos\Delta] - j\sin\alpha \cos\theta_o \sin\Delta \qquad (16)$$

$$E_T(\theta_1) = [\cos\alpha \cos\theta_o + \sin\alpha \sin\theta_o \cos\Delta] + j\sin\alpha \sin\theta_o \sin\Delta \qquad (17)$$

From (16) and (17)

$$|E_T(\theta_o)|^2 = \cos^2\alpha \sin^2\theta_o + \sin^2\alpha \cos^2\theta_o - 2\sin\alpha \cos\alpha \sin\theta_o \cos\theta_o \cos\Delta \quad (18)$$

$$|E_T(\theta_1)|^2 = \cos^2\alpha \cos^2\theta_o + \sin^2\alpha \sin^2\theta_o + 2\sin\alpha \cos\alpha \sin\theta_o \cos\theta_o \cos\Delta \quad (19)$$

From (18) and (19), $|E_T(\theta_1)|^2 > |E_T(\theta_o)|^2$ which indicates that $E_T(\theta_1)$ is the maximum field and is separated from the minimum field $E_T(\theta_o)$ by 90° as shown in Figure 2. Replacing the dummy variable $\theta_o = \theta$, the maximum and minimum field expressions from (10) and (17) can be rewritten as,

$$E_{max}(\theta) = E_T(\theta_1) = (\cos\alpha \cos\theta + \sin\alpha \sin\theta \cos\Delta) + j\sin\alpha \sin\theta \sin\Delta \quad (20)$$

$$E_{min}(\theta) = E_T(\theta_o) = (\cos\alpha \sin\theta - \sin\alpha \cos\theta \cos\Delta) - j\sin\alpha \cos\theta \sin\Delta \quad (21)$$

Now let the ratio of minimum and maximum field amplitudes be defined as:

$$r \triangleq \left|\frac{E_{min}(\theta)}{E_{max}(\theta)}\right| \quad (21)$$

such that:

$$\frac{|E_{max}|^2 - |E_{min}|^2}{|E_{max}|^2 + |E_{min}|^2} = \frac{1-r^2}{1+r^2} \quad (22)$$

Substituting values of E_{max} and E_{min} from (18) and (19) in (22), results, after some manipulation, in:

$$\cos 2\theta \cos 2\alpha + \sin 2\theta \sin 2\alpha \cos\Delta = \frac{1-r^2}{1+r^2} \quad (23)$$

Substituting $\cos\Delta$ from (12), in (23) then yields:

$$\cos 2\alpha = \frac{1-r^2}{1+r^2}\cos 2\theta \qquad (24)$$

Equations (12) and (24) relate the four variables r, θ, α and Δ controlling the behavior of the rotating radiation pattern. The plots of these equations are periodic in nature and possess symmetry about $\Delta = \frac{\pi}{2}$ and $\alpha = \frac{\pi}{4}$ axes as shown in Figure 3. Because of symmetry, all pertinent information is contained in the range $0 \leq \alpha \leq \frac{\pi}{4}$ and $0 \leq \Delta \leq \frac{\pi}{2}$. Furthermore, it can be seen that for any two prescribed parameters of the required rotating pattern, the remaining variables can be determined from Figure 3.

For example, suppose it is required to generate a rotating pattern with a rotation rate of 15 revolutions per second and with 80% modulation (r=0.2). In such a case, the azimuth angle $\theta(t)=2\pi$ is scanned in 6.66×10^{-2} seconds. For graphical convenience, let this time interval be divided into 32 intervals each of duration $t \simeq 2.062 \times 10^{-3}$ seconds corresponding to an angular change of $\frac{\pi}{16}$. Using the plots of Figure 3, the corresponding values of Δ and α can be determined and are drawn in Figure 4. An electronic implementation of these values will generate the desired 15 revolutions per second rotation rate.

Two special cases of interest can be inferred directly from Figures 2 and 3.

(a) For 100% modulation (r=0) the contour lies on the abcissa which means $\Delta=0$ and $\alpha=\theta$. This implies that to realize a rotating beam in case c in Figure 2, no relative phase shift in the carrier frequency is required or allowed. The antenna excitation current angle α will be synchronous with the azimuthal angle θ of the rotating beam. The electronic hardware in the transmitter designed for the Surface Electrical Properties experiment has been designed to operate in this 100% modulation mode.

(b) For the zero percent modulation case (r=1), $\Delta=\frac{\pi}{2}$ and $\alpha=\frac{\pi}{4}$. This is the special case represented by the conventional turnstile antenna.

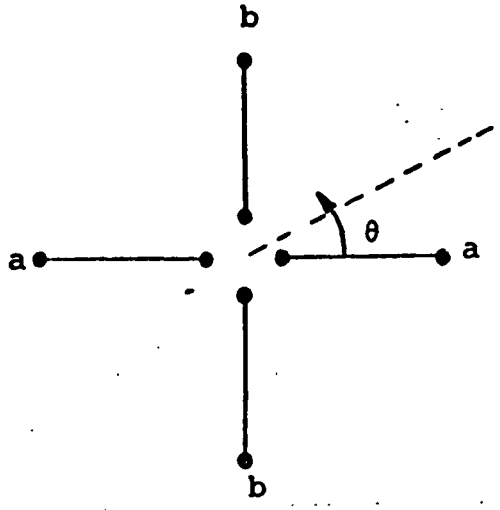

Figure 1. Set of Two Orthogonal Dipoles Antennas

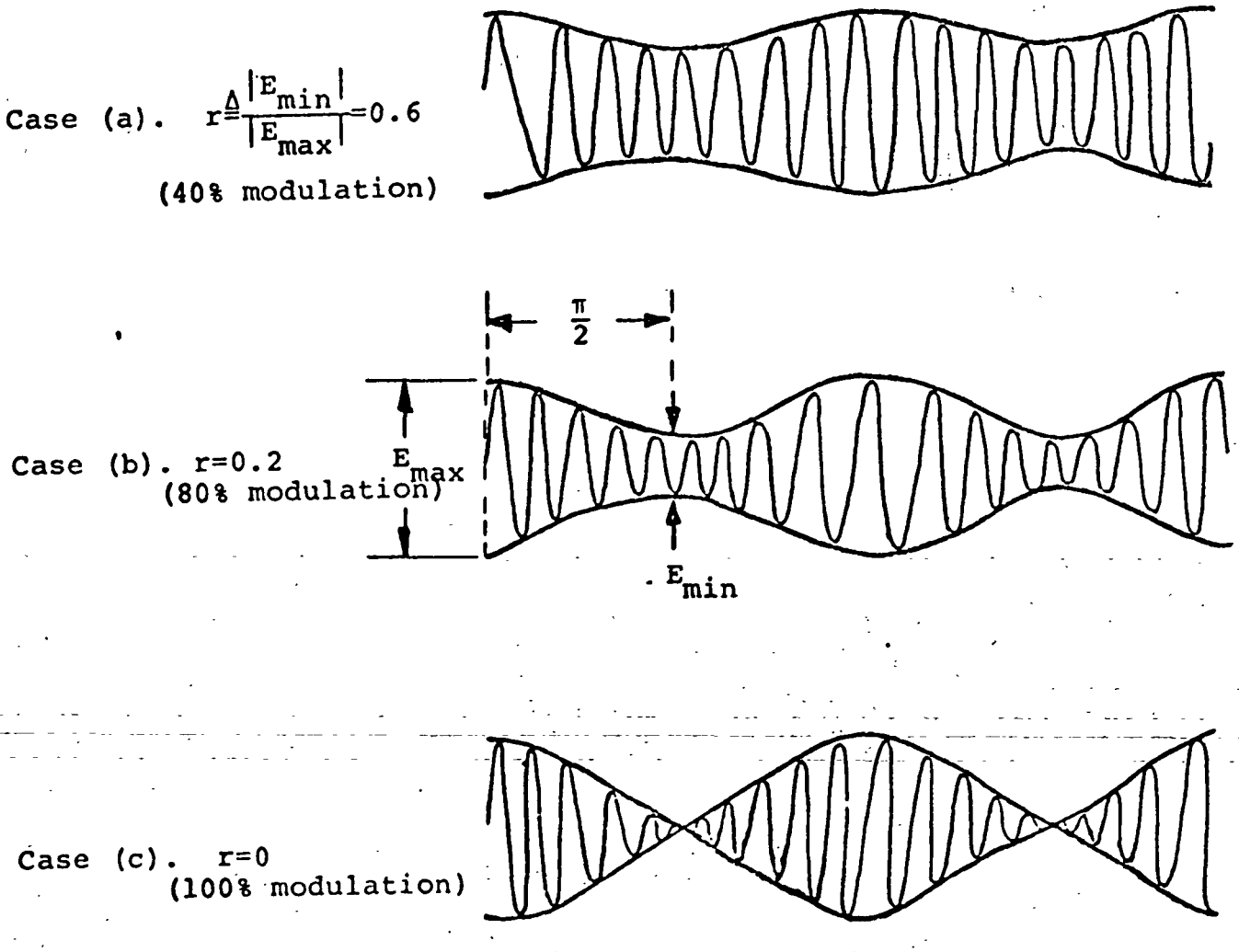

Figure 2. Maximum and Minimum of Electric Field for Rotating Radiation Pattern

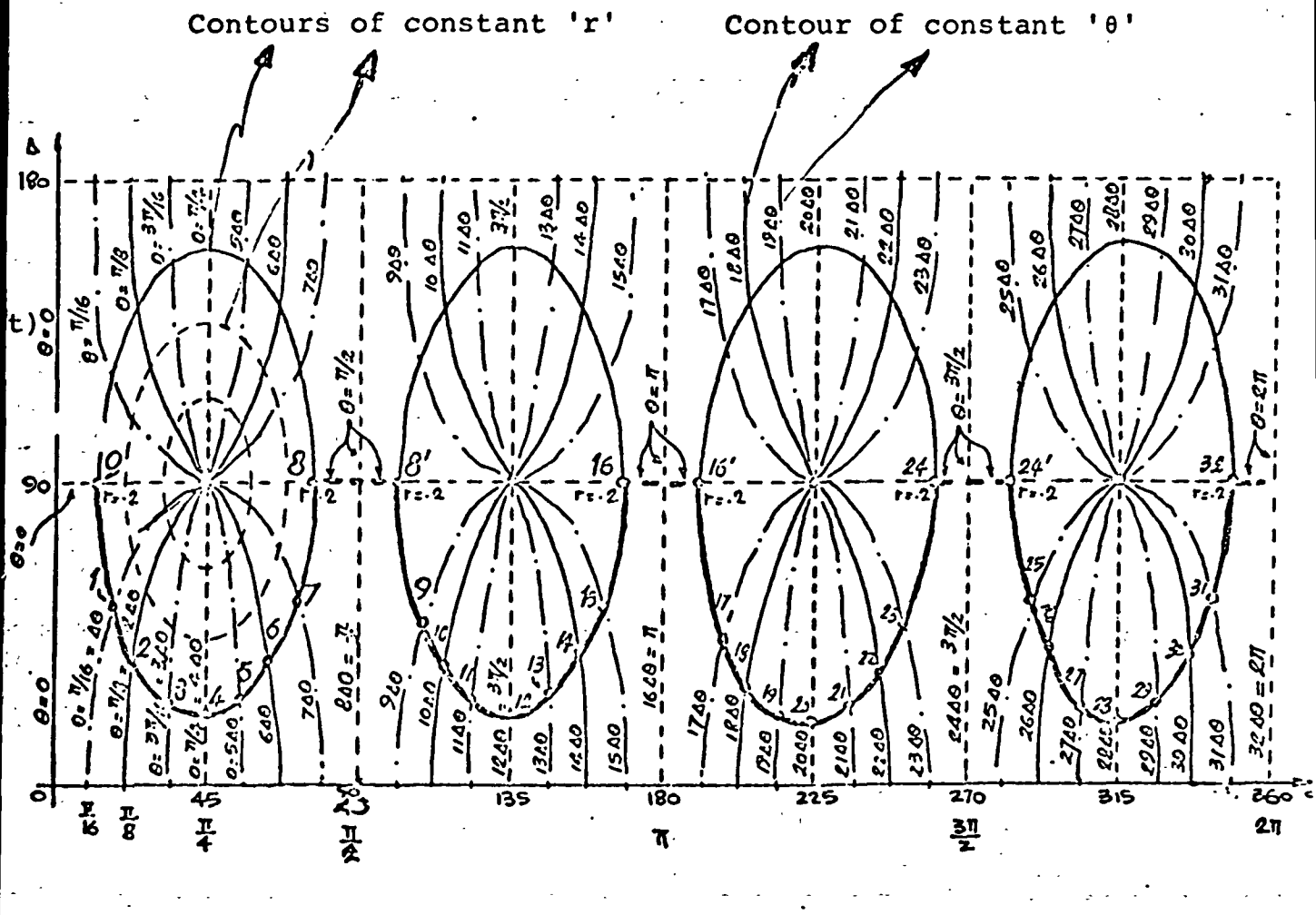

Figure 3. Plots Relating the Variables r, θ, Δ, α

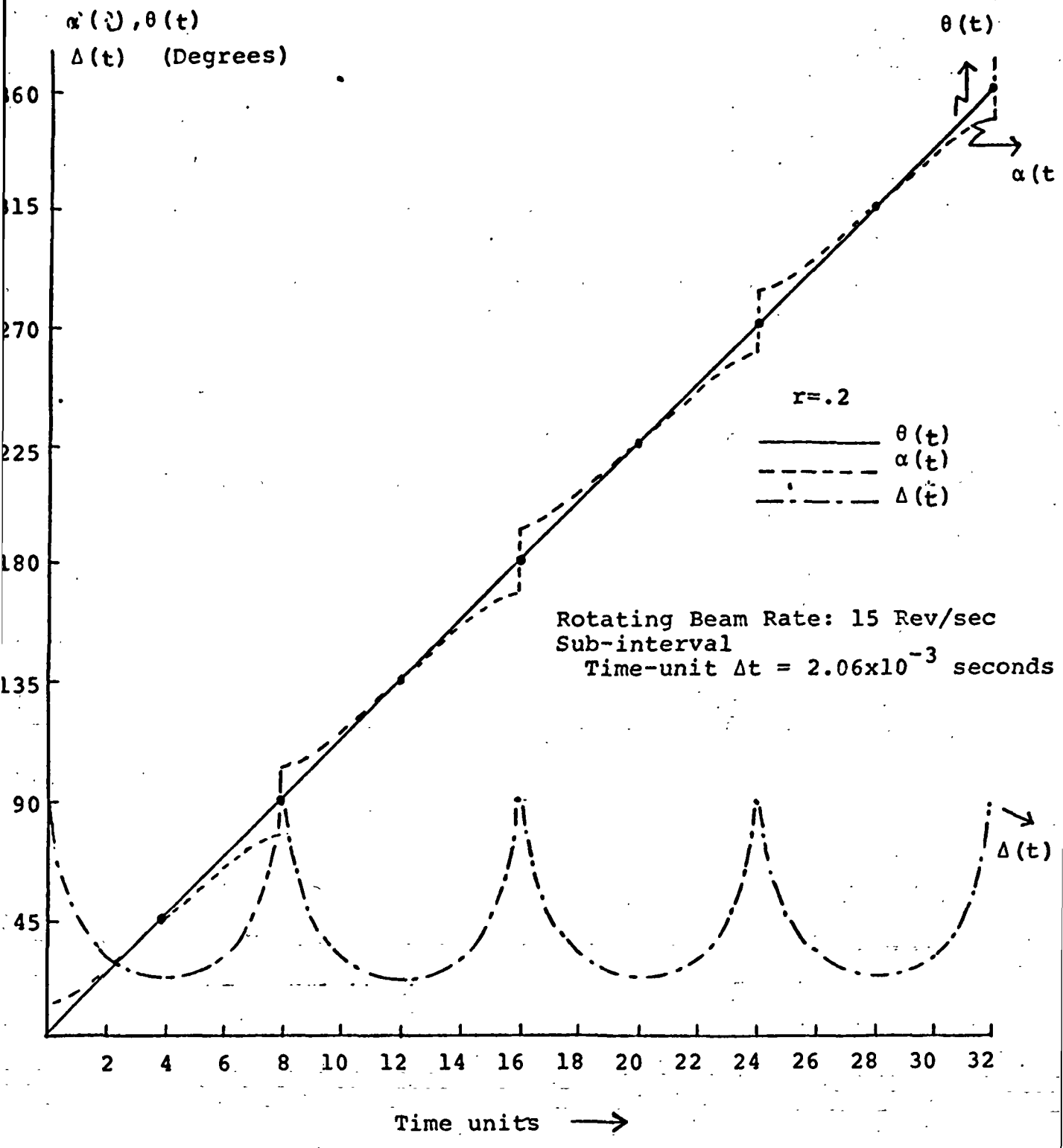

Figure 4. Parameter Values for 80% Modulated, 15 Revolutions per second Rotating Pattern